2-1964

Compatibility studies of several molten uranium and thorium alloys in niobium, tantalum, and yttrium

Robert James Cash
Iowa State University

Ray M. Fisher
Iowa State University

Merl R. Core
Iowa State University

Compatibility studies of several molten uranium and thorium alloys in niobium, tantalum, and yttrium

Abstract
Niobium, tantalum, yttrium, and Inconel have been used to contain molten aluminum, lead, tin, zinc, and several of their respective uranium and thorium alloys for various times up to 3000 hours and at temperatures ranging from 600 to 1100° C. Altogether 76 capsule tests were run, almost all in a static isothermal condition. Tantalum showed the best resistance followed by niobium, Inconel, and yttrium respectively. The systems, lead in tantalum and lead in niobium, showed the greatest potentials for possible liquid-metal fuel carrier systems. An alloy of uranium-bismuth-tin contained in tantalum also exhibited promising possibilities . The tabulated test data include a classification of the type of corrosion attack which occurred and a measured value of the amount of corrosive penetration. Each test was also given an arbitrary rating for easy reference comparisons. A number of photomicrographs are included for each set of tests.

Disciplines
Engineering | Metallurgy

IS-888

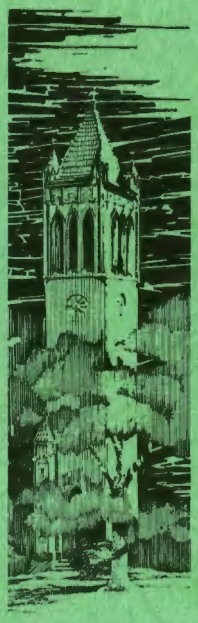

IOWA STATE UNIVERSITY

COMPATIBILITY STUDIES OF SEVERAL MOLTEN URANIUM AND THORIUM ALLOYS IN NIOBIUM, TANTALUM, AND YTTRIUM

by

Robert James Cash, Ray M. Fisher and
Merl R. Core

AMES LABORATORY

RESEARCH AND DEVELOPMENT REPORT

U.S.A.E.C.

IS-888

Engineering and Equipment (UC-38)
TID-4500, June 1, 1964

UNITED STATES ATOMIC ENERGY COMMISSION

Research and Development Report

COMPATIBILITY STUDIES OF SEVERAL MOLTEN URANIUM AND THORIUM ALLOYS IN NIOBIUM, TANTALUM, AND YTTRIUM

by

Robert James Cash, Ray M. Fisher and
Merl R. Core

February 1964

Ames Laboratory
at
Iowa State University of Science and Technology
F. H. Spedding, Director
Contract W-7405 eng-82

IS-888

This report is distributed according to the category Engineering and Equipment (UC-38) as listed in TID-4500, June 1, 1964.

Printed in USA. Price $ 2.75 Available from the

Office of Technical Services
U. S. Department of Commerce
Washington 25, D. C.

TABLE OF CONTENTS

IS-888

COMPATIBILITY STUDIES OF SEVERAL MOLTEN URANIUM AND THORIUM ALLOYS IN NIOBIUM, TANTALUM AND YTTRIUM *

Robert James Cash, Ray W. Fisher and Merl R. Core

ABSTRACT

Niobium, tantalum, yttrium, and Inconel have been used to contain molten aluminum, lead, tin, zinc, and several of their respective uranium and thorium alloys for various times up to 3000 hours and at temperatures ranging from 600 to 1100° C. Altogether 76 capsule tests were run, almost all in a static isothermal condition. Tantalum showed the best resistance followed by niobium, Inconel, and yttrium respectively. The systems, lead in tantalum and lead in niobium, showed the greatest potentials for possible liquid-metal fuel carrier systems. An alloy of uranium-bismuth-tin contained in tantalum also exhibited promising possibilities . The tabulated test data include a classification of the type of corrosion attack which occurred and a measured value of the amount of corrosive penetration. Each test was also given an arbitrary rating for easy reference comparisons. A number of photomicrographs are included for each set of tests.

A background of the advantages and disadvantages of fluid-fuel reactors are compared with those for solid-fuel reactors. Differences between aqueous fuels and liquid-metal fuels are also discussed. The various types of corrosive attack of solid metals by liquid metals are defined and illustrated with several photomicrographs. The variables affecting liquid-metal corrosion attack are given and driving forces for the various types of attack presented. Methods of corrosion inhibition are mentioned. The various criteria for selecting fuel and fertile alloys and suitable container materials were also considered.

* This report is based on an M. S. thesis by Robert James Cash which was presented February, 1964, to Iowa State University, Ames, Iowa.

INTRODUCTION

The greatest stimulus to the development of liquid metals technology was undoubtedly the advent of nuclear energy and the concept of the liquid-metal-fuel reactor. With the growth of the atomic energy program, liquid metals were first considered as reactor coolants and later as fuel carriers. In addition, liquid metals were suggested for pyrometallurgical processing, that is, high temperature fuel reprocessing. Present trends of development in nuclear power reactors are towards higher operating temperatures to improve thermal efficiency, and towards more irradiation-resistant fuels to achieve increased reactor stability and greater fuel utilization.

The liquid-metal-fuel-reactor concept was first suggested by von Halban and Kowarski in 1941 (51), but it did not receive much attention until 1947. The first so-called liquid-metal-fuel-reactor (LMFR) as proposed by the Nuclear Engineering Department of Brookhaven National Laboratory was a thermal, power-breeder reactor. A solution of uranium in bismuth was selected for the fuel because of the low melting point and low thermal neutron-absorption cross section of bismuth. Moreover, bismuth has a high boiling point [1477°C; (65)] which makes possible the high temperature operation of a bismuth-cooled reactor at fairly low pressures. One of the most outstanding features of the LMFR is the proposed method for fuel reprocessing. Pyrometallurgical experiments (5, 56) have shown that the removal of volatile fission products can be effected by vacuum degassing, whereas nonvolatile fission products from the fluid fuel can be removed by extraction with a fused salt. Furthermore, this process can be put on a continuous basis which should show a low operating cost.

Modern conventional power plants have an approximate thermodynamic efficiency of 40 per cent. For a nuclear power plant to achieve similar efficiencies, it is necessary to have the reactor outlet temperature above 500°C. With the LMFR, such temperatures are obtainable, and it represents one of the few potentialities for producing electric power competitive with the best of the present conventional steam power plants. Moreover, the flexibility of liquid-metal-fuel systems is such that they range over several different reactor categories. Liquid-metal-fuel reactors may be designed as fast, intermediate, or thermal systems, with either circulating or static fuel systems (44).

In order to understand better the characteristics and development problems of a liquid-metal-fuel reactor, fluid- and solid-fuel reactors should be compared. In particular, a distinction between the features of fluid fuels and those of liquid-metal fuels should be made (1, 36, 44, 46, 47, 60).

The advantages of a reactor using a circulating fluid fuel over one with solid-fuel elements can be listed as follows:

1. Simple design and structure Fluid-fuel reactors can employ external heat exchangers separate from the core region, so that the nuclear requirements of the core do not have to compromise with the heat flow requirements of the exchanger since both need not be satisfied at the same place. Therefore, materials of high neutron absorption cross sections, which could not be used in the core of a thermal reactor, could be used for the heat exchanger construction. Furthermore, the heat transfer problem is simpler, because, in addition to conduction, advantage can be taken of the fluid fuel in transferring heat.

2. Easy fuel handling and reprocessing Since the fluid fuel is circulated through a continuous loop, fission products and uranium and/or plutonium buildup could be removed from the reactor system by constant bleeding in such a manner that reprocessing could be accomplished at other sites. This continuous removal of fission products would improve the neutron economy and permit a higher percentage of fuel burnup. Radiation damage to the fuel would heal itself and only the radiation damage to the container need be of concern. In addition, there would be no down time while the reactor was being charged or discharged. Fuel element fabrication and canning would be eliminated, and complete decontamination would be unnecessary; thus the cooling time would be shorter, resulting in a smaller holdup of fuel material.

3. Safety and ease of control Any liquid-fuel reactor which expands with a temperature increase would have a negative temperature coefficient of reactivity. Such an effect tends to make the reactor self-regulating since the change in reactivity is immediate and is not delayed by any heat-transfer process. Changing the fuel concentration also changes the reactivity, so that the reactor could be controlled by this means. Furthermore, the hazard to the community is reduced since the fission products are not allowed to accumulate in the reactor.

On the other hand, several disadvantages are also inherent in circulating fluid-fuel reactors. These are listed below:

1. Unpredictable reactivity changes Sudden density or concentration changes in the fuel due to voids, such as bubbles, can affect the reactivity of the reactor.

2. Loss of delayed neutrons During that part of the cycle when the fuel is outside of the core region, delayed neutrons are lost through decay of their precursors.

3. External holdup of fissionable material This disadvantage is not as serious as it may seem since most solid-fuel reactors have a second set of fuel elements on hand for which a use tax is charged.

4. High radiation levels Hazardous levels of radiation will require remote maintenance of pumps, heat exchangers, and component piping.

5. Corrosion, erosion, and mass transfer problems Each reactor fuel system has particular corrosion problems, and in every case corrosion is usually the most difficult aspect which must be considered.

Several aqueous homogeneous reactor designs have been proposed and one design in particular (Homogeneous Reactor Experiment-1) went critical in 1957 (47). However, a distinct disadvantage of the aqueous solution reactor is that it cannot operate at the competitive high temperatures without high pressures. This is one advantage that a liquid-metal-fuel system has over the aqueous-fuel system. Some additional advantages are listed as follows:

1. Free from radiation damage Liquid-metal-fuel solutions are free from radiation damage and do not give off bubbles as commonly encountered with aqueous solutions.

2. Better heat-transfer properties Liquid metals are widely used because their heat-transfer properties are better than those of water.

3. Suitable for electromagnetic pumping If necessary, electromagnetic pumps can be used to circulate the molten metal system even though the efficiency may be low.

4. Diversity of reactor choice Molten-metal systems can be used for fast, intermediate, and thermal reactors provided the critical mass requirements are not excessive.

5. Economy Some suitable metals are cheaper than heavy water which was used in the Homogeneous Reactor Experiment-2 (HRE-II).

6. Useful by-products Some metal by-products formed by neutron capture, such as polonium from bismuth, may be valuable for other uses.

Again, as in the comparison of fluid fuels with solid fuels, liquid-metal systems have several disadvantages when compared to aqueous solutions. These are given below:

1. Low heat capacities The heat capacities of the various molten metals are less than that of water.

2. Higher densities Metal solutions have higher densities than water solutions.

3. Special pumping facilities Liquid metals require special, elaborate pumping techniques because of their corrosive nature.

4. Higher cross sections The absorption cross sections of the best metals are higher than that of heavy water and at most are only comparable with light water.

5. Economy Because of the limited solubility of uranium in a number of metals, enriched U-235 or U-233 must be used as a fuel. Some authors (60), however, consider this feature a distinct advantage, for in this case the reactor size can be made smaller than if natural uranium is used. In addition, if enriched materials are used, the drastic limitations on materials which arise from nuclear properties are not nearly so serious.

6. Moderator problems A moderator must be included in the design, if the reactor is to operate with thermal neutrons.

7. Difficulties with start-up The start-up of liquid-metal-fuel reactors is difficult from the standpoint that the metal fuel melts at a high temperature. This requires that the entire loop system must be molten before pumping can commence.

8. Corrosion problems Corrosion, erosion, and mass transfer problems are much more severe with liquid-metal systems, especially at the high operating temperatures, than with aqueous-fuel solutions.

Around the core of a liquid-metal-fueled, breeder reactor there would be a fertile blanket material. This blanket could be a solid or liquid dispersion of thorium-232 or uranium-238 in some metal such as bismuth. If a molten metal blanket were used, the continual reprocessing of the fertile material could be accomplished in a manner similar to the molten fuel in the core. The fertile material would be converted into a fissile material by the absorption of neutrons as illustrated by the following equations:

$$ {}_{90}Th^{232} + {}_{0}n^{1} \longrightarrow {}_{90}Th^{233} \xrightarrow[23.3\ m]{\beta^-} {}_{91}Pa^{233} \xrightarrow[27.4\ d]{\beta^-} {}_{92}U^{233} \qquad (1) $$

$$ {}_{92}U^{238} + {}_{0}n^{1} \longrightarrow {}_{92}U^{239} \xrightarrow[23.5\ m]{\beta^-} {}_{93}Np^{239} \xrightarrow[2.33\ d]{\beta^-} {}_{94}Pu^{239} \qquad (2) $$

Figure 1 illustrates a schematic diagram of a liquid-metal-fuel--liquid-metal-blanket, power-breeder reactor showing the principal cooling and processing streams. First, the main fuel stream is circulated through a sodium (or other liquid coolant) heat exchanger, the sodium carrying the

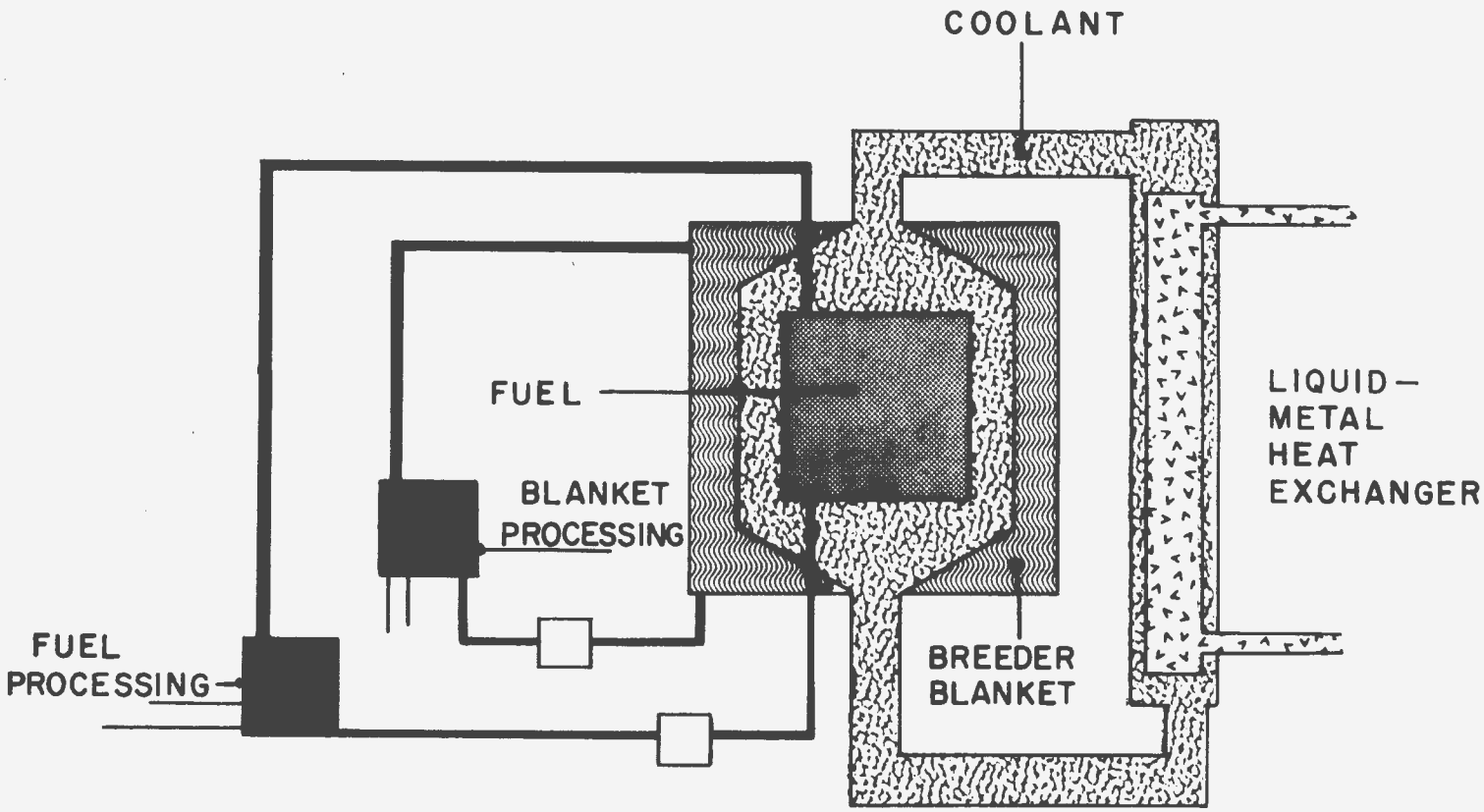

Figure 1. Schematic diagram of a liquid-metal-fuel--liquid-metal-breeder reactor for power production

heat to the steam boiler. The thorium and/or uranium bearing blanket stream is also circulated through a heat exchanger for cooling since up to 30 per cent of the total heat generation of the reactor can occur within the blanket material. A small part of the main fuel stream flows through the reprocessing system where the fission products are removed and additional fissile material is added. A second process stream flows from the blanket for removal of fissile fuel produced therein, as well as for fission product removal. Finally, volatile fission products could be carried away from the surface of the molten fuel by a helium stream.

The fact that the liquid-metal-fuel-reactor concept has been under development for about 15 years without the operation of a single design indicates that a number of technological difficulties still remain to be solved (32). Perhaps the biggest problem now facing the successful operation of such a reactor is the containment problem of a suitable fissile-fuel alloy, one which would not necessarily be an alloy of uranium and bismuth.

CORROSION BY LIQUID METALS

The use of liquid metals in nuclear technology introduces a corrosion problem unlike that commonly encountered in aqueous or gaseous media. The principal driving force is the chemical equilibrium between the solid and liquid metals. In general, corrosion may be defined as "the destruction by chemical or electrochemical agencies in contrast to erosion which means destruction by mechanical agencies." The above definition (50) denotes the transfer of electrons, but this is not always the method of attack by liquid metals. Therefore, this definition should be expanded to allow for the solution or solubility of a solid metal in a liquid metal in which no electron transfer is involved. That is, the essential first step in corrosion is one of transfer of atoms from the containing solid surface to the liquid metal.

Along these same lines, compatibility with a liquid metal can be defined as the extent to which components can co-exist in a certain environment without chemical or metallurgical change (3). Several different mechanisms reduce compatibilities. They act by either chemical or metallurgical change, or by a combination of the two. Decreased compatibility characterized by a loss of weight of the solid constituent in the system is often called "liquid metal corrosion."

Liquid metal corrosion in most instances is dependent upon the solubility rate and the extent of solubility of the solid metal in the liquid metal. Often, however, solubility and diffusion barriers, in the form of surface intermetallic compounds and metal oxide or nitride films, may be developed from the metal components, or from impurities present in the

system. In addition, temperature gradients and multimetallic systems can cause an increase in the amount of attack over that expected. Each of these factors can combine or act separately to complicate the determination of the solubility rate or the attainment of the solubility limit.

Types of Corrosion Attack

According to Brasunas (6), corrosive attack by a liquid metal in contact with a solid metal can be classified as a combination of one or more of seven basic types of attack. Since alloys behave in a manner different from pure metals, the types of liquid-metal attack are arranged in the following categories.

Pure metals

1. Solution of solid metal with the liquid metal may occur as
   a. uniform simple solution,
   b. intergranular solution, or penetration of liquid metal into grain boundaries because of surface tension phenomena, or
   c. crystalline facet development caused by different solubility rates in various crystal directions.
2. The liquid-metal atoms may diffuse uniformly or intergranularly into the solid-metal lattice, which may or may not result in a phase transformation.
3. An intermetallic compound layer may be formed on the surface.
4. Mass transfer of three various types may occur:
   a. isothermal mass transfer caused by concentration gradients,
   b. thermal-gradient mass transfer,

c. mass transfer by energy gradient; that is, a reorientation of the surface contour to one of lower energy state.

Alloys

5. One or more alloy constituents may be leached from the surface of the alloy because of selective solution, which can result in phase transformations and/or subsurface voids within the grains or along grain boundaries.

6. Inward diffusion of liquid-metal atoms and interaction with the alloy components may cause subsurface precipitation of an intermetallic compound.

Impurities

7. Since impurities are almost impossible to exclude, they may form simple or complex substances on the metal surface or beneath it which can stimulate or suppress interaction. Familiar examples are oxides and nitrides which have frequently been detected on metal surfaces.

Each of these seven types of liquid-metal corrosion attack will now be described in detail and illustrated by photomicrographs, which were furnished through the courtesy of Oak Ridge National Laboratory.

The first example of liquid-metal corrosion to be considered is uniform-solution-type attack. Figure 2a illustrates the even removal of titanium metal from the surface exposed to molten lead at 1000°C for 40 hours. Uniform solution causes a significant weight loss to the container metal, but metallographic examination shows practically no signs of attack other than the somewhat wavy surface or interface contour that is shown.

In fact, the presence of a rough surface generally indicates solution-type attack.

If phase diagrams of all the liquid-metal--solid-metal systems were known, an ascertainment could be made of the amount of attack that would occur in a static system as a result of uniform solution. This could be accomplished by examination of the solubility limit of the solid metal in the liquid metal at the operating test temperature. However, there would be no conception of the rate at which the solubility limit would be reached, since this rate can be greatly influenced by other variables such as impurities in the system.

Intergranular corrosion attack (Type 1b) is illustrated in Figure 2b for the case of liquid lead contained in nickel for 40 hours at 1000°C. Comparison of this photomicrograph with Figure 5b, which depicts the selective removal of nickel from type 304 stainless steel by lithium penetrating the grain boundaries, indicates that intergranular corrosion attack is characterized by chunks of solid metal surrounded by the liquid metal. Note that intergranular attack and solution attack work together. In all types of corrosion attack, solution of the solid metal by the liquid metal usually occurs.

The development of crystal facets is shown as Type 1c attack in Figure 2c. Polarized light was used to bring out the crystallographic facets on a beryllium sample after exposure to liquid lead at 1000°C for 40 hours. This type of solution attack occurs at the interface between the liquid and solid metals as crystalline projections extending from the solid metal and sometimes overlapping the boundary of the liquid metal.

Type 2 corrosion attack, diffusion of a liquid metal into a solid metal, occurs when sodium is contained in OFHC grade copper at 815°C. The photomicrograph in Figure 2d shows this penetration and the resultant intermetallic phase which is blue-gray in color. A simple bend test showed that the entire cross section of the copper was embrittled. After exposure to the air for one year, a stainless steel specimen, which had been tested with sodium at 1000°C for 400 hours, became coated with a Na_2CO_3 layer--further evidence of sodium penetration (6).

Intermetallic compound formation (Type 3) was observed when liquid lead and vanadium were in contact with each other for 100 hours at 1000°C. This phenomenon is shown in Figure 3a as the narrow horizontal band between the original two constituents. The diamond shaped impressions were made during a check on the hardness. The smallest diamond impressions appear in the intermetallic phase, indicating a harder composition. This is usually a sure sign of intermetallic compound formation and a useful tool of examination if the band is wide enough for hardness measurements.

The next type of liquid-metal corrosion to be discussed is isothermal mass transfer (Type 4a), also referred to as dissimilar-metal or concentration-gradient mass transfer. The best example obtained by Brasunas and Manly (6, 50) at Oak Ridge National Laboratory is the interalloying between molybdenum and nickel shown in Figure 3b. In this test conducted at 1000°C the molybdenum sample was in contact with sodium contained in a nickel capsule. After 100 hours, enough nickel had migrated through the sodium and alloyed onto the molybdenum surface to produce a Ni-Mo intermetallic compound, indicated by the sizes of the diamond hardness impres-

Figure 2. Types of liquid-metal corrosion attack (reduced 33 1/3 per cent)

a. Type 1a: uniform solution attack--even removal of titanium metal from the surface exposed to liquid lead at 1000°C for 40 hours (250X, 0.5 % HF etch)

b. Type 1b: intergranular attack--liquid lead contained in nickel at 1000°C for 40 hours (100X)

c. Type 1c: crystalline facet development--beryllium sample after exposure to liquid lead at 1000°C for 40 hours (250X, polarized light)

d. Type 2: inward diffusion into solid-metal lattice by liquid-metal atoms--OFHC grade copper in sodium at 815°C (750X)

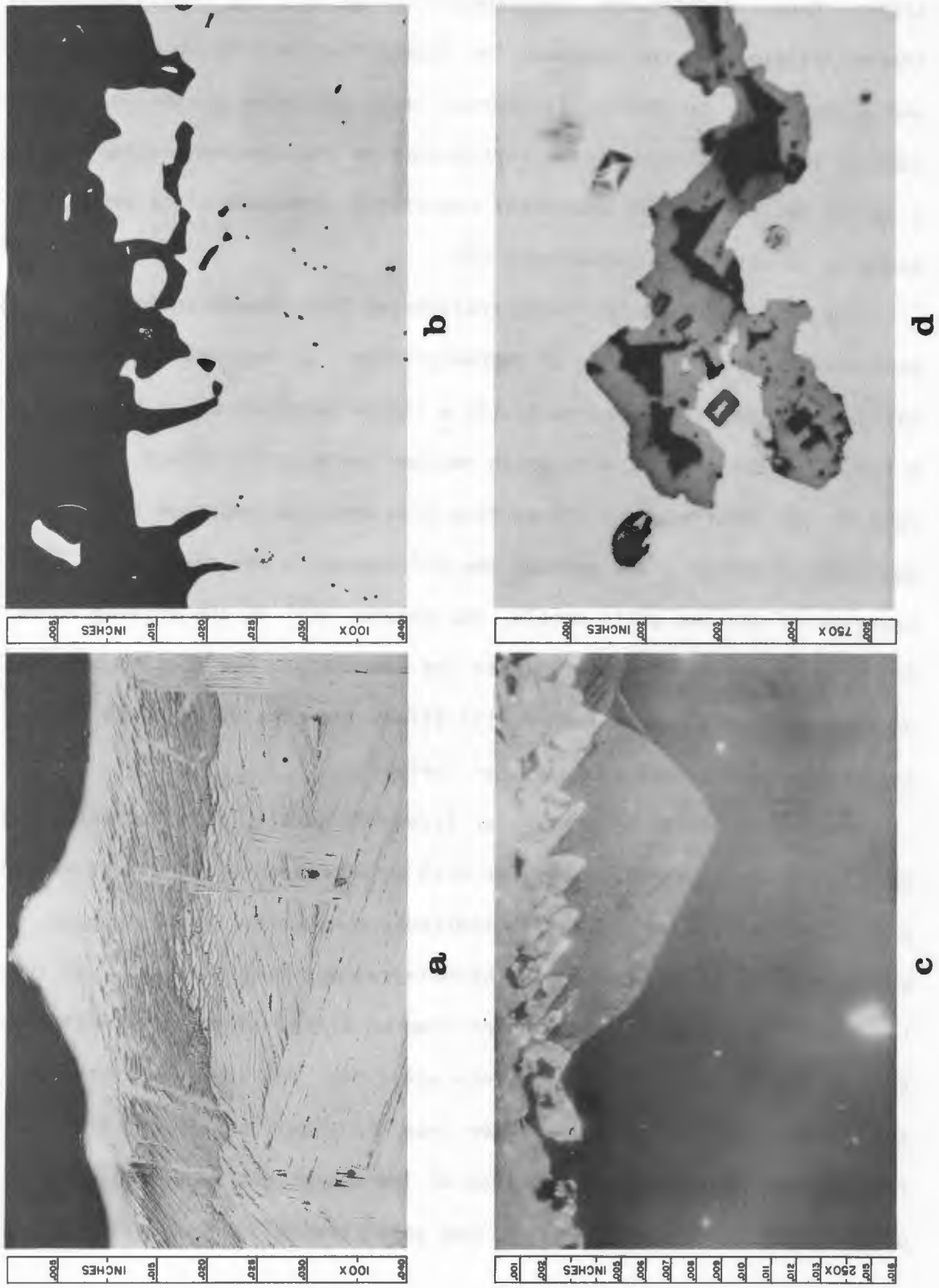
a
100X
INCHES
b
100X
INCHES
c
250X
INCHES
d
750X
INCHES

sions. This indicates the importance of using only two component-tests, thereby eliminating the tendency for interdiffusion between the capsule and a specimen. In static, isothermal tests employing a specimen, the capsule material should always be the same as the specimen, unless such a system is intended for practical operation. Brasunas cites several examples to verify this statement (6).

The driving force for concentration-gradient mass transfer is simply explained by the principles of thermodynamics. If two metals that alloy with one another are in contact with a liquid metal in which both have a finite solubility but with which neither forms solid alloys, alloys form at the interfaces as the surface free energies decrease to their equilibrium values. The greater the difference in the chemical free energies of the two solid metals, the greater will be the driving force for mass transfer. Therefore, both the temperature and the solubilities of the two metals in each other will affect the rate of reaction, increasing with an increase in either variable.

Thermal-gradient mass transfer (Type 4b) results from the existence of a temperature gradient together with an appreciable solubility within a liquid-metal system. Figure 4 indicates the various steps through which metallic atoms must go in thermal-gradient mass transfer. If there is selective removal of one element from an alloy, these atoms must diffuse to the surface and then go into solution. The atoms then travel through the stagnant boundary layer into the liquid stream and are finally carried to the cold portion of the system where nucleation will occur. Either crystal growth follows until the solidified material

reaches a stable size and drops from the liquid,or the atoms supersaturate close to the wall, diffuse through the boundary layer, and then nucleate on the metallic container wall or diffuse into it to commence plug formation. An example of crystalline plug formation is shown in Figure 3c for a type 410 stainless steel thermal-convection loop operated at 1000°C for 40 hours with lithium.

Thermal-gradient mass transfer is usually the most damaging type of liquid-metal corrosion to occur, if the materials and conditions are right for it to happen. And even though the solubility of the container material in the liquid metal may be very low, over a period of time large amounts of material can be transformed. Long before any weakening of the container could result, the material transferred would have begun to form a plug, reducing and eventually stopping flow. Prevention of this plugging, through proper selection of materials, corrosion inhibitors, and perhaps continuous corrosion product removal is of great importance in the successful operation of a liquid-metal system.

Energy-gradient mass transfer (Type 4c) as defined by Brasunas (6) may be illustrated by Figure 3d showing the surface of type 316 stainless steel as recovered from a sodium bath after 400 hours at 1000°C. One should note the crystal face developments on certain grains, an indication that energy-gradient mass transfer has occurred. The classification of this type of mass transfer by Brasunas is really a misnomer since in all types of liquid-metal corrosion an energy gradient is present, else corrosion attack would not occur. However, in this case such action is not accompanied by any perceptible weight changes since the surface layer is simply rearranged to a more stable configuration.

Figure 3. Types of liquid-metal corrosion attack (reduced 33 1/3 per cent)

a. Type 3: intermetallic compound formation--vanadium specimen immersed in liquid lead at 1000°C for 100 hours (200X, KOH + $K_3Fe(CN)_6$ etch)

b. Type 4a: concentration-gradient mass transfer--molybdenum surface after exposure to sodium in a nickel capsule at 1000°C for 400 hours (500X)

c. Type 4b: thermal-gradient mass transfer--crystalline plug formation in Armco iron capsule with type 416 stainless steel tested in lithium (5X)

d. Type 4c: energy-gradient mass transfer--surface of type 316 stainless steel as recovered from a sodium bath after 400 hours at 1000°C (500X)

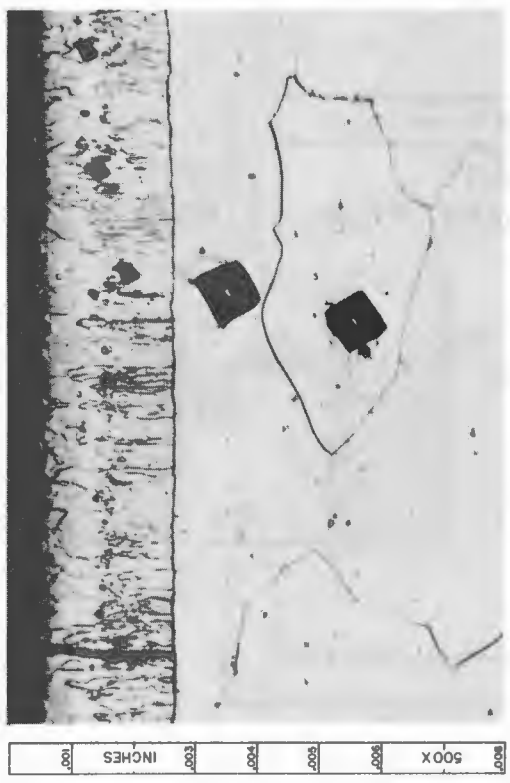

b

d

a

c

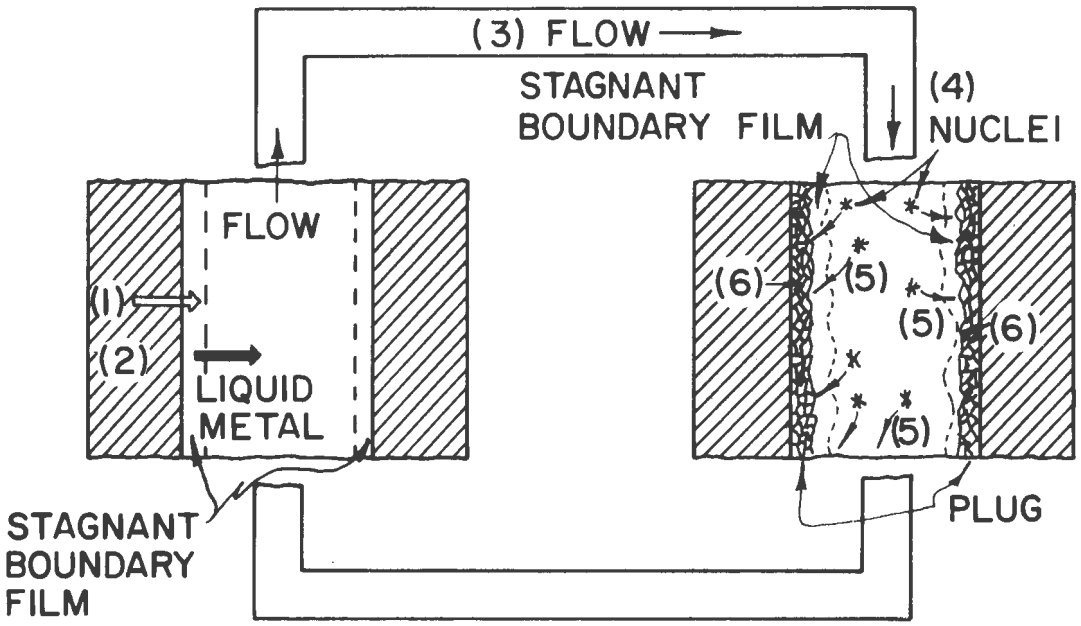

Figure 4. Mechanism of thermal-gradient mass transfer

Selective solution (Type 5) of one constituent (nickel) from type 304 stainless steel into a lithium bath is shown in Figure 5a. As shown, contact with the lithium for 400 hours at 1000°C resulted in a phase transformation at the surface and in the neighboring grain boundaries. This phenomenon is quite common in systems where an alloy is used to contain the liquid metal. Another form of preferential leaching is the decarburizing action by lithium shown in Figure 5b. In this test, lithium having a low carbon content was contained in type 430 stainless steel for 40 hours at 1000°C. By the process of simple solution, carbon was drawn from the surface of the stainless steel to equalize the affinity of the lithium. Further explanation of this type of attack is found in a paper by Brasunas (8).

Figure 5c gives evidence of inward penetration of liquid-metal atoms to cause subsurface precipitation of an unknown phase (Type 6 corrosion attack). Here type 316 stainless steel was exposed to 1000°C sodium for 40 hours. Often times it is difficult to distinguish this mode of liquid-metal corrosion attack from intergranular attack. However, the presence of the black spots within the individual grains near the surface indicates that the attack was other than intergranular.

The last type of corrosion attack to be discussed is that attributed primarily to impurities in the liquid metal. Oxygen, nitrogen, and carbon are the most common impurities found in liquid metals and are practically impossible to eliminate completely. At times their presence can exert an appreciable influence on the rate of attack. As an illustration, the carburization, after a long exposure period, of type 347 stainless steel

Figure 5. Types of liquid-metal corrosion attack (reduced 33 1/3 per cent)

a. Type 5: selective solution attack--selective leaching of nickel from type 304 stainless steel by lithium at 1000°C for 400 hours resulting in phase transformation (250X)

b. Type 5: decarburization--type 430 stainless steel after 40 hours in lithium at 1000°C (750X)

c. Type 6: inward diffusion of liquid-metal atoms causing subsurface precipitation of an intermetallic compound--type 316 stainless steel exposed to sodium at 1000°C for 40 hours (250X)

d. Type 7: solid-metal contamination by impurities in liquid metal--carburization of type 347 stainless steel by sodium contaminated with carbon after long time service (250X)

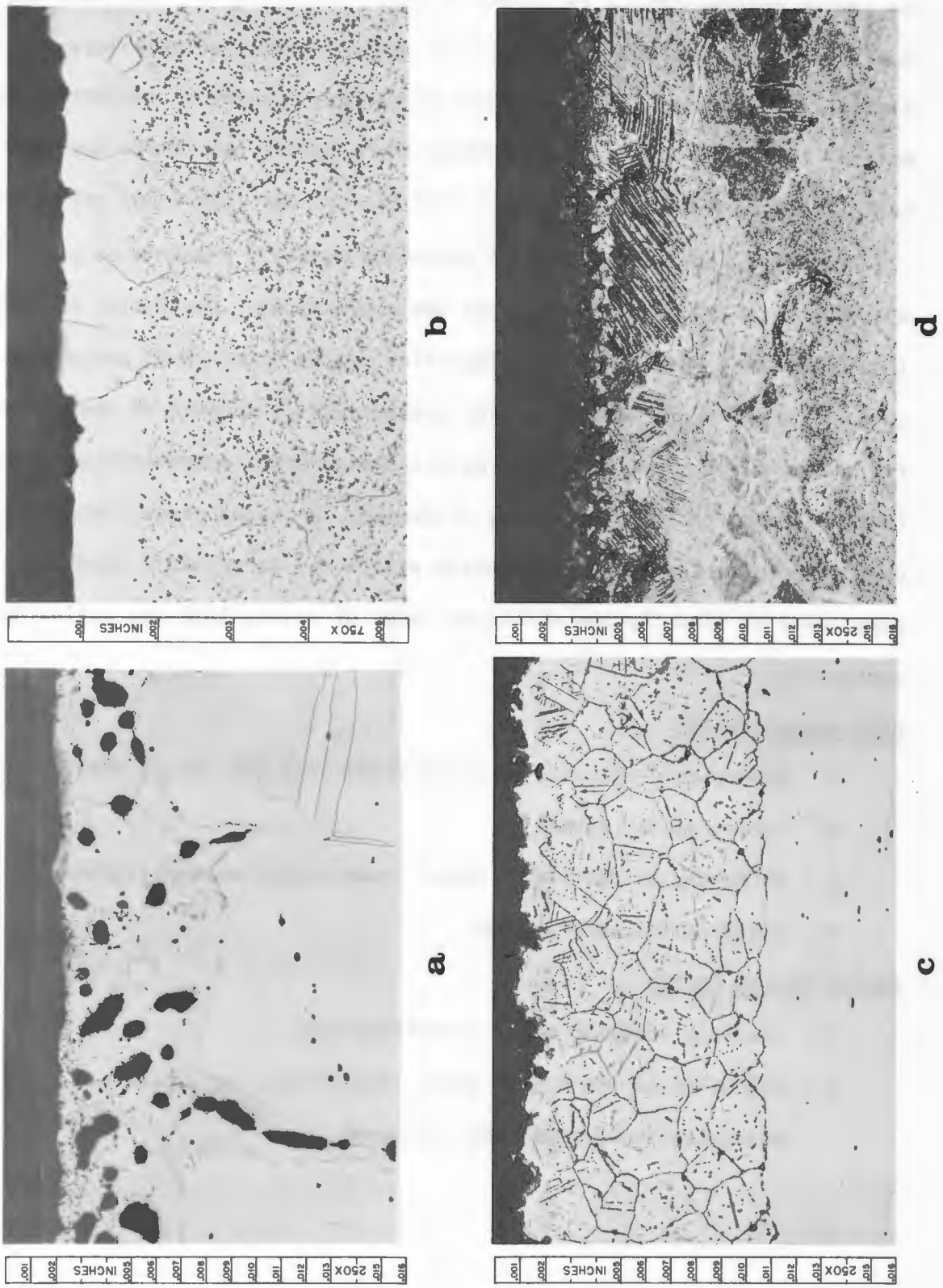
a
b
c
d
250X
750X
INCHES

by sodium contaminated with carbon is shown in Figure 5d. On the other hand, oxide and nitride films can also act as corrosion inhibitors. In liquid lead the oxygen contamination decreases the rate of corrosion since most of the constituents of high-temperature alloys can reduce the lead oxide and form a diffusion barrier film between the liquid and solid metals.

Quite probably, liquid-metal corrosion actually encountered would be a complex combination of several of the above types. Obviously, changes in the physical and mechanical properties of the metals will accompany changes in the chemical composition and physical structure of the surface regions affected. Hence, simple weight change measurements are unsatisfactory in determining the amount of damage. From the above discussions on the seven basic types of corrosion attack, it is possible through experience to classify the different types of attack into the following categories:

<u>High damage factor</u>

1. appreciable solution of solid metal into the liquid metal,
2. intergranular attack,
3. diffusion of the liquid metal inward--causing embrittlement,
4. appreciable mass transfer.

<u>Medium damage factor</u>

1. leaching--causing phase transformation,
2. diffusion of the liquid metal inward--causing subsurface precipitation without embrittlement.

Low damage factor

1. leaching--decarburization,
2. impurities--surface films.

Evaluation of the Degree of Corrosion Attack

The quantitative determination of the extent of corrosion attack which has occurred is always a problem. The field of liquid-metal corrosion is particularly difficult in this respect, and the problem deserves careful study.

A careful evaluation of the material to be used in contact with a given molten metal should include consideration of the following:

1. dimension changes of the container or specimen metal,
2. weight changes of the specimen,
3. changes in composition of the molten metal,
4. changes in the chemical composition of the metal surface by analytical or spectrographical analysis,
5. changes in crystal structure of the metal surface by X-ray or electron diffraction, and
6. nature and depth of attack as determined by careful metallographical study.

Dimensional and weight changes can be quite useful in determining a rate of corrosion attack if a specimen is used in the corrosion test. But, it may be difficult to obtain accurate measurements because of excess liquid metal which cannot be easily removed. Observation of the types of corrosive attack illustrated previously indicates that conven-

tional weight-change measurements may be unsatisfactory since they can actually be misleading. Weight-loss measurements would only be valid in the instance of Type Ia attack, where uniform solution has occurred. Weight-change measurements of intergranularly attacked specimens cannot indicate the depth of such attack. A small weight loss due to intergranular attack could be much more damaging than a larger weight loss representing uniform attack. Thus, metallographical examination must be employed.

The last item mentioned is one of the most important tools in evaluating corrosion attack. In some cases, it may be advisable to also determine the hardness changes or gradients as a means of corroborating the metallographical analysis. Simple bend tests are often useful in determining possible embrittlement of the material.

There are several variables which affect liquid-metal corrosion (2, 50). It is important to know how each variable influences the degree of attack since each in turn affects the evaluation of the corrosion attack. These nine variables as listed by Manly (50) appear below:

1. Temperature
2. Temperature gradient
3. Cyclic temperature fluctuation
4. Surface area to volume ratio
5. Purity of liquid metal
6. Flow velocity or Reynolds number
7. Surface condition of container material
8. The number of materials in contact with the same liquid metal

9. Condition of the container material, such as the presence of a grain-boundary precipitate, the presence of a second phase, the state of stress of the material, and the grain size.

In all liquid-metal corrosion tests, these variables must be considered and controlled to obtain information that will be useful in the overall understanding of the suitability of solid metals as containers for various liquid metals. For that reason, each variable should be examined more closely to fully understand its effect on the corrosion process.

Temperature is probably the most important factor in liquid-metal corrosion. Higher temperatures result in increased solubility of the solid metal in the liquid metal and in greater corrosive effects. Also, as the temperature increases, the diffusion rate increases, a significant factor in certain types of liquid-metal corrosion.

Cyclic temperature fluctuations can also increase the corrosion rate in liquid-metal--solid-metal systems and may cause erroneous static-corrosion results if neglected. In a supposedly isothermal condition in a poorly controlled furnace, the liquid-metal--solid-metal interface temperature can fluctuate quite appreciably around a set value. During the high temperature part of the fluctuation more material goes into solution, and subsequently, at the low temperature part of the fluctuation the liquid becomes supersaturated. The excess may precipitate in the bulk liquid, deposit on container walls as dendrites, or form a uniform layer on the walls. Thus greater amounts of temperature fluctuation about a mean set point may result in a greater degree of corrosion. The fluctuation should be kept less than $\pm 5^{\circ}C$.

The ratio of the exposed area of the solid material to the volume of the liquid metal will determine the rate and amount of corrosion of the solid-metal container in a static system. The container metal will corrode sufficiently to saturate the liquid metal at the operating temperature; thus, as the ratio of surface area to volume decreases, the amount of corrosion increases.

The purity of the liquid metal has important effects on corrosion, especially the rate at which the solubility limit is reached. Purity can also markedly affect the wetting tendencies of the liquid metal for the solid container. The oxygen content of sodium, for example, significantly influences the corrosion of refractory metals.

The flow velocity or Reynolds number is only important in a forced-circulation loop, since increased flow velocity decreases the thickness of the lamellar layer of stagnant liquid metal in the hot and cold legs of the loop. Thus, when metal atoms pass from the hot leg to the cold leg, the diffusion paths are shorter in these two regions. And, by Equation 9 (see page 34) the corrosion rate, R, would increase.

The condition of the surface of the container material is a less-important variable as long as the surface is free of films. However, if there is a film on the surface, it can greatly accelerate or retard the corrosion rate. But after equilibrium is reached between the liquid metal and the solid metal, the surface conditions should have little or no effect. Its principle effect is to change the rate at which the liquid metal becomes saturated. The degree of roughness of the surface will affect this rate since the greater the surface area that is exposed, the faster the liquid becomes saturated.

Concentration-gradient mass transfer is likely to occur when two or more solid metals are in contact with the liquid metal or when the system consists of three or more constituents, such as a molten-fuel alloy contained in a metal (pure or alloy) container. In this case, equilibrium is achieved only when the chemical potential of each component in any given phase is equal to its chemical component in every other phase. Therefore, the components will naturally tend to redistribute themselves between the phases of the system until equilibrium of chemical potentials is attained. This driving force results in a decrease of the free energy of the system.

The condition of the solid material, with respect to grain size and other variables, must be considered. The wettability of individual grains and the wettability of grain boundaries may differ, thus determining whether corrosion attack will be general or intergranular. Also, the grain boundaries can greatly increase or decrease corrosion attack.

Rate-Controlling Processes of the Corrosion Mechanisms

The rates of the various corrosion mechanisms depend in part on the structure at the solid-liquid interface. However, very little is known about the factors which control this rate of corrosion. The principle driving force is known to be the chemical equilibrium between the solid and liquid metals.

The chief concern of the engineer in the design of a liquid-metal system, from the corrosion aspect, is the amount of attack which the container material will undergo. In the present section the equations for the corrosion rates will be presented for two cases of liquid-metal corrosion.

In a static isothermal assembly, the corrosion rate for uniform-solution-type attack can be determined by classical theory (68) involving the solution-rate constant α . Taking the case of a pure liquid metal contained in a pure metal capsule, the net rate of entry of solid atoms into the solution, dN/dt, is given by

$$dN/dt = k_f A n_a - k_b A n \tag{3}$$

where n_a is the number of atoms per unit area of liquid-solid interface, A is the area of the interface, and n is the concentration of the solute atoms of the liquid metal. The rate constants k_f and k_b represent the frequency at which solute atoms enter the liquid metal, or reprecipitate on the solid metal surface, respectively. Equation 3 would be equal to zero at equilibrium; hence

$$k_f n_a = k_b n_o \tag{4}$$

where n_o is the concentration of solid atoms in the liquid metal at saturation. Solving Equation 4 for k_b and letting N = nV, where V is the volume of liquid metal, yields

$$d(nV)/dt = k_f n_a A - (nAk_f n_a)/no \tag{5a}$$

or

$$dn/dt = k_f n_a (A/V) \cdot [1 - n/n_o]. \tag{5b}$$

Integration of Equation 5b, assuming n = 0 at time t = 0, gives the variation of container metal concentration in the melt with time,

$$n/n_o = 1 - \exp[-k_f(n_a/n_o)(A/V)]t. \quad (6)$$

Given a system at constant temperature, $k_f(n_a/n_o)$ becomes fixed; this reduces Equation 6 to the familiar equation (26)

$$n/n_o = 1 - \exp[-\alpha (A/V)t]. \quad (7)$$

Determining the rate at which the solid metal goes into solution by Equation 7 involves the knowledge of the parameters α and n_o as well as the geometrical values of A and V. The experimental determination of α can best be accomplished by measuring n as a function of t usually by the use of radioactive tracers. The initial slope of the curve according to Equation 7 is $\alpha(A/V)$.

It has been found that the values of α can be classified into two classes, depending upon whether the rate controlling process is solution of the solid metal or diffusion of the dissolved metal through the boundary layer of the fluid. These two cases are illustrated in Figure 6 for mercury in iron and sodium in iron. Weeks and Klamut (69) state that for most liquid metals, it has been found that the diffusion-limited mechanism is of predominant importance (Figure 6a). In this case it is assumed that the boundary layer of the liquid in contact with the solid becomes quickly saturated with solute. The net result is that the transfer of material from the solid to the dissolved state is the rate at which the container metal moves by diffusion through this surface film into the main body of the melt. For the second case (Figure 6b), the diffusion step is fast compared to the initial rate of solution, so that the liquid boundary layer is not saturated. Excellent discussions of these two types of liquid-

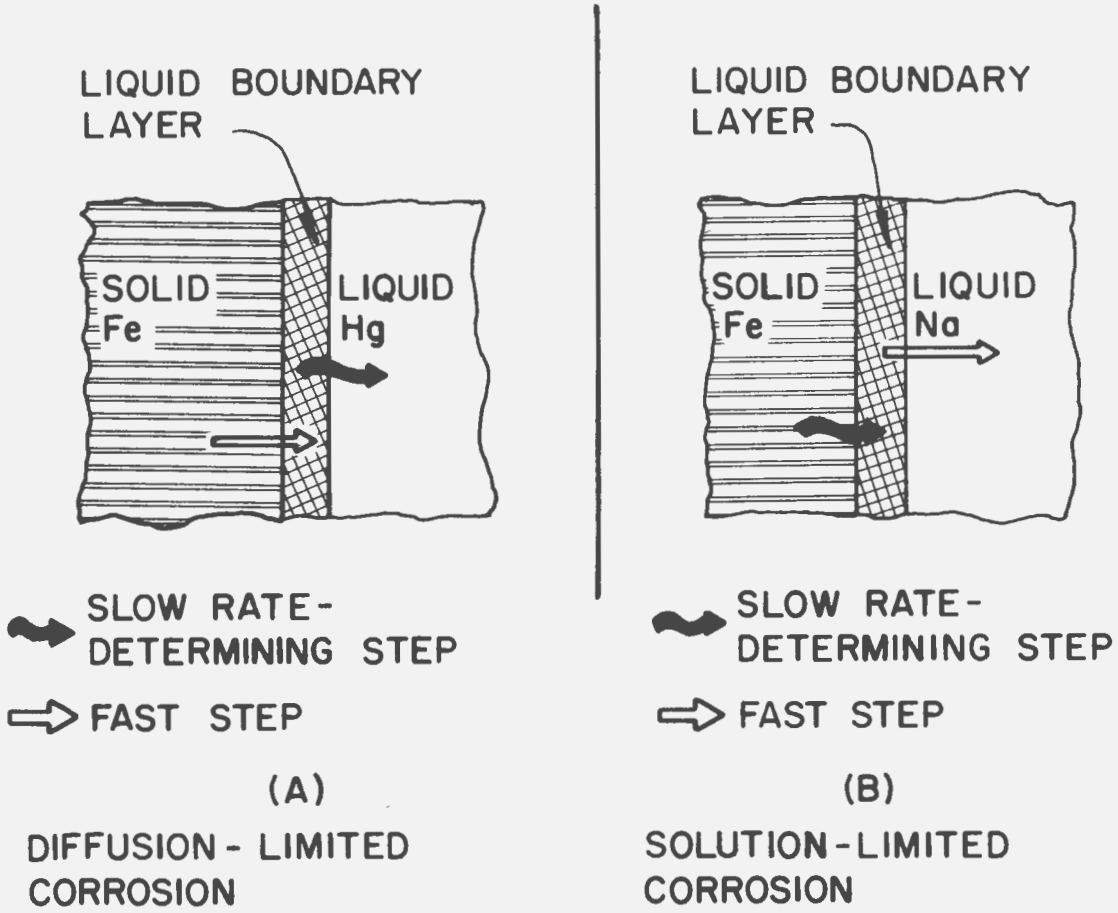

Figure 6. Dissolution of a solid metal into a liquid metal

metal-corrosion kinetics are found in papers by Weeks and Gurinsky (68), Weeks and Klamut (69), Epstein (25, 26), and Finniston (27).

When a temperature gradient exists, such as in the case of a liquid-metal-loop system, the difference in solubility of the dissolved metal in the liquid metal in the hot and cold zones of the system gives rise to thermal-gradient mass transfer. This difference in solubility is the driving force for thermal-gradient mass transfer, and a check of the phase diagram of the two metals to be used in such a system will give an indication of this driving force. However, no information concerning the rate of the process can be determined from the phase diagram. Finniston (27) has stated that D. H. Kerridge and J. W. Taylor et al. have shown that of two rate-controlling steps, solution and crystallization, the former is slower and therefore the rate-determining factor. These results are stated only for the systems of copper-bismuth and iron-bismuth, and thus, they may not apply to all systems since any of the six processes involved in thermal-gradient mass transfer (Figure 4) could be rate-controlling for a given system.

For the special case of a temperature-gradient mass transfer system in a closed circular loop, Epstein (26) has derived an expression for the mass transfer rate based on heat-transfer analogy. Referring to Figure 3b, when the solution rate is the rate-controlling factor of mass transfer, the average rate of solution ($g/cm^2/sec$) of the hot leg of the loop is given as

$$R_{\bar{T} + \Delta T/2} = - (\alpha /2) \ (dS^\circ/dT) \ \Delta T \qquad (8)$$

where α is the solution-rate constant (cm/sec) at the mean loop temperature, and $dS°/dT$ is the mean temperature coefficient of solubility ($g/cm^3 °K$) over the temperature gradient $\Delta T(°K)$.

However, if diffusion is the rate-controlling step (Figure 6a), then

$$R_{\bar{T} + \Delta T/2} = -0.023 \, (D/d) \, (vd/\nu_o)^{0.8} \, (\nu_o/D)^{0.4} \, (dS°/dt) \, \Delta T \quad (9)$$

where D is the diffusion coefficient (cm/sec) of solute in solvent at the mean hot leg temperature, d is the inside diameter of the loop, v is the flow velocity (cm/sec) in the loop, and ν_o is the kinematic viscosity of the liquid.

It must be pointed out that these equations were developed for the case of a pure liquid metal contained within a pure metal container wherein the method of corrosion attack is primarily that of uniform solution (Type Ia). In the present study with liquid alloys, these equations would not be applicable except in the case of the eutectic compositions at which alloys supposedly act as pure metals.

At present only the rate controlling processes for the two types of liquid-metal corrosion described above have been determined and then only to the degree mentioned. The rate controlling steps for the other corrosion mechanisms are being studied, but these rates are more difficult to ascertain because of the fact that these other types of corrosion attack are not encountered as often as uniform solution and thermal-gradient mass transfer.

Corrosion Attack Inhibitors

In the first part of this section it was mentioned that oxygen, nitrogen, and other impurities in a liquid metal could form diffusion barrier films between the solid metal and the liquid, and thus possibly promote or inhibit liquid-metal corrosion.

On the one hand, if it can actually be determined that active impurities such as oxygen, nitrogen, or carbon promote corrosion, the best inhibition would simply involve removal of the contaminates from the reaction. This is done in a variety of ways such as the well-known "cold-trapping" of sodium to remove dissolved oxygen by precipitation, oxygen-gettering by active solid metals (Ti, Y, Zr) or by active soluble getters (Ca, Si, Mg, Ba), and the scavenging of carbon and nitrogen by titanium, yttrium, or zirconium. If, however, one or more of these active impurities is known to inhibit corrosion by liquid metals, then the problem becomes that of trying to keep the liquid metal saturated with the inhibitor.

In a static isothermal system, where there is a solid in contact with a liquid metal, the fluid tends to become partially saturated with the solid after a certain amount of time, and further reaction is hampered since the driving force is cancelled. For such systems, an effective method for inhibiting corrosion is the presaturation of the liquid at the operating temperature with the material to which it must be exposed.

Inhibition of solution corrosion is classified in two categories, depending upon whether the inhibition requires a reduction in the solid-metal solubility or the formation of an impervious barrier at the solid-

liquid metal interface. The first type of corrosion inhibition is called thermodynamic inhibition and was described in the preceding paragraph. The latter category of solution corrosion inhibition is called kinetic inhibition. The type of inhibition mechanism results from the precipitation of the dissolved inhibitor on the solid-metal surface by dissimilar metal mass transfer, followed by a reaction of the precipitated inhibitor with the solid metal to form an adherent surface film that is inert and hopefully impervious to the liquid metal. Precipitation of the inhibitor alone is not sufficient unless the reaction film is formed (69).

For example, zirconium additions to liquid lead, lead-bismuth mixtures, bismuth, or mercury inhibit corrosion of iron from steels by the formation of adherent deposits of ZrN and/or ZrC on the steel surface (69, 27). Zirconium will also deposit on pure iron from liquid bismuth to help reduce, but not prevent, mass transfer. The effectiveness of the inhibitor has been shown to be directly related to the activity of the nitrogen and carbon in the steel. Similarly, titanium also has a tendency to form TiN or TiC films on steel surfaces.

Static solution-rate measurements have also been made with various systems to demonstrate the effect of inhibitors on the solution-rate constant α (Equation 7). In the presence of inhibitors α decreased with time, presumably resulting from simultaneous dissolution and formation of the inhibiting films (68, 69). Such a decrease in α results in a lower number of container-metal atoms entering the fluid. Ideally, no corrosion attack with time would occur only if α was equal to zero.

The simple stratagem of presaturating the liquid metal before contacting it with the container material will not readily work for the case

of a dynamic loop system. In these cases there is always a high-temperature region and a low-temperature region, relatively speaking. In the hot region the liquid can become saturated with the solute, but when it reaches the cold zone there will tend to be precipitation of the solute. On the next passage through the hot zone the liquid will tend to saturate again. Thus, it is quite clear that in this case presaturation at either zone would be ineffective as the only means of mass transfer inhibition. Since thermodynamic inhibition has not been demonstrated in flowing systems with a usefully-large temperature differential, it has been necessary to resort to a combination of kinetic and thermodynamic inhibitors. Protective film formation and stabilization of cold-leg supersaturations by crystal growth or nucleation inhibitors may greatly reduce the corrosion rate (68). These results have been achieved exclusively in experiments with small temperature differentials, and practical use requires a temperature, and therefore solubility differential, too large for precipitation control. Hence, in the practical sense the effectiveness of inhibition becomes a function of the relative rates of film formation and container material dissolution.

Although one key to the problem of corrosion inhibition is to find a solid-liquid metal system in which there is little or no differential solubility over the operating range of temperature, the main effort has been to find practical containment metals which form no solid alloys with liquid metals. Most useful solid metals are the high melting point, body-centered cubic metals: iron, cobalt, niobium, tantalum, molybdenum, tungsten, and their alloys. Such selection of various container materials will be discussed further in the section titled Discussion of the Problem.

More discussion of inhibition of liquid-metal corrosion can be found in papers by Taylor (61) and Finniston (27). Inhibitors which give varying degrees of protection and their mechanisms are mentioned by Weeks et al. (71), Weeks and Gurinsky (68), Weeks and Klamut (70), and Kammerer et al. (43). In addition these references contain excellent bibliographies which list previous work done in this area.

OBJECT OF THE INVESTIGATION

The goal of the research described in this report is an investigation of the compatibility of several suitable molten fuel and blanket alloys with various containment materials. The work is intended to serve as a basis from which engineering scale studies involving liquid-metal fuels could be made. Among some of the problems encountered in these compatibility studies are the selection of suitable molten fertile and fuel alloys and the selection of adequate container metals. Originally, it had been planned to examine a number of alloy systems in three or four container materials using isothermal, static tests, and then to incorporate one of the successful molten systems into an operating dynamic test loop. However, it was discovered that the time involved for the preparation of a dynamic loop after completion of the compatibility studies would be excessive. As a result, the scope of this investigation was narrowed, and the idea of operating a circulating loop was rejected. The work presented is limited to static and dynamic capsule tests of several molten fuel and fertile alloy systems in five container metals with recommendations for further study of several systems in dynamic test loops. Each of the various systems studied will be classified according to the type of corrosion which occurred. These various types of corrosion have been discussed in the previous section of this report.

It is hoped that the information resulting from these tests will aid in the design and operation of engineering scale liquid-metal-fuel systems.

DISCUSSION OF THE PROBLEM

Containment of molten alloys at high temperatures is a major problem in the successful operation of a liquid-metal-fuel reactor. The containment problem when using sodium or a sodium-potassium alloy differs remarkably from that involving uranium and thorium alloys because of the high uranium and thorium concentration and the comparatively high temperatures required to maintain the molten state. Therefore, it was necessary to develop and test new container materials--those which would not only withstand the high temperatures but would also resist mass transfer, erosion, and corrosion by the various feasible fuel alloys.

Several criteria are necessary, first of all, for the selection of container materials and, secondly, for the various molten fuel systems which must be contained (41). Selection of the container metals and molten fuels are described in more detail in the following two sections.

Selection of the Containment Metals

The corrosion tests conducted in this investigation were restricted to the three metals: niobium, tantalum, or yttrium--with the exception of several static tests in Inconel and an alloy of 90 % tantalum-10 % tungsten by weight. These were the materials which had been suggested by Fisher and Fullhart (28, 29) as promising container materials for molten alloys of uranium and thorium. The other refractory metals, molybdenum and tungsten, although recommended for liquid-metal containment (6, 24, 38, 45, 48), were not used because of the difficulties which would be encountered in the fabrication and welding of capsules (12). Capsule

tests using specimens were not conducted, thus eliminating the possibility of concentration-gradient mass transfer (Type 4a attack) occurring when three dissimilar metals are present in one system.

It is necessary to consider the following properties of a proposed containment material:

1. Melting point The melting point of the container material should be relatively higher than that of the liquid-metal system it is to contain. The containment metals used in this investigation all melt above 1500°C.

2. Solubility The material which is to be used as a container for liquid metals should, ideally, be one which does not form compounds, liquid solutions, or solid solutions with the liquid metal at temperatures between the melting points of the container and the liquid metal. The phase diagram for such a system would look like that shown in Figure 7.

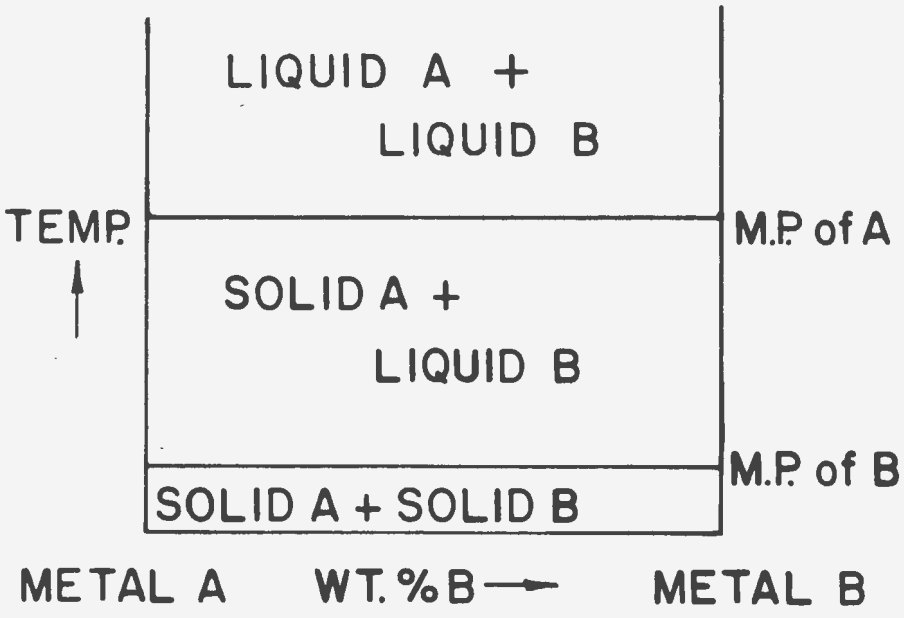

Figure 7. Ideal phase diagram for solid container--liquid metal system

Theoretically, complete insolubility is impossible, but such a phase diagram is justified if one supposes that the range of liquid and solid solubility is too small to be shown accurately on the diagram. Eldred (24) has correlated restricted solubility in the solid state with large differences in size between the atoms of the metals concerned. Such a criterion might be useful in container selection but should not be considered as totally reliable.

3. Phase diagrams The existence of intermetallic compounds between the container material and the liquid metal as well as their mutual solubilities can be determined from the phase diagrams. Likewise, when alloys are used as container materials, Cathcart and Manly (10) have shown that those alloys whose compositions either coincided with or were very close to that for intermetallic compounds exhibited the best corrosion resistance. Useful information for this experimental investigation was found in phase diagrams by Hansen and Anderko (39), Gschneidner (34), Weinberg et al. (72), and Udy et al. (66).

4. Strength at high temperatures The container must be capable of withstanding the stress and strain placed on it by the weight of the molten metal and the expansion and contraction over the operating range of temperature.

5. Porosity Low porosity, preferably zero, is desired at all operating temperatures in order to insure against gas losses. This would be a necessity in the case of volatile fission products in a molten-metal fuel.

6. Neutron absorption cross section The containment material should have a relatively low neutron absorption cross section whether used

for a thermal or fast reactor. Consequently, the radioactive constituents formed under neutron bombardment should also be considered in making the selection.

7. Fabrication and welding characteristics Some materials, such as graphite and tungsten, provide excellent corrosion resistance to liquid metals, but a practical system employing them is difficult to fabricate or weld.

8. Oxidation resistance If possible, the container material should have a resistance to high-temperature oxidation such as materials like Inconel and stainless steel. This problem is not unsurmountable, however, since low-oxidation-resistant materials can be sheathed within other materials, provided the two are compatible. Unfortunately, this adds to the fabrication problems.

9. Availability and purity High purity metals are being used with an increasing rate for the containment of liquid metals. The expense and availability of such pure materials may be an important factor in the selection of adequate containers and should not be overlooked.

Tantalum was of interest because it has previously been used as a successful crucible material to prepare some thorium alloys, and it has also been used very successfully in some earlier corrosion tests with alloys of uranium-bismuth and thorium-magnesium (28, 29, 30). Niobium, which closely resembles tantalum, was also of interest since this metal had been used successfully by Fisher and Fullhart (29) to contain the thorium-magnesium eutectic. Tantalum and niobium are both available from commercial distributors at purities of 99.99+ or better in the form of

tubing, sheet, and other required forms; both metals can be worked at room temperatures. The major differences between tantalum and niobium are density, neutron absorption cross section, and corrosion resistance. As can be seen from the table of properties of the materials used in this investigation found in Appendix B, the density of niobium is about one-half that of tantalum. Likewise, tantalum's thermal neutron absorption cross section is almost 20 times that for niobium. Even though niobium has good resistance to corrosion, it has been found that tantalum has a greater degree of chemical inertness than any other metal yet tested (12).

Both tantalum and niobium are classified as refractory metals because of their high melting points. However, the metals undergo accelerated oxidation in air at about 425°C, necessitating the use of a protective sheathing or coating. Tensile and yield strengths of all the refractory metals are substantially retained at high temperatures. In addition, several high-temperature refractory-metal alloys also provide similar strength properties. Niobium, as well as tantalum, may be welded to itself and certain other metals by resistance or inert-gas welding. However, because of the low-oxidation resistance, most welds are performed in an inert atmosphere. Porosity is not a problem since both metals are quite dense.

The tantalum-10 wt. % tungsten alloy was chosen because it was a new refractory alloy and the National Research Corporation had provided several pieces of 0.040-inch sheet to the Ames Laboratory as samples. Properties of this alloy will also be found in the Appendix. Since the alloy was not available in the form of tubing, it was necessary to fabricate

capsules from the sheet. The material was brittle, making the fabrication and welding difficult to accomplish with the result that only two capsule tests were conducted with this alloy.

Yttrium, when it first became available in large quantities in 1957, was found to be immiscible with uranium. A subsequent investigation by Haefling and Daane (37) of the immiscibility of the rare earths with uranium suggested that yttrium would be a possible container for uranium and uranium-base alloys. Fisher and Fullhart (29) have successfully contained the uranium-5 wt. % chromium eutectic at temperatures up to 1100°C, and the containment of uranium-6 wt. % manganese in yttrium looks very promising (62).

Although yttrium has a lower melting point and lower strength at high temperatures than the refractory metals, its use at 1000°C has already been tested. The neutron absorption cross section is about the same as that for niobium, but it has only about one-half the density. The first yttrium tubing available in 1959 was extruded by special order from Nuclear Metals, Inc. on a best effort basis. The billets of yttrium were supplied by the Ames Laboratory and were 99.6 wt. % pure; the common impurities are given in Appendix A. The extrusion process consisted of coating the ingot with an alundum paste and canning in $\frac{1}{4}$-inch thick copper before a series of size reductions in a 1000-ton extrusion press (33, 35). Removal of the copper cladding was accomplished by pickling in a 50 % HF-50 % HNO_3 solution which did not attack the yttrium. After annealing at 1000°C, it was necessary to make all welds in an inert atmosphere. Welding is more difficult than with the refractory metals

because yttrium is a softer and lower melting metal than tantalum or niobium. The procedure used for oxidation protection is explained in the section titled Experimental Procedures.

Inconel Alloy 600 was used as the sheathing material to withstand the oxidizing atmosphere present in the muffle furnaces. In addition, it was used as a container material for several comparison tests with the above mentioned materials.

Inconel, a nickel-chromium-iron alloy, was found to be compatible with tantalum and niobium at all test temperatures up to 1200°C, but not with yttrium (28). In the latter case, yttrium combines with the nickel to form an intermetallic compound; however, this was remedied by placing a tantalum spacer between the yttrium capsules and the Inconel. The properties of Inconel Alloy 600 are found in Appendix B and will not be discussed here, since Inconel was not intended as a possible container material.

Ceramic coatings and refractories (19), which show promising corrosion resistance to liquid metals, were not considered as container materials because of the immediate disadvantages inherent to their use. The art of applying coatings has not yet been developed to enable their utilization to the full extent required. The coatings are generally brittle and unable to withstand the shock of thermal cycling.

Selection of the Liquid-Metal Alloys

The selection of the uranium or thorium alloy system to be employed as the molten constituent must conform to certain requirements if it is

to be used in a liquid-metal-fuel reactor (32, 46). Some stipulations to be considered are listed as follows:

1. Percentage of uranium or thorium content Preferably, the system should contain a high percentage of the uranium or thorium constituent; however, sometimes the high percentage must be sacrificed to keep the melting temperature within a permissible range. Such was the case with the uranium-bismuth fuel proposed by Brookhaven National Laboratory for the LMFR.

2. Melting point The melting point of the alloy system should be low enough (usually less than 800°C) not to tax the capabilities of the container material and to facilitate the start-up as a dynamic system.

3. Neutron absorption cross section The constituent combined with the uranium or thorium should have a low neutron absorption cross section to preserve neutron economy. Consequently, the radioactive species formed should be of low intensity and preferably "short-lived." Such elements as Cobalt-59 should be avoided.

4. Heat transfer characteristics High thermal conductivity, high specific heat, and low viscosity combine to define a good heat transfer fluid. Since these characteristics are known for uranium and thorium, an improvement should be sought by the choice of suitable constituents to the alloy system.

5. Vapor pressures Metals with low vapor pressures at the elevated temperatures are desirable over those with high vapor pressures. This is reflected directly in the boiling point, which should be high in order to minimize the possibility of exceeding design pressures due to

unexpected boiling. In addition, a high boiling point will tend to exclude the deposit of vapor in undesirable locations.

6. Alloy characteristics Such characteristics as ease of fabrication, machinability, and brittleness of the alloy should also be considered. Some alloys are difficult to produce at a specified composition, and special techniques must be employed to produce them. In some cases it is not necessary to fuse the constituents to form the alloy, because the solubility of the components is such that the alloy is formed upon raising the capsule to the test temperature. Since the alloys are usually cast, it is necessary to remove the outer crust before it is used in a capsule test. Brittleness plays an important roll in how this crust is removed. In addition, problems may be encountered if the alloy has a negative coefficient of expansion as in the case of bismuth. A number of equipment failures caused by the expansion upon freezing have been reported with this system.

7. Phase diagrams Most of the phase diagrams of the common elements with uranium and thorium have been determined. These diagrams greatly facilitate the selection of suitable binary alloys since data on the melting points and solubilities are given. Also, the phase diagram of the container metal and the constituent added to the uranium or thorium should be checked for the possible formation of liquid, solid, or intermetallic compounds at or below the temperatures of operation.

8. Previous corrosion experience Particular interest should be placed on compatibility between the container material and the uranium or thorium alloy, if such information is available, and at least upon the

compatibility between the container and the constituent added to the uranium or thorium. As far as compatibility between the container and the uranium or thorium is concerned, very few materials exist which will contain these elements, although solid solution formation at the temperature of operation might give a clue to what could happen. Nevertheless, when alloyed, uranium and thorium may become less corrosive, especially if the temperature can be lowered.

Selection of suitable molten alloys of uranium and thorium for this investigation started by studying the various phase diagrams (34, 39, 58, 65, 66, 72) and by searching the literature for corrosion information on tantalum, niobium, and yttrium (6, 9, 17, 19, 45, 48, 52, 53, et al.). A list of all the binary systems for which information was available was made and is shown in Tables 1 and 2. Only alloys with melting points below 800°C were considered. The systems to be studied were further scrutinized by consideration of the other seven items mentioned above. This narrowed the selection down to six uranium-alloy systems: U-Al, U-Bi, U-Mn, U-Hg, U-Sn, and U-Zn; and to six thorium-alloy systems: Th-Al, Th-Bi, Th-Pb, Th-Mg, Th-Sn, and Th-Zn. Of these 12 systems, U-Bi and Th-Mg had been tested in the three containment materials, niobium, tantalum, and yttrium (9, 29, 30), but the systems were included because the available corrosion data on these systems were helpful in the investigation and recommendation for further study. The system U-Mn was not tested since the alloy was already under study by another investigator, as mentioned in Table 1. Methods of preparing the alloys were then considered and reviewed in light of available information (21, 39, 65, 72).

Table 1. Possible molten uranium systems with composition ranges melting below 800°C

Reference	Alloy system	U composition range wt. %	Molten-state range °C	Melting points of eutectics[a] °C	Rejected	Remarks
39	U-Al	0 - 30	640 - 800	640	No	Eutectic at 13.0 wt. % U
39	U-Sb	0 - ?	630.5 - ?	?	Yes	No phase diagram
39	U-Bi	0 - 11	271 - 800	None	No	
39	U-Co	87.5 - 92	734 - 800	734	Yes[b]	Eutectic at 89 wt. % U
39	U-Ga	0 - 6.5	30 - 800	None	Yes	Ga is very expensive
39,58	U-In	0 - ?	156 - ?	?	Yes	No phase diagram
39,58	U-Fe	88 - 94.5	725 - 800	725	Yes	Previously run in Ta, Nb, and Y (9)
39,58,65	U-Pb	0 - 0.1	327 - 800	None	Yes	Low U solubility
39	U-Mg	0 - 0.06	650 - 800	None	Yes	Very low U solubiligy
39,58	U-Mn	92 - 95	716 - 800	716	No	Under investigation by Fullhart[c]
39,58,65	U-Hg	0 - 56	(-40) - 800	None	No	
39,58	U-Ni	59 - 76	740 - 800	740	Yes	Previously run in Ta, Nb, and Y (9)
65,67	U-Pu	0 - 46	612 - 800	612	Yes	Pu is highly toxic; 16.25 at. % eutectic
39	U-Se	0 - ?	220 - ?	?	Yes	No phase diagram
39	U-Na	0 - ?	98 - ?	?	Yes	Low U solubility
39	U-Te	0 - ?	450 - ?	?	Yes	No phase diagram
39	U-Tl	0 - ?	303 - ?	?	Yes	No phase diagram
39,58,65	U-Sn	0 - 5	232 - 800	None	No	
39	U-Zn	0 - 8	420 - 800	None	No	

[a]This covers only the range of stated composition.

[b]Forms a highly radioactive constituent.

[c]Fullhart, C. B., Ames, Iowa. Data on containing U-Mn. Private communication. 1961.

Table 2. Possible molten thorium systems with composition ranges melting below 800°C

Reference	Alloy system	Th composition range wt. %	Molten-state range °C	Melting points of eutectics[a] °C	Rejected	Remarks
39,66,72	Th-Al	0 - 36	632 - 800	632	No	Eutectic at 25.6 wt. % Th
39	Th-Sb	0 - ?	630 - ?	?	Yes	No phase diagram
39,66,72	Th-Bi	0 - 3.3	271 - 800	None	No	
66	Th-In	0 - ?	156 - ?	?	Yes	No phase diagram
39,66	Th-Pb	0 - ?	327 - 800	None	No	Th dissolves in Pb and solidifies out in elementary form on cooling
39,58,66	Th-Mg	0 - 70	596 - 800	596	No	Previously run in Ta, Nb, and Y (9)
39,66	Th-Hg	0 - ?	(-40) - ?	?	Yes	No phase diagram; low Th solubility
65,67	Th-Pu	0 - 11	605 - 800	605	Yes	Pu is highly toxic
39,66	Th-Na	0 - ?	92 - 800	92	Yes	(58) disputes correctness of diagram in (39)
39	Th-Te	0 - ?	450 - ?	?	Yes	No phase diagram
66	Th-Tl	0 - ?	303 - ?	?	Yes	No phase diagram
39	Th-Sn	0 - ?	232 - 800	None	No	Th dissolves in Sn and solidifies out in elementary form on cooling
14,66	Th-Zn	0 - 3.8	420 - 800	None	No	

[a]This covers only the range of stated composition.

The capsule corrosion tests conducted as part of this investigation were divided into two phases--those in which the constituent added to the uranium or thorium was tested separately in the container materials, and those in which the uranium or thorium alloy itself was tested with the container materials. The reasons for conducting the corrosion tests in this manner were twofold:

1. In order to utilize higher concentrations of a fissionable or fertile component in liquid metals, dispersions in which the solid contains this constituent must be considered (44). Such dispersions or slurries usually made-up either as an intermetallic compound of the fissionable or fertile component with the liquid-metal components or as an ionic compound dispersed in the liquid phase. An example of the former type of slurry would be U_3Bi_5 or U-Bi dispersed in bismuth or a lead-bismuth alloy (49). Table 3 lists a number of possible intermetallic-compound dispersions in liquid-metal systems. The ionic compound dispersions are formed simply by adding the ionic compound to the liquid-metal surface. An example of this latter type of dispersion is UO_2 or U_3Si in Na or NaK. A table listing common ionic-compound dispersions and their dependence upon the contact angle of wetting may be found in Volume 1 of the Reactor Handbook (65).

Although it is possible to produce liquid-metal dispersions, their satisfactory containment still remains a problem of great, if not controlling, importance. Essentially, the liquid-metals in which the intermetallic or ionic compound is dispersed must be contained. For this reason separate tests with the non-fuel or non-fertile constituents were conducted as one phase of the investigation.

Table 3. Possible intermetallic-compound dispersions in liquid-metal systems[a]

Dispersion system	Solid-intermetallic compound		Liquid-metal carrier			
	Composition	Density g/cm^3	Composition wt. %	Temperature °C	Density g/cm^3	Freezing point °C
U-Bi	UBi_2	12.4	Bi	350	10.0	271
U-Pb	UPb_3	12.98	Pb	350	10.6	325
U-Sn	USn_3	10.0	Sn	400	6.8	231
U-Bi-Pb	UBi_2	12.4	0-81 Pb; Bi	350	10.1-10.5	125-271
	U_3Bi_4	12.59	81 Pb-19 Bi	350	10.5	260
	UBi	13.6	81-95 Pb; Bi	350	10.5	260-310
	UPb_3	12.98	95-100 Pb; Bi	350	10.5-10.6	310-325
U-Bi-Sn	UBi_2	12.4	0-11 Sn; Bi	350	10.0-9.5	271-230
	U_3Sn_5	----	11-12 Sn; Bi	350	9.5	230
	USn_3	10.0	12-100 Sn; Bi	350	9.5-6.8	230-139
U-Pb-Sn	UPb_3	12.98	0-2 Sn; Pb	350	10.5-10.3	325-320
	$USn_3 + UPb_3$	10.0-10.5	2-100 Sn; Pb	350	10.3-6.8	320-183
U-Bi-Pb-Sn	$USn_3 + UPb_3$	10.0-10.5	56 Bi-16 Sn-32 Pb	350	9.7	95
U-Bi-Na	UBi_2	12.4	4 Na-96 Bi	350	7.0	340
U-Hg	UHg_4	14.6	Hg	100	13.3	-38.9
U-Cd	U	19.8	Cd	---	----	321
U-Ga	UGa	9.69	Ga	---	----	30
U-Na	U	19.8	Na	---	----	98
Th-Bi	Th_3Bi_5	10.5	Bi	350	10.0	271
Th-Bi-Pb	Th_3Bi_5	10.5	0-45.5 Pb; Bi	350	10	125-271
Th-Bi-Pb	ThBi	10.8	3 Bi-97 Pb	350	10.5	318
Th-Pb	$ThPb_3$	12.3	Pb	350	10.5	325
Th-Na	Th	11.6	Na	---	----	98

[a]Reproduced from Reference 65.

2. The liquid-metals which looked promising in the first phase of the investigation were then rerun as constituents with uranium or thorium. In this manner, a check could be made to determine whether the addition of uranium or thorium accelerated or hindered the corrosion attack. The results of the various corrosion tests are listed in tabular form in the section titled Results and Discussion.

REVIEW OF LITERATURE

Considerable work in the field of liquid metals has been undertaken in the past fifteen years, especially under the topic of liquid-metal corrosion. Only a fraction of the information about corrosion has appeared in the open literature.

After selecting the liquid-metals to be used in the investigation, a search of the available information in the literature was conducted. A number of references were found on corrosion by the four basic pure liquid-metals to be tested, but little information was available on the corrosion resistance of the thorium and uranium alloys of these pure metals. A general summary of corrosion by numerous pure liquid metals was found in Kelman et al. (45) and Lyon (48). Corrosion resistance of ferrous metals and various refractory coatings, in particular, was not considered in the literature review since selection of the container materials had already been decided.

Corrosion by Liquid Aluminum

A search of the literature quickly gave an indication that aluminum was quite corrosive in its liquid state. Lyon (48) reports that no known metals are totally immune to attack by liquid aluminum. Above 660°C almost all solid metals and alloys suffer severe attack. Some success has been achieved, however, with inert metallic oxide coatings. Even liquid metal solutions containing more than 50 wt. % aluminum will attack materials in the same fashion as the pure metal. Unknown resistance of the refractories was listed by Lyon. Kelman et al. (45) did not consider the corrosiveness

of aluminum in their report. Although Miller (52) considers corrosion of tantalum and niobium by several liquid metals including uranium, he fails to consider attack by molten aluminum. No phase diagrams for aluminum-niobium or aluminum-tantalum were found, but Hansen and Anderko (39) indicate the existance of $NbAl_3$ and $TaAl_3$ as intermediate compounds. No melting point data or methods of preparation were given.

With tests using a 2.0 at. % uranium-aluminum alloy at 1000°C, Brasunas (6) found that a niobium specimen was severely attacked by heavy solution while a tantalum specimen showed only 0.003 inch of surface irregularity. Both tests were run for 4 hours. Of the materials tested, tantalum was best and rated at a "9" on the basis of a possible 10 points, and niobium received a "3".

Fisher et al. (28, 29) have studied an alloy of 76 wt. % aluminum-18 wt. % thorium-6 wt. % uranium melting at 630°C (4) in tantalum and yttrium. Tantalum failed in 96 hours at 1000°C, but yttrium suffered only 0.010 inch attack after 1340 hours at 800°C. Additional tests by the same authors (9) showed that 1200 hour tests at 800°C in niobium and tantalum were only slightly attacked. A better grade of tantalum was used in the latter tests, however.

Holman (41) considers aluminum too corrosive and having too high of a melting point temperature to be considered as a possible liquid metal. His main concern, however, was for use as reactor coolants. Gschneidner (34) lists five intermediate compounds between yttrium and aluminum, with a eutectic composition at 90 wt. % aluminum melting at 650°C. This latter reference would seem to indicate that yttrium and aluminum would not be

compatible above 650°C. Tantalum and niobium, however, need definite investigation. Information on Inconel and the tantalum-tungsten alloy was not discovered in the literature cited.

Corrosion by Liquid Lead and Lead Alloys

Numerous reports have appeared in the literature on corrosion by lead, lead-bismuth eutectic, lead-tin, and other common lead alloys. A number of these reports are summarized in Lyon (48) and Kelman et al. (45). Both sources quote niobium and tantalum as having good resistance to attack by lead and bismuth-lead at temperatures up to 1000°C. Unknown resistance to bismuth-lead-tin eutectic above 600°C was indicated, however. Inconel was shown to have limited capabilities up to 850°C and poor resistance to attack above 850°C. Kelman et al. considers structural materials containing appreciable amounts of tungsten as unsuitable for lead containment, thereby inferring that tantalum-10 wt. % tungsten would be inadequate.

In a series of tests with liquid lead at 1000°C for periods of 40 hours, Brasunas (6) investigated the corrosion resistance of niobium and tantalum. Specimen tests were used in iron capsules containing the lead. Niobium suffered 0.013 inch of decarburization, 0.004 inch of film formation, and a +0.003 inch change in thickness. Tantalum, on the other hand, alloyed with iron from the capsule wall (Type 4a attack) and was covered with a 0.0002 inch hard, surface film. Brasunas rated niobium at "8" and tantalum at "9" on the basis of "10". In a two component test, tantalum did not indicate any evidence of attack after 100 hours exposure with liquid lead at 1000°C and was consequently rated at "10"; niobium

was not investigated with such a test. Inconel was also tested with lead at 1000°C for 100 hours and found to undergo deep intergranular attack (rated at "6"). Brasunas also tested a 2.0 at. % uranium-lead alloy in niobium and tantalum for 4 hours at 1000°C. Intermetallic formation to a depth of 0.001 inch occurred in niobium, and tantalum suffered 0.005 inch of subsurface precipitation. Surprisingly, tantalum (rated "6") was more severely attacked than niobium (rated "9").

In selecting liquid metals as reactor coolants, as liquid-metal fuels, and as heat transfer fluids in fuel elements, Holman (41) selected as possible choices: lead, lead-bismuth, and lead-tin. Stipulations to follow in selecting suitable containers were also presented, but actual materials for containment were not suggested.

Miller (52) reports that tests with tantalum at 1000°C showed an apparent solubility of 0.007 grams of tantalum loss per 100 grams of lead corresponding to a penetration of 0.006 mil/month. A gray film was noted but showed no signs of attack. A specimen test was used, but microscopic examination showed no reaction layer nor was the edge of the specimen attacked. Similar tests with niobium showed a penetration of 0.1 mil/month with the appearance of a 0.1 mil thick inner reaction layer. Mass transfer tests showed niobium to have high resistance with a thermal gradient of 800 to 300°C. Both metals were reportedly attacked by the bismuth-lead eutectic.

Cathcart and Manly (10, 11) have described a method of corrosion testing in liquid lead using specimens exposed in a thermal convection loop constructed of quartz, a material supposedly inert to concentration-

gradient mass transfer (Type 4a). The loops were run until plugging by mass transfer caused stoppage of the flow unless the tests were purposely halted after a certain number of hours. Niobium did not show any mass transfer after 545 hours of operation at a hot leg temperature of 800°C and a cold leg temperature of 500°C. Yttrium and tantalum were not tested. Inconel caused plugging in only 90 hours under the same test conditions.

Collins and Stephan (17) checked a number of materials for solubility in the bismuth-lead eutectic at temperatures from 900°F (482°C) to 2200°F (1204°C) by means of isothermal agitated capsules. They concluded that tantalum and niobium showed considerable promise since less than 100 ppm of the metals was detected as being soluble in the liquid eutectic. Inconel showed the worst resistance of the materials tested and should, therefore, be avoided.

Clifford (15, 16) conducted a series of experiments with the lead-bismuth eutectic by using dynamic spinner tests and thermal convection loops at temperatures from 600 to 900°C. Of the materials tested, type 446 stainless steel and a chromium-molybdenum alloy showed the best resistance at 600°C. Above that temperature none of the materials tested showed sufficient corrosion resistance for long term application. The corrosion studies and equipment design were helpful in the over-all investigation.

Corrosion by bismuth, uranium-bismuth, bismuth-lead, uranium-bismuth-lead, bismuth-lead-tin, and uranium-bismuth-lead-tin was studied by Cordovi (18) by means of 500 to 200 hour static capsule tests at 550°C. Although tantalum and niobium were not investigated, the refractory metal molybdenum

was tested. All of the six liquid metals tested showed promising results although data were incomplete in some cases and the test temperature was rather low. From the basis of these results, tests with tantalum and niobium employing the six liquid metals seems to be warranted.

Although bismuth was not one of the pure metals tested as a regular part of this investigation, it was used in several tests as a liquid-metal constituent. Therefore, the corrosive nature of bismuth was of importance. Bismuth has been shown to be more corrosive (15) than lead under the same conditions. Pray et al. (55) tested bismuth with 50 possible container materials at 750 and 850°C over test periods varying from approximately 11 to 31 days. Most of the materials tested were iron, chromium, or nickel alloys; tantalum, niobium, and yttrium were not tested. Inconel appeared to alloy with bismuth and was deemed unsatisfactory as a container material. Fisher et al. (28, 29, 30) have conducted numerous tests with bismuth and alloys of uranium-bismuth in niobium, tantalum, and yttrium at temperatures up to 1050°C. Static, isothermal tests showed that bismuth and 5 wt. % uranium-bismuth solutions severely attacked niobium and yttrium; however, tantalum was not attacked. A forced circulation loop test with 10 wt. % uranium-bismuth in tantalum run at temperatures up to 1160°C proved feasible with less than 0.001 inch attack in 957 hours. Another loop test ran for 4500 hours at 1050°C, again with less than 0.001 inch attack. Samples taken during operation of the loop systems showed less than 6 ppm of tantalum present in the liquid-metal alloy.

Lyon (48) and Kelman et al. (45) list niobium as satisfactory up to 730°C when in contact with bismuth. Above that temperature, however, limited use is recommended. No information was cited for tantalum, Inconel, or yttrium. On the other hand, various sources in Miller (52) say that tantalum suffers pronounced intergranular attack at 1000°C after 227 hours. The solubility of tantalum and niobium in bismuth, however, was determined and found to be low and little affected by increase in temperature. Brasunas (6) also reports that tantalum and niobium show good corrosion resistance to bismuth at 1000°C, but his results are based on 4 hour and 40 hour tests only. In 4 hour static tests with 2.0 at. % uranium-bismuth at 1000°C, niobium was rated "7" on a basis of "10" while tantalum received a "9". Information about the system bismuth-yttrium is missing from Gschneidner (34), and possibly the system has not been extensively studied.

Weeks et al. (71) through their work with uranium-bismuth fuel are able to present helpful suggestions which carry over to other corrosion systems. Solubility data, information on corrosion inhibitors, and methods of corrosion testing were helpful in the overall investigation. Testing methods and procedures outlined in Bett (3), Brasunas (7), Cygan (20), Deville and Foley (23), and Frost et al. (32) were also helpful.

Corrosion by Liquid Tin and Tin Alloys

Alloys of tin with lead and lead-bismuth were considered previously; therefore, only corrosion by tin and bismuth-tin will be considered here. Kelman et al. (45) states only that niobium and tantalum have been

suggested for use with liquid tin, and tantalum is considered as a better container. No corrosion and temperature data were given. Lyon (48) cites the same reference.

Holman (41) considered tin in selection of liquid metals and found it to be worthy of investigation. Both Nb_3Sn and Ta_3Sn intermetallic compounds have been identified according to Hansen and Anderko (39), but the alloys are apparently formed by peritectic reaction between 1200 and 1500°C. Phase diagrams for the metals with tin are not available.

More rigorous tests (52) with tin in tantalum at 1740°C for one hour showed that some tantalum was dissolved in the tin to the extend of 0.33 wt. %. No such test was conducted with niobium, however.

Coultas (19) has conducted a number of static corrosion tests with tin at 1800°F (982°C) using several refractory materials. Many of the specimens tested were ceramics, but several tests were made with tantalum. Vycor capsules, judged by the experimenter to be inert, were used to contain the liquid tin and the specimens. The tantalum test was run for 40 hours; suggestion of solution attack and wetting by tin were the only results reported. Two more tests were run at 3160°F (1738°C) for one hour in Al_2O_3 capsules. Solution of the tantalum in tin was evident in both tests, but marked intergranular corrosion had occurred in only the second test.

Gschneidner (34) did not list any properties of the yttrium-tin binary system, since apparently the system has not been fully investigated. It appears that adequate corrosion information is lacking with the systems niobium-tin, tantalum-tin, and yttrium-tin. Therefore, further investigation seems to be warranted.

Corrosion by Liquid Zinc and Zinc Alloys

Both Kelman et al. (45) and Lyon (48) in quoting the same source state that niobium and tantalum are suggested for possible use in liquid zinc in the order listed. Holman (41) rejects zinc as a possible liquid metal on the grounds that it is too corrosive and melts at a fairly high temperature (419.5°C).

Commercially pure tantalum and niobium foil when tested dynamically with molten zinc at 440°C were found to be completely dissolved after a period of less than 50 hours (52). Hansen and Anderko (39), however, do not list any information or phase diagrams.

DeKany et al. (22) conducted a number of 100 hour isothermal static tests at temperatures up to 750°C on various materials by using liquid zinc and zinc-base systems. Both tantalum coupons and capsules were run with zinc at 750°C. Mild corrosion through formation of an intermetallic layer (Type 3 attack) was noted. By alloying the zinc with 46 wt. % magnesium, the same test conditions yielded a system with no reported corrosion. Other tests in tantalum capsules with various additions of magnesium also showed no corrosion after 100 hours at 750°C.

A check of available literature by Nathans (53) on the solubilities of a number of metals in liquid zinc has shown that niobium has a relatively high degree of solubility. He was unable to find information on the solubilities of tantalum and yttrium, however. Gschneidner, nevertheless, reports that the solubility of yttrium in liquid zinc at 600°C is 0.8 wt. %. Additional information was not listed.

Brasunas (6) considered the corrosion resistance of a 2.0 at. % uranium-zinc alloy in several refractory metals at 1000°C. Examination of a 4 hour tantalum test capsule showed that 0.013 inch of grain boundary penetration had occurred. Tantalum was arbitrarily rated at "7" on a scale of 10 possible points. Niobium was not tested. Molybdenum and tungsten, two metals previously considered in the Corrosion by Liquid Metals section, were rated at "9" and "10", respectively.

Of the three metals selected, the literature review indicates that tantalum shows the highest resistance to corrosion attack by the liquid metals used in this investigation. Corrosion attack by high percentage uranium alloys has also been studied.

Attack by 95.0 wt. % uranium-chromium has been investigated in yttrium, tantalum, and niobium (9, 28, 29). Yttrium appears to be unattacked whereas tantalum undergoes slight solution attack up to several mils during test periods of 2000 hours at 950°C. Miller (52) reports that tantalum dissolves slowly in pure uranium at all temperatures up to 1300°C and its upper limit as a container material is about 1450°C. Intergranular penetration makes the metal permeable to liquid uranium between 1200 and 1250°C. Niobium would be practical up to 1400°C under fast heating rates according to Miller's source. No significant intergranular mode of attack was detected at any temperature even though some inward diffusion of uranium into niobium was observed during long term tests at 900°C. These reports on niobium conflict with information in Cash (9) and Fisher et al. (28, 29) for uranium-chromium, uranium-iron, and uranium manganese in niobium.

Additional container materials for containment of uranium-chromium and other high content uranium alloys have been suggested and investigated by Powell (54). Tests from 860°C up to 950°C with capsules made from 95 wt. % uranium-5 wt. % niobium and 90 wt. % uranium-10 wt. % niobium were successfully run with the uranium-chromium eutectic for periods up to one month. An essential element of these capsules, however, is the oxide layer (UO_2 and U_3O_8) separating the capsule material from the molten uranium eutectic. This oxide layer must be built up before the actual containment can be effected by passing oxygen over the surfaces for several minutes at 400°C. Powell concludes that the 89 wt. % uranium-11 wt. % nickel eutectic severely attacks the uranium-5 wt. % niobium capsules, even at 800°C. In addition, thermal cycling causes a breakdown of the oxide layer.

EXPERIMENTAL PROCEDURES

There are two general experimental methods for determining the corrosion of metals by liquid metals, depending upon whether dynamic or static conditions are applicable (3). Static tests are used primarily to select from a number of materials those few which seem most resistant. These tests are conducted under isothermal conditions and may or may not employ metal specimens held in a bath of liquid metal at the desired temperature for a specified time. Upon completion of the test, the capsule and specimen, if used, are sectioned and examined for evidence of corrosion.

Once a number of possible container materials and possible fuel systems have been screened in this manner, further evaluation is normally conducted through dynamic tests where conditions more closely approach those anticipated in actual service. Dynamic tests consist of agitating the liquid metal over the solid metal (such as the so-called "see-saw" or rocker tests) or in maintaining a flowing current of liquid metal by force or by natural thermal convection in a circuit (so called "loop tests"). Rocking tests are used to simulate flow of a liquid metal over a solid-metal surface and are usually performed under isothermal conditions, although some authors (7) have maintained temperature gradients at opposite ends of the test specimens. Rocking tests employ sealed capsules of the test material partially filled with liquid metal. These capsules are heated and rocked in such a manner that the liquid metal periodically moves from end to end. After the initial screening tests, rocking tests are usually conducted to further evaluate the system of materials before

justifying the design and construction of an engineering test loop. Much corrosion information can be gained from static and rocker tests because of their convenience and low cost.

Thermal and forced circulation loop tests, however, provide a better means of ascertaining the behavior of the system under actual operating conditions (63). Only an in-pile test loop under neutron irradiation (64) would give a clearer picture save for a full-scale operational system. Both the thermal and forced circulation loops allow investigation of temperature-gradient mass transfer, while the forced circulation loop also permits the study of erosion. Thermal loops work on the principle of a closed circulating system under the influence of convection forces from a heated section and a cooled section. Flow rates obtained in this manner are relatively small (1-4 gallons per minute); therefore, the forced circulation loop becomes necessary for attaining high velocities.

It is necessary to keep in mind the merits and demerits of these testing schemes when evaluating data obtained from these tests, for a material which shows promise in one type of test may fail completely in another. Even when the results of the same type of test are being compared, it must be remembered that small variations in operating conditions can produce quite different results. In the same way, it cannot be assumed that rates of corrosion established in small-scale tests of short duration will apply to large systems for longer periods of time.

Corrosion Test Procedures

The experimental investigation has been limited almost entirely to the attack of liquid metals on three solid metals and two alloys in a

static, isothermal condition. Approximately one-third of the tests completed were run with uranium or thorium alloys in the molten state while the remaining capsules contained only a pure liquid metal. Selection of these metals and alloys was discussed earlier.

The general procedure consisted of first testing the uranium and thorium counterpart constituent (pure metal) in annealed niobium, tantalum, and yttrium; in capsules constructed of the tantalum-tungsten alloy; and in Inconel. These tests were run as static, isothermal capsule tests. Secondly, some of the metals which showed promising corrosion resistance were run individually as dynamic, isothermal capsule tests. These tests were performed in a rocker furnace oscillating through an arc of 135° and in a specially designed 360° rotary furnace. Several molten alloys of uranium and thorium were also run in these furnaces. As the third phase of testing, the most corrosion resistant pure metals were prepared as molten uranium and thorium alloys and run for long durations as static, isothermal corrosion tests. From these data, recommendations for further study were made as discussed on page 131.

The results to be described were obtained with the liquid metal in contact with only one container material at a time in order to avoid interactions inherent with three-component systems as previously discussed. Specimens were not used, and thus only interactions between the inner capsule surface and the liquid metal were possible. In addition, no satisfactory way of removing bath metals from specimens is yet available, so that the idea of using specimens was not even considered. The present method merely involves heating to slightly above the melting point and

removing the specimens, which usually means encountering wetted surfaces retaining some of the liquid metal, thus making weight change measurements unreliable as a method for evaluating the degree of corrosion attack.

Niobium, tantalum, and yttrium capsules were prepared by cutting off two-inch lengths of the annealed stock tubing with a Carborundum cut-off wheel. In the case of niobium and tantalum, the tubing was 0.75 inch O.D. with 0.030 inch wall thickness. Caps for the tubing ends were spun on the metal lathe from 1.00 inch circular slugs punched from 0.030 inch sheet. For yttrium the tubing was 0.75 inch O.D. with 0.040 inch wall thickness. Since satisfactory caps could not be spun from yttrium for this diameter tubing, punched circular slugs approximately 0.71 inch in diameter were used for end caps. The capsule ends were recessed with a 0.020 inch lip to support the end caps and provide a ridge of metal which was melted down over the cap to form the welding bead.

After removing loose burrs of metal present from the cutting operation, each capsule was fitted with end caps for welding. Before each weld was made, both metal surfaces were thoroughly cleaned with carbon tetrachloride to remove any grease and dirt which might have caused inclusions within the weld. The bottom caps were usually welded in place and examined before the test materials were added to the capsules. All welds were made with a heliarc welder under an inert helium atmosphere. Each capsule was purged and filled with argon before and after insertion of the test sample. The top cap was then placed in position while the capsule continued to remain in a helium atmosphere. The final weld was then completed and carefully examined for possible cracks and/or inclusions. At times it was

necessary to make a second pass of the heliarc gun to produce a satisfactory weld.

For the tests conducted in the tantalum-tungsten alloy, it was necessary to fabricate square 3/4 inch capsules from the 0.040 inch sheet. Capsules were constructed by bending a $2\frac{1}{4}$ inch x 2 inch sheet in a U-shape. The fourth side was then welded in place, followed by two 3/4 inch square caps. Inconel capsules were simply constructed from 3/4 inch, schedule 40 pipe by machining lips at the ends of three-inch pieces of pipe, in much the same manner as for the yttrium capsules. The 0.125 inch Inconel end slugs were cut from 0.875 inch diameter bar stock.

The metal containers, except for the Inconel capsules, were then sealed in bombs of Inconel containing an argon atmosphere added with the heliarc gun. These Inconel bombs consisted simply of three-inch pieces of 3/4 inch, schedule 40 pipe sealed exactly the same way as Inconel capsules. Since yttrium readily combines with the nickel present in Inconel, these capsules were first encapsulated in a 0.005 inch sheath of tantalum to avoid contact with the walls. A typical test capsule arrangement is shown in Figure 8 for the case of tin contained in niobium.

Preparation of the molten alloys consisted of either separate fabrication beforehand or of adding the proper amount of the materials to the container capsule before sealing. In the case of the alloys of uranium and thorium, wherein the fuel or fertile metal was soluble to a given degree in its counterpart constituent, the latter method proved somewhat satisfactory. However, in most instances the liquid alloys were prepared in electric arc vacuum furnaces as buttons or in induction furnaces in separate graphite crucibles.

After completion of the final encapsulation of the test container in the Inconel, the samples were introduced into muffle furnaces already at test temperatures. The bank of six muffle furnaces used for the majority of tests is shown in Figure 9. Short duration tests under 100 hours in length were usually run in the Inconel bomb furnaces illustrated in Figure 10. These tests could be run without having to encapsulate the capsule in Inconel for protection against the atmosphere. An inert helium atmosphere of 5.0 psig was used for these tests. Timing for all tests was always figured as beginning five minutes after the sample was inserted into the furnace and ending the moment it was removed. All test capsules were allowed to cool by standing in the air at room temperature immediately upon removal from the furnaces. Although oil quenching (6) might allow more accurate correlation of analytic data to the test temperature, the method of cooling was not changed from that decided upon for the first tests, in order to maintain a standard testing procedure.

The dynamic, isothermal tests were performed in a rocker furnace constructed from a furnace like that shown in Figure 10, and in the 360° rotary apparatus shown protruding from muffle furnace Number 5 in Figure 11. The rocker furnace operated at a rate of one cycle every 107 seconds, and the rotary furnace at the rate of one revolution per minute. The rotary furnace was capable of holding two capsules at the same time. The supporting bearings were adequately cooled by means of the centrifugal blower shown in the figure.

Temperature control was achieved with chromel-alumel thermocouples connected to Wheelco temperature controllers. The guaranteed accuracy is

Figure 8. Typical static, isothermal test capsule before sealing

Figure 9. Bank of six muffle furnaces used in the investigation

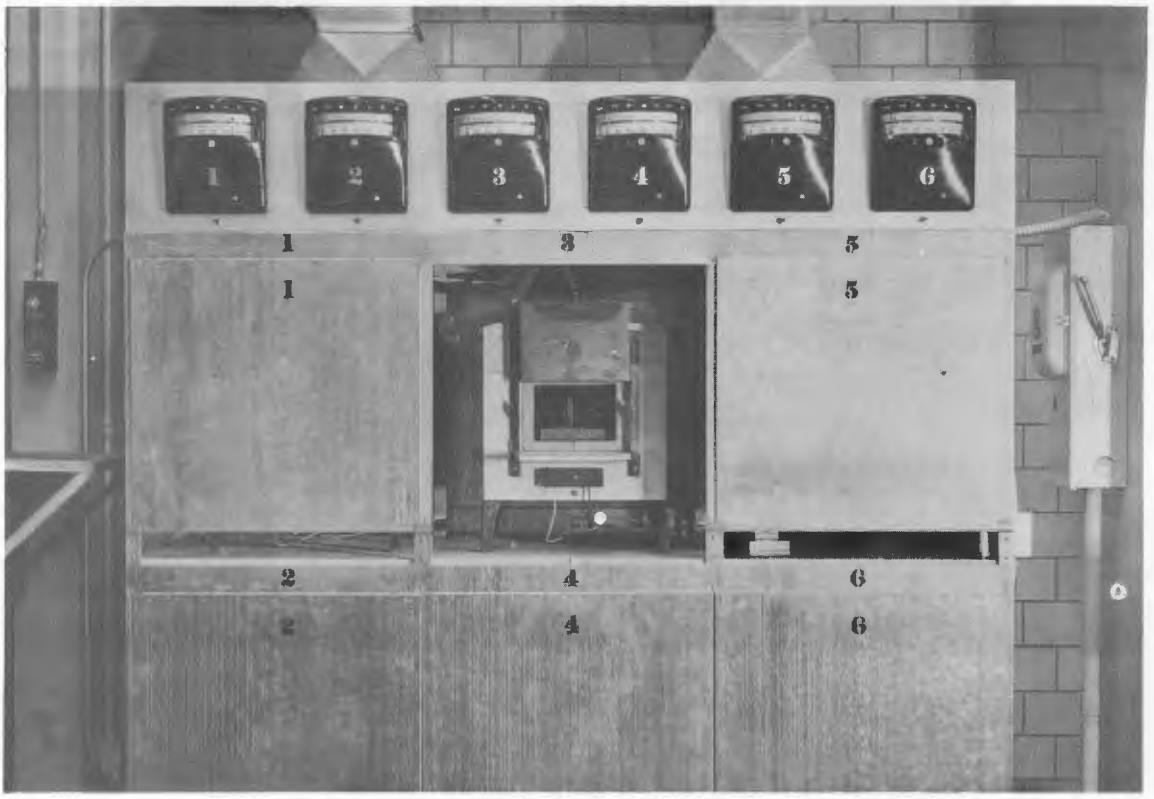
1
2
3
4
5
6
1
3
5
1
5
2
4
6
2
4
6

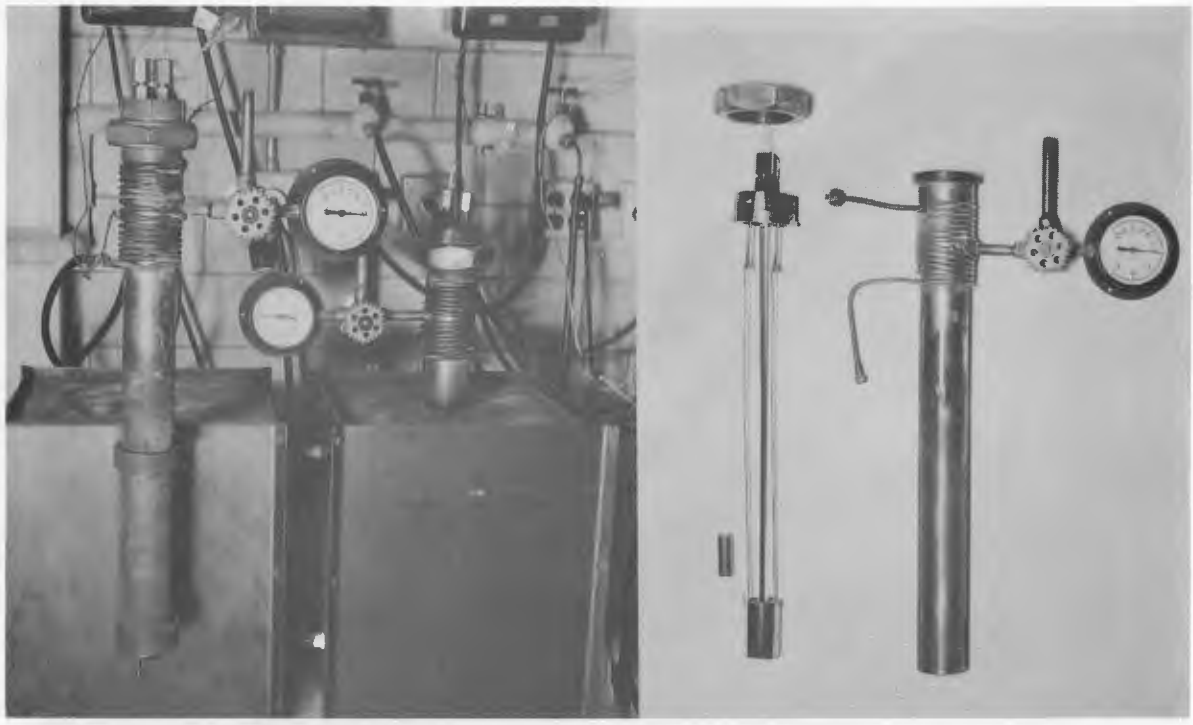

Figure 10. Inconel bomb furnaces used for short term tests

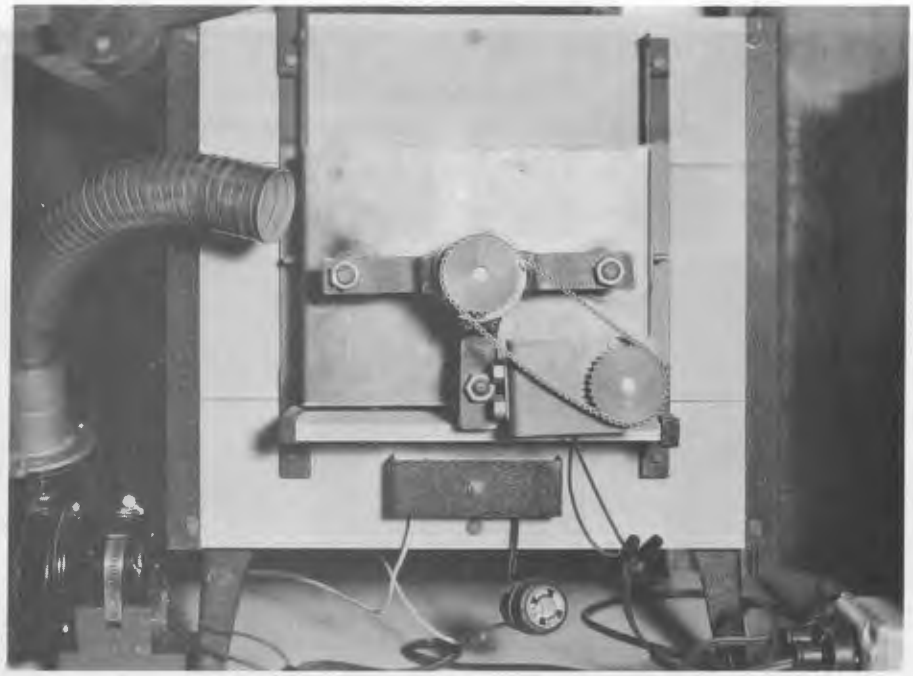

Figure 11. 360° rotary apparatus for dynamic, isothermal tests

$\pm \frac{1}{2}$ % of full scale or in this case ± 6°C. However, accuracy of ± 5°C was easily obtained for the tests conducted under this investigation. Temperature fluctuation was rather substantial considering it can be an important factor which influences the corrosion rate. Fluctuations of ± 1°C or less would have been much more satisfactory but unfortunately were unattainable with the existing equipment. Test temperatures varied from 600°C to 1100°C for different samples, but each test was always run at a constant temperature setting.

In all tests the surface to volume ratio was maintained within the range of 7.29 ± 1.36 in^2/in^3 since this factor is also quite important. This value was slightly higher (averaging 14.84 ± 2.27 in^2/in^3) for the rocker and rotary furnace test capsules since more surface area was contacted by the liquid metal.

Methods of Specimen Examination

At the conclusion of the high-temperature exposure, the capsules were sectioned once along the tubing's center axis. This method produced two equal halves giving full view of the vertical plane from top to bottom. In a number of cases where the liquid metal had completely penetrated the container wall, the capsule could not be removed from its Inconel sheath. For these samples the entire Inconel capsule was sectioned axially.

The examination then involved a visual observation of the entire capsule to check for swelling, possible oxidation, and points at which corrosion attack was most likely to occur. A check of the meniscus was always made in order to note whether or not wetting of the container walls

had occurred and to see if the liquid metal also showed any tendency to climb the walls and completely cover the available surface area. After this, the examination consisted primarily of observation under a metallurgical microscope. In many cases the liquid-metal phase was also analyzed spectrographically. Analytical methods of analysis proved fruitless in the cases of lead and tin in niobium and tantalum, because precipitation of undesired phases inhibits the detection of niobium or tantalum impurity in the liquid metal.

Specimens to be analyzed metallographically were prepared using normal polishing procedures outlined in Hopkins and Peterson (42). The examination of the polished sections consisted of two studies: (1) photomicrography of the interface regions at different magnifications and fields of light; and (2) measurement of the capsule wall thickness for depth of corrosion penetration. With the aid of the microscope, photomicrographs, and Reference 6, the various types of corrosion attack which occurred were classified. Photomicrographs were taken at magnifications of 50X, 100X, 150X, 250X, and 500X under a bright field of light and under polarized light. Magnification and light fields varied from sample to sample depending upon which seemed to work best at the moment. Over 200 photomicrographs were taken, a number of which will be shown in the next section of this report.

Measurement of wall penetration was made with a screw micrometer eyepiece which was calibrated at each magnification. Original capsule wall thicknesses were assumed to be within ± 0.001 inch of their specified values except for the extruded yttrium tubing where a variation of ± 0.003

inch was assumed. In each case the mean value was used to determine depth of penetration. Tabulations of the data for corrosion tests will be found in the section titled Results and Discussion.

RESULTS AND DISCUSSION

In interpreting the results presented here, the purpose of the investigation should be kept in mind. The compatibility tests were planned to provide a basis in the selection of a possible fertile or fuel alloy for possible use in a liquid-metal-fuel reactor. It was realized at the start that such a combination of a low melting point metal with uranium or thorium which was compatible with the chosen containers might not exist. Nevertheless, it was felt that compilation of corrosion data on these systems would still be useful.

During the investigation no provisions were made for outgassing the metals used, purifying the inert cover gas, or conditioning the container surfaces for removal or application of films. For these and other reasons, the present data are by no means considered complete or conclusive. Additional tests are planned in order to extend the present knowledge and to verify some of the test data which may be in error due to excessive amounts of impurities, temperature cycling, or other possible extraneous effects.

For purposes of presentation the compatibility data including the photomicrographs pertaining thereto are divided into four sections according to the liquid metal involved. Data on each capsule test conducted has been tabulated for easy reference. The tabular form used shows the extent of interaction observed by the methods of examination described previously, its classification according to the section titled Corrosion by Liquid Metals, and an arbitrary comparative rating as a basis of container evaluation. In addition, the conditions of the test such as duration and test temperature are also tabulated.

The arbitrary comparative rating quickly indicates which systems showed little or no signs of interaction and those which showed appreciable reaction. The systems have been rated from one to ten, where one represents complete destruction and ten represents excellent resistance to corrosion. In the author's opinion, the systems rated at nine or ten appeared resistant enough to corrosive attack to warrant consideration under more practical testing involving temperature gradients, dissimilar metals, and forced circulation. The systems rated seven or eight are of questionable interest, and their utilization would be dependent upon the amount of corrosion which could be allowed for a particular application. Systems rated at six or below are those in which the attack is too severe to be recommended for further consideration except for necessary short term service.

Corrosion by Aluminum and Uranium-Aluminum

Ten capsule tests were run using aluminum and uranium-aluminum as the liquid metals. The uranium-aluminum alloy chosen was the eutectic composition at 13.0 wt. % uranium (39) with a melting point of approximately 640°C. The alloy was prepared in an electric arc vacuum furnace, but no analytical check of the composition was made. The tests were all run in the range from 800 to 900°C for various lengths of time and only in a static, isothermal condition. These tests and their results are tabulated in Table 4 while photomicrographs of the interfaces between the container walls and the liquid metals are shown in Figures 12 and 13. A check of Table 4 and the figures show that further tests were not warranted in the

Figure 12. Photomicrographs showing corrosion attack by aluminum and uranium-aluminum eutectic (reduced 20 per cent)

a. Aluminum in niobium at 800°C for 36 hours; Test Number 1 (2.8X)

b. Aluminum in niobium at 800°C for 74 hours; Test Number 2 (100X, polarized light)

c. Uranium-aluminum in niobium at 800°C for 74 hours; Test Number 3 (50X, HF, HNO_3, H_2SO_4 etch)

d. Aluminum in tantalum at 800°C for 232 hours; Test Number 4 (150X)

e. Uranium-aluminum in tantalum at 800°C for 212 hours; Test Number 5 (50X)

f. Uranium-aluminum in yttrium at 850°C for 137 hours; Test Number 6 (top specimen, 2.8X)

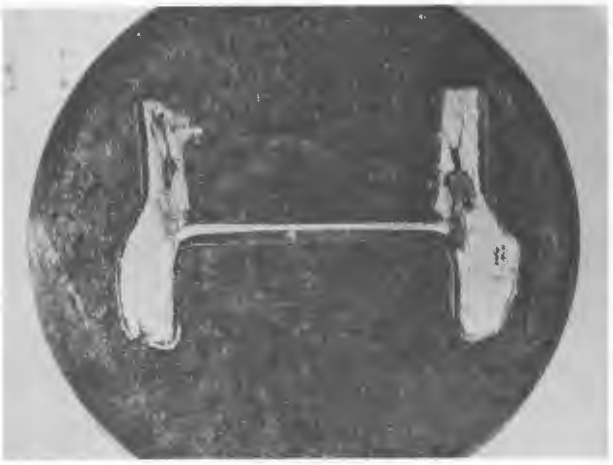

a

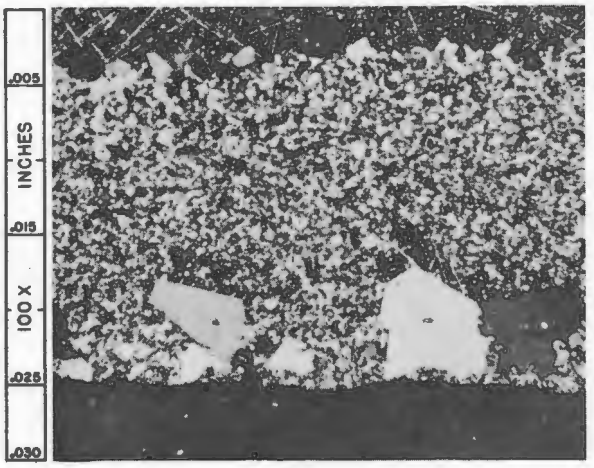
.005
INCHES
.015
100 X
.025
.030

b


.005
.010
INCHES
.025
.030
.035
50 X
.045
.050
.055
.060

c

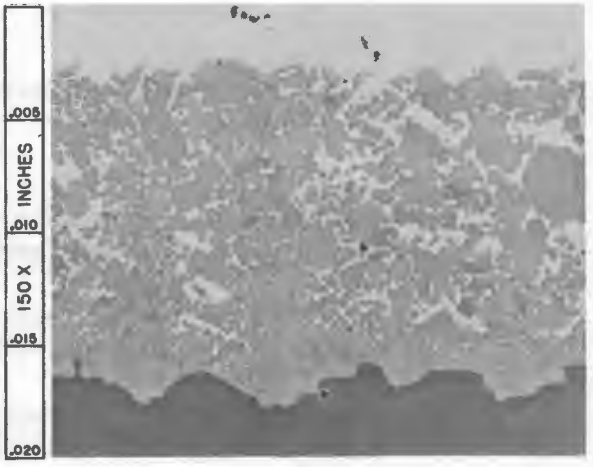
.005
INCHES
.010
150 X
.015
.020

d


.005
.010
INCHES
.025
.030
.035
50 X
.045
.050
.055
.060

e

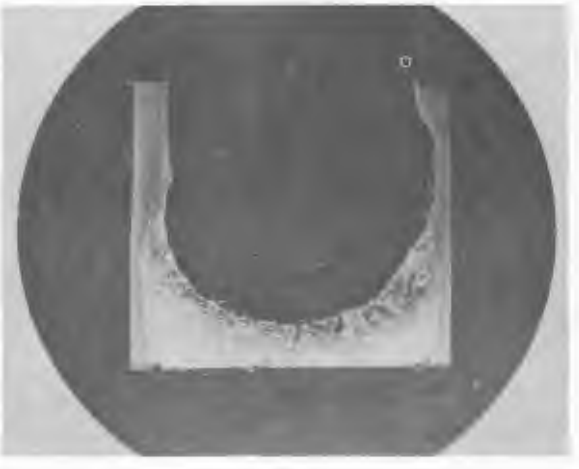

f

Figure 13. Photomicrographs showing corrosion attack by aluminum and uranium-aluminum eutectic

a. Uranium-aluminum in yttrium at 850°C for 137 hours; Test Number 6 (bottom specimen, 500X)

b. Uranium-aluminum in tantalum-tungsten at 800°C for 466 hours; Test Number 8 (150X)

c. Uranium-aluminum in tantalum-tungsten at 900°C for 432 hours; Test Number 9 (250X, polarized light)

d. Aluminum in Inconel at 800°C for 36 hours; Test Number 10 (500X)

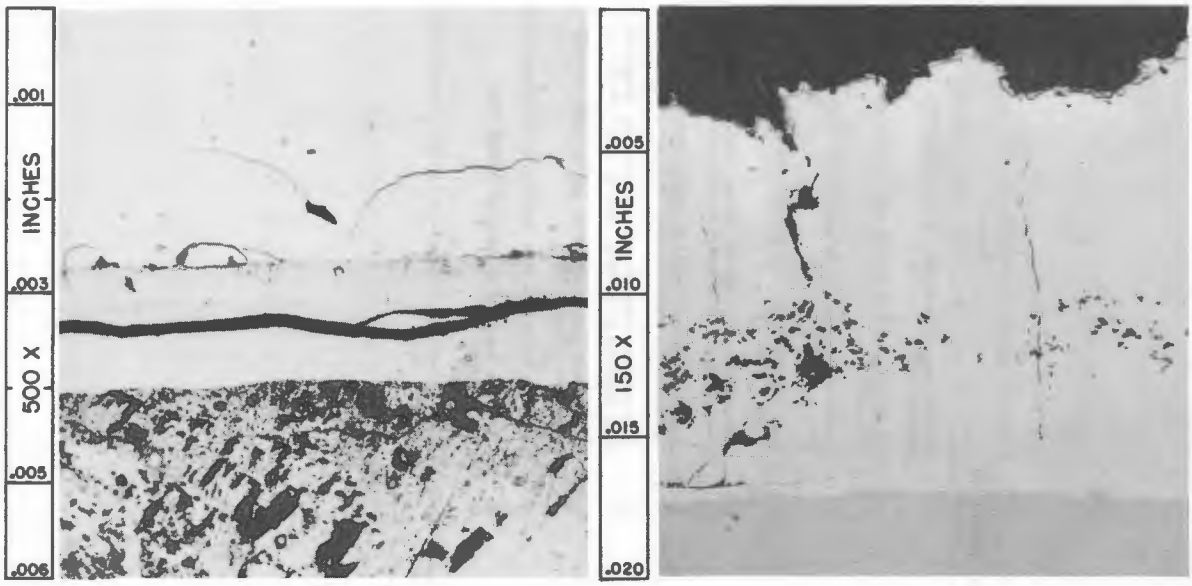
.001
INCHES
.003
500 X
.005
.006
.005
INCHES
.010
150 X
.015
.020

a b

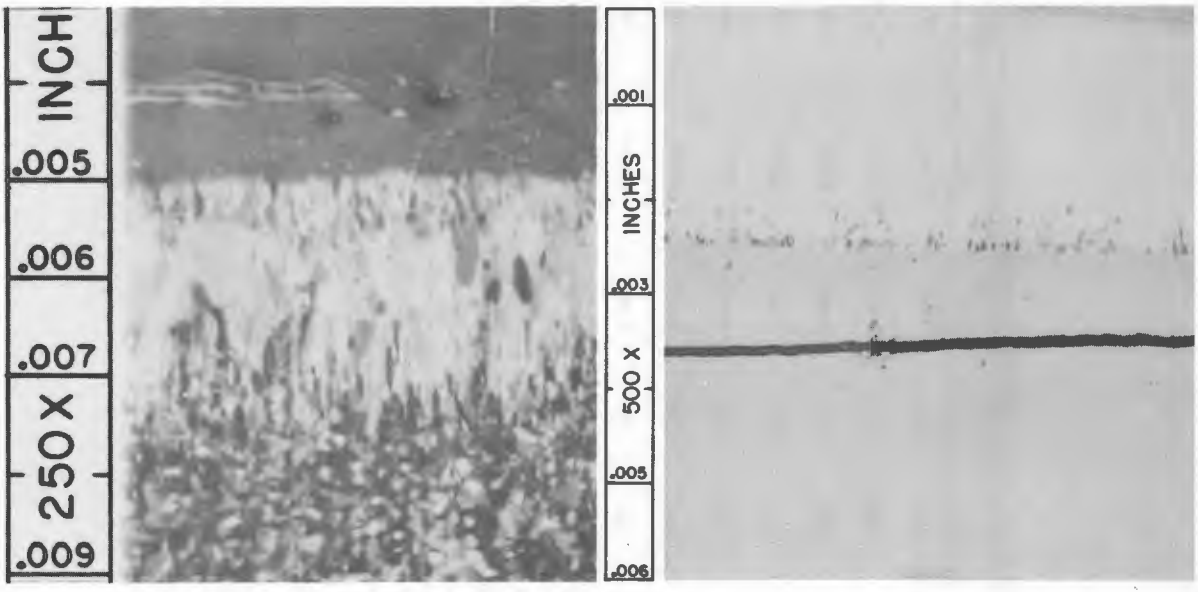
INCH
.005
.006
.007
250X
.009
.001
INCHES
.003
500 X
.005
.006

c d

Table 4. Corrosion test data for aluminum[a] and uranium-aluminum[b]

Test Number	Corrosion system	Test temperature °C	Duration of test hours	Container wall thickness[c] inches	Penetration depth of corrosion inches	Type of corrosion attack[d]	Intermetallic compound formation inches	Arbitrary comparative ratings	Remarks
1	Al in Nb	800	36	0.030	Complete	Ia, 3	>0.030	2	Capsule ends flared out. Al climbed walls (Figure 12a).
2	Al in Nb	800	74	0.030	Complete	Ia, Ic, 3	0.024	2	Al corroded through bottom cap. Al climbed walls (Figure 12b).
3	U-Al in Nb	800	74	0.030	0.015	Ia, 3	0.024	3	Irregular interface. Nb detected in U-Al as weak to moderate[e] (Figure 12c).
4	Al in Ta	800	232	0.030	0.006	Ia, 3	0.017	5	Swelling at bottom. Ta wet but did not climb walls (Figure 12d).
5	U-Al in Ta	800	212	0.030	0.015	Ia, 3	0.060	4	Subsurface void formation in the intermediate phase (Figure 12e). Ta detected as moderate[e].
6	U-Al in Y	850	137	0.074	0.062	Ia, 3	0.017	3	Greatest attack at meniscus region (Figure 12f). Intermetallic compound shown in Figure 13a.
7	U-Al in Y	800	146	0.055	Complete	Ia, 3	--	3	U-Al corroded through wall at meniscus. Remaining U-Al analyzed at Al-44 %, U-22 %, and Y-34 %[f].
8	U-Al in Ta-W	800	466	0.040	Complete	Ia, 3	>0.040	5	U-Al spread over inner walls and corroded through two sides (Figure 13b).
9	U-Al in Ta-W	900	432	0.040	0.032	Ia, 3, 5	>0.040	5	Seems to be preferential leaching of Ta (Figure 13c).
10	Al in Inconel	800	36	0.113	0.047	3, 5	0.012	3	Selective leaching to depth of 0.0008 inch (Figure 13d).

[a] Melting point of aluminum is 660°C.

[b] Melting point of 13.0 wt. % uranium-aluminum eutectic is 640°C.

[c] Tolerance of ±0.001 inch.

[d] Refer to section titled Corrosion by Liquid Metals.

[e] Spectrographical analysis.

[f] Analytical analysis.

container materials chosen for this investigation. Since aluminum is so corrosive as a liquid metal, original plans to test the thorium-aluminum eutectic were dropped as the result of these first ten tests.

Although a number of the tests with aluminum and uranium-aluminum resulted in complete penetration of the container walls, arbitrary competitive ratings above the value of "1" were still given. A comparison of the values will show that some materials are more resistant to attack than others. In particular, tantalum and the tantalum-10 wt. % tungsten alloy showed the best corrosion resistance. Alloying aluminum with uranium also seemed to inhibit some of the corrosive nature of aluminum. This is especially true for niobium, since with aluminum alone there was considerable swelling of the ends of the capsule in less than 36 hours, while alloyed aluminum did not cause any swelling at all after 74 hours. The primary mode of corrosion attack seemed to be uniform solution attack (Type 1a) followed by intermetallic compound formation (Type 3). In the cases of the two alloys, Inconel and tantalum-tungsten, preferential leaching of one or more of the constituents (Type 5) was also noticeable as evidenced by the photomicrographs. Inconel was used as a container strictly as a test material for a basis of comparison. Used to contain aluminum, Inconel was rated as a slightly better container than niobium.

Corrosion by Lead and Its Thorium and Uranium Alloys

Lead, uranium-lead, and thorium-lead were tested in the container metals. Only two capsule tests were run with the alloys of lead, and

Figure 14. Corrosion attack of niobium and tantalum by lead (500X reduced 20 per cent)

a. Lead in niobium at 900°C for 2115 hours; Test Number 14 (Vilella's etch)

b. Lead in niobium at 900°C for 2115 hours; Test Number 15 (Vilella's etch)

c. Lead in niobium at 1100°C for 1255 hours; Test Number 16

d. Lead in tantalum at 700°C for ~ 216 hours; Test Number 18

e. Lead in tantalum at 800°C for ~ 216 hours; Test Number 19

f. Dynamic capsule test of lead in tantalum at 900°C for 1030 hours; Test Number 20

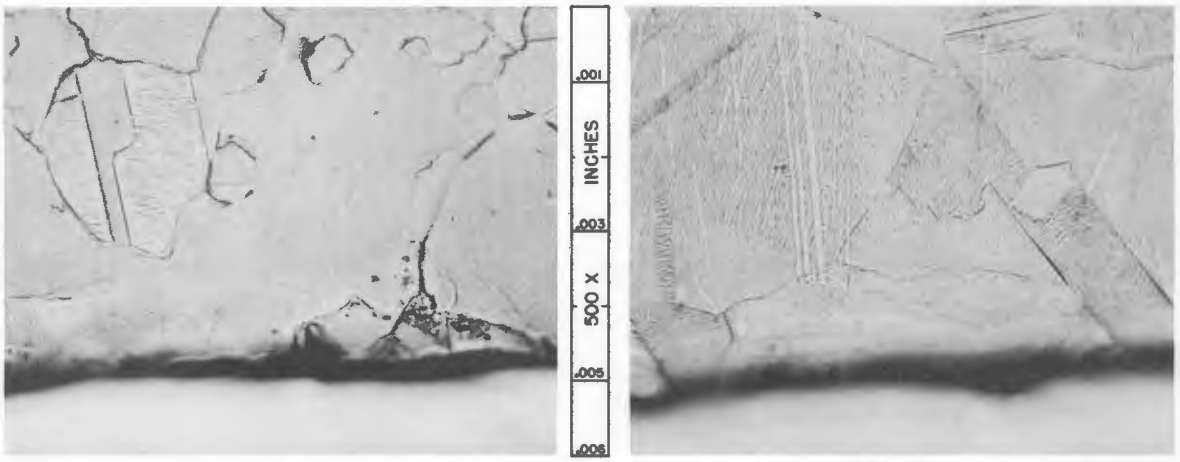
.001
INCHES
.003
500 X
.005
.006

a b

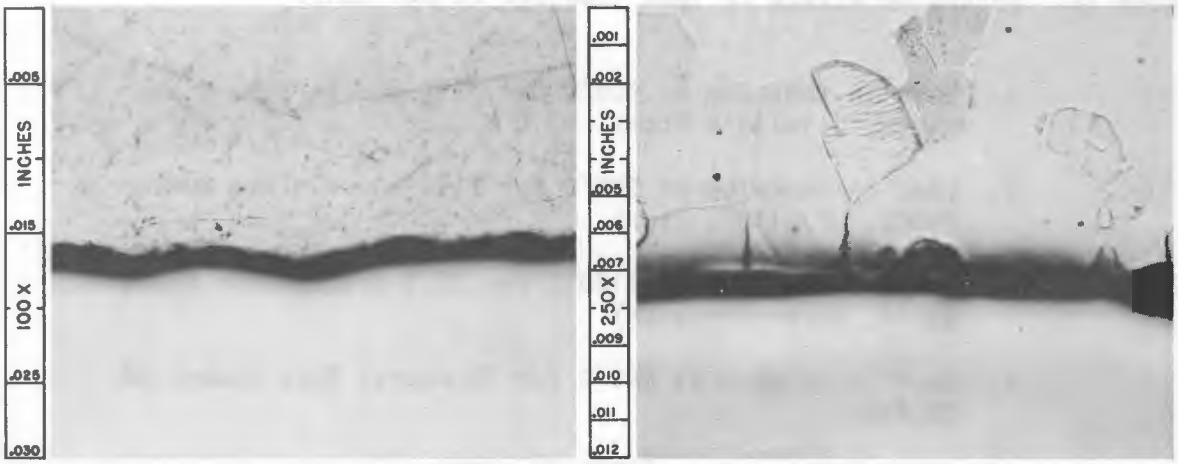
.005
INCHES
.015
100 X
.025
.030
.001
.002
INCHES
.005
.006
.007
250 X
.009
.010
.011
.012

c d

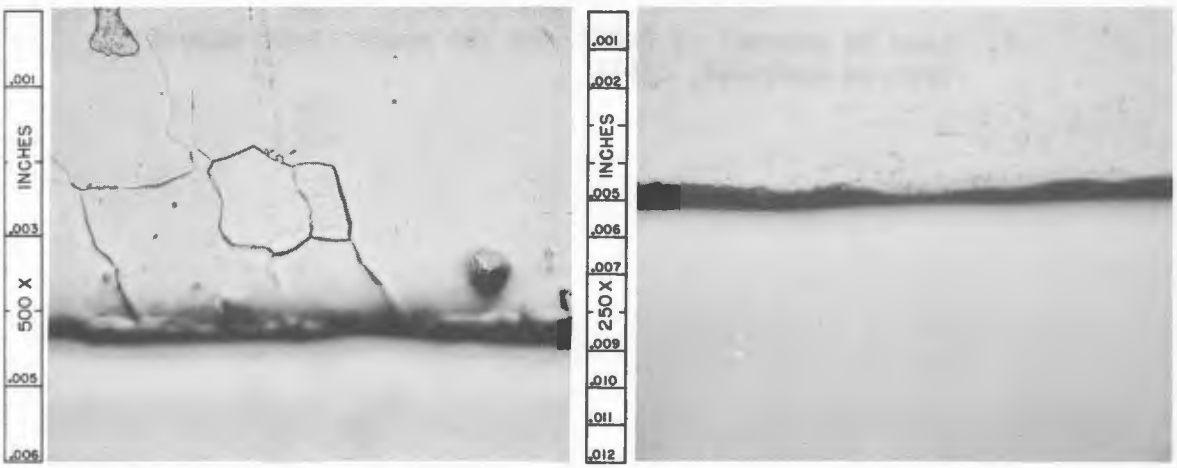
.001
INCHES
.003
500 X
.005
.006
.001
.002
INCHES
.005
.006
.007
250 X
.009
.010
.011
.012

e f

Figure 15. Corrosion attack by lead (reduced 20 per cent)

a. Lead in tantalum at 900°C for 2115 hours; Test Number 21 (500X, Vilella's etch)

b. Lead in tantalum at 900°C for 2115 hours; Test Number 22 (500X, Vilella's etch)

c. Lead in tantalum at 1100°C for 1255 hours; Test Number 23 (500X, Vilella's etch)

d. Lead in yttrium at 800°C for 12 hours; Test Number 28 (2.8X)

e. Lead in Inconel at 800°C for 100 hours; Test Number 29 (top specimen, 250X)

f. Lead in Inconel at 800°C for 100 hours; Test Number 29 (bottom specimen, 250X)

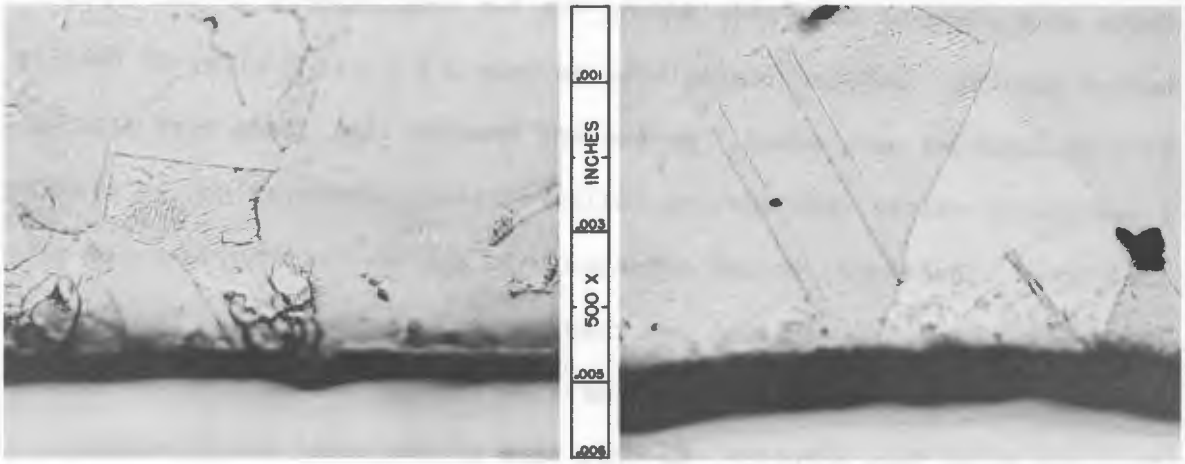
.001
INCHES
.003
500 X
.005
.006

a b

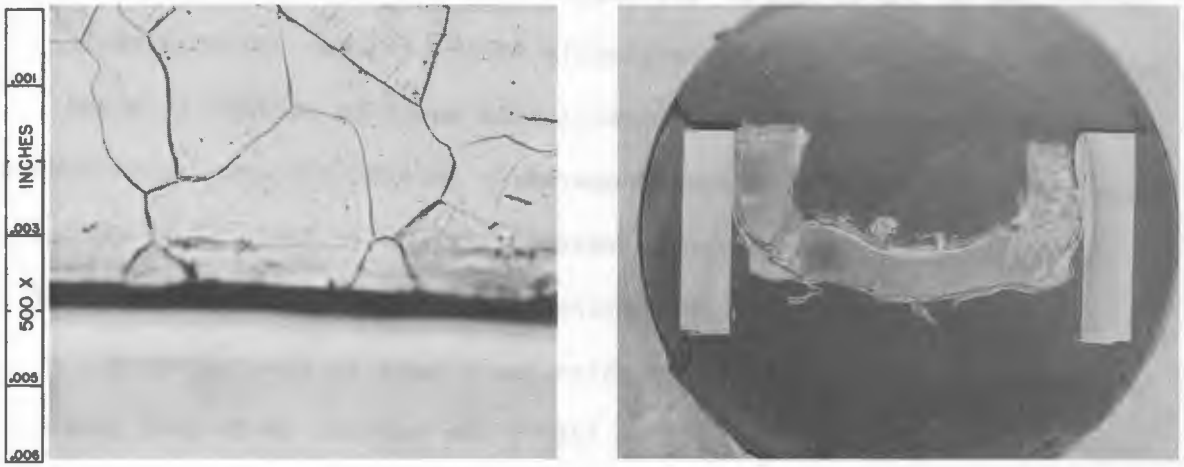
.001
INCHES
.003
500 X
.005
.006

c d

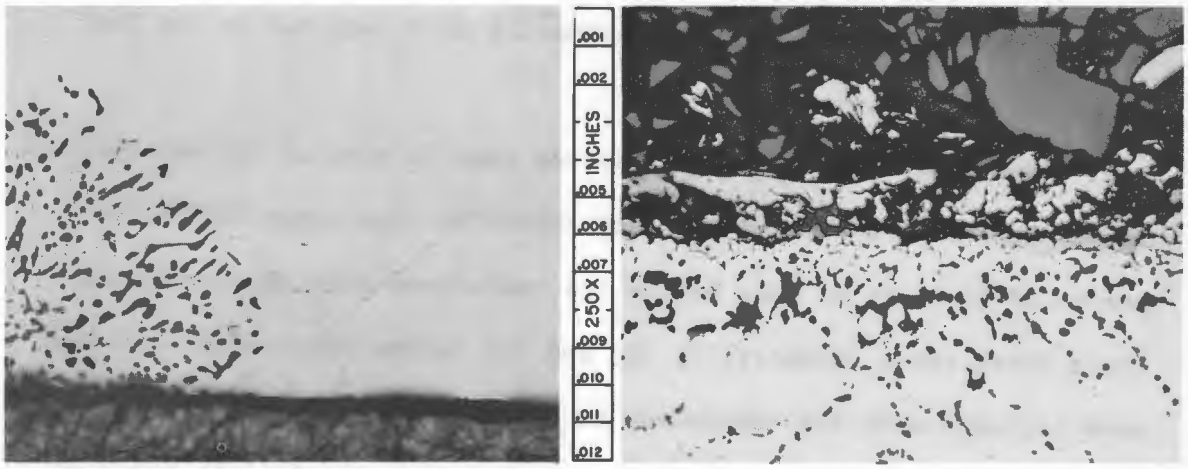
.001
.002
INCHES
.005
.006
.007
250 X
.009
.010
.011
.012

e f

these were prepared by simply adding the two constituents to the capsule before sealing. Weighed ingredients to make a 2.0 wt. % alloy of fertile or fuel material were added. Hansen and Anderko (39) state that thorium dissolves in molten lead and, on solidification, separates out in elementary form. Therefore, it was expected that all of the thorium would go into solution during the test and then precipitate out during the cooling process. For uranium-lead only a small percentage of the uranium was expected to go into solution, so that some of the metal would remain undissolved on the bottom of the capsule. In this way the solution would remain saturated. If the capsule tests had been run as dynamic, isothermal tests where the two constituents would be constantly mixed, then the alloys would have been prepared in an electric arc vacuum furnace.

The results of the corrosion tests are shown in Table 5. Figure 14 through Figure 15 represent photomicrographs of the interface region of the various systems tested. Corrosion tests made in this category ranged in temperature from 650° to 1100°C for periods up to 2115 hours. Overall, thirteen capsule tests were run, all in a static, isothermal state with the exception of Test Number 20 which was run in the 360° rotating muffle furnace.

Three static tests with the system lead in niobium failed when two faulty controllers allowed the temperature to rise above 1200°C for a period of 24 hours or more before the resistance windings burned out. These three tests (Numbers 11, 12, and 13) failed completely, but they were included with the tabulation as a comparison with Test Numbers 18 and 19 which were also in the same furnaces when the failure occurred.

Table 5. Corrosion data for lead and its thorium and uranium alloys

Test Number	Corrosion system	Test temperature °C	Duration of test hours	Container wall thickness[a] inches	Penetration depth of corrosion inches	Type of corrosion attack[b]	Intermetallic compound formation inches	Arbitrary comparative ratings	Remarks
11	Pb in Nb	700[c]	<216	0.030	Complete	--	--	--	Capsule disintegrated when faulty controller allowed temperature to go above 1200°C. No metallographic data.
12	Pb in Nb	700[c]	<12	0.030	Complete	--	--	--	See note above.
13	Pb in Nb	800[c]	<216	0.030	Complete	--	--	--	See note above.
14	Pb in Nb	900	2115	0.031	<0.0005	Ia[d]	None	10	Little or no corrosion attack. Pb wet but did not climb walls (Figure 14a).
15	Pb in Nb	900	2115	0.031	<0.001	Ia	None	9	Slight amount of solution attack. Capsule walls were wet to 3/8 in. above meniscus (Figure 14b).
16	Pb in Nb	1100	1255	0.029	0.001	Ia	None	9	Varying degrees of solution attack up to 0.001 in. Wetting up to meniscus region (Figure 14c).
17	Th-Pb in Nb[e]	650	230	0.030	None	--	None	10	Th-Pb could be easily removed from capsule. Meniscus was turned down as alloy did not wet walls.
18	Pb in Ta	700[c]	<216	0.031	<0.0005	Ia[d]	None	10	Short exposure to >1200°C temperature did not cause any noticeable attack (Figure 14d).
19	Pb in Ta	800[c]	<216	0.030	<0.0005	Ia[d]	None	10	Pb wet walls only to meniscus region (Figure 14e).
20	Pb in Ta	900	1030	0.030	<0.0005	Ia[d]	None	10	Interface slightly irregular but varies <0.0005 in. 360° rotating capsule test. Pb wet walls (Figure 14f).
21	Pb in Ta	900	2115	0.031	None	--	None	10	Slight gap at interface caused by contraction during cooling (Figure 15a).
22	Pb in Ta	900	2115	0.0315	<0.0005	Ia[d]	None	10	Interface slightly irregular but varies <0.0005 in. See Figure 15b. Separation at interface.

[a] Tolerance of ±0.001 inch.

[b] Refer to section titled Corrosion by Liquid Metals.

[c] Faulty temperature controller allowed temperature to rise above 1200°C.

[d] Corrosion is probably Type Ia if attack occurred.

[e] Melting point data are not available since Th precipitates out upon cooling.

Table 5 (Continued)

Test Number	Corrosion system	Test temperature °C	Duration of test hours	Container wall thickness[a] inches	Penetration depth of corrosion inches	Type of corrosion attack[b]	Intermetallic compound formation inches	Arbitrary comparative ratings	Remarks
23	Pb in Ta	1100	1255	0.031	None	--	None	10	Smooth interface. Pb wet walls slightly. No corrosion at 500X (Figure 15c).
24	U-Pb in Ta[f]	650	230	0.031	None	--	None	10	U-Pb could be easily removed from capsule. Meniscus was turned down as alloy did not wet walls.
25	Pb in Y	700	67	0.055	Complete	1a, 3	>0.055	1	Pb alloyed directly with Y to form a new system and did not climb the walls.
26	Pb in Y	800	50	0.055	Complete	1a, 3	>0.055	1	See note above.
27	Pb in Y	700	50	0.055	Complete	1a, 3	>0.055	1	See note above.
28	Pb in Y	800	12	0.055	Complete	1a, 3	>0.055	1	Figure 15d shows bottom of capsule sandwiched between Inconel. Y has been completely absorbed into the lead.
29	Pb in Inconel	800	100	0.113	Top[g] 0.011 Bottom 0.011	1b, 5 1b, 5	None None	8	Decarburization of Inconel to 0.011 in. depth along grain boundaries--apparent on etched specimens. More prominent on bottom specimen (Figures 15e and 15f).

[f] Melting point at approximately 600°C.

[g] Two metallographic specimens were examined.

The latter two tests did not fail and showed very good signs of corrosion resistance. In general, the tests with lead in niobium showed slight amounts of solution attack except for Test Number 17, thorium-lead in niobium, which was run at only 650°C for 230 hours. This test showed no signs of attack. Spectrographical analysis of the liquid metals from Test Numbers 16 and 17 were inconclusive when compared to the metallographic analyses. Test Number 16 showed signs of about 0.001 inch of solution attack, but the spectrographic analysis indicated that no niobium was detected, meaning less than 20 ppm present. On the other hand, Test Number 17 which showed no metallographic signs of attack indicated niobium present as a faint trace with interference. In this case the interference indicates that niobium may not conclusively be present. In most cases, however, the results of the metallographic examinations were considered as more conclusive.

Tests with lead in tantalum showed a greater resistance to liquid-metal corrosion than the tests in niobium. All of these tests suffered little or no attack even at temperatures up to 1100°C. Any attack which may have occurred with the lead in tantalum system was less than 0.0005 inches. The slight irregularity of the interfaces of some of the metallographic specimens examined indicates that very slight uniform solution attack (Type 1a) may have resulted. As a check, spectrographical analyses were run on the liquid metals upon completion of the tests. In all cases a blank sample of lead was submitted which had not been contacted with the tantalum. Unfortunately tantalum was detected in both the blank samples and the liquid metals run in the capsules as a faint trace with

interference. Because of this fact, no conclusions could be made from the spectrographical analyses for the lead run in tantalum.

Test Number 24 showed that the uranium had partially settled in the bottom of the capsule; hence two specimens were prepared for analytical analysis. The top layer contained 0.008 wt. % uranium while the bottom layer was reported as 9.96 wt. % uranium. Actual compositions present during the test were not determined since no method of sampling was devised.

The 360° rotating furnace test (Number 20) did not show any definite signs of attack except for a slightly irregular interface between the liquid metal and solid metal as shown in Figure 14f. This test compared with its companion tests equally well, if not better. Hansen and Anderko (39) do not give any information about the binary systems lead-tantalum or lead-niobium while Miller (52) states that there is little reaction between lead and tantalum or lead and niobium. The results of these tests seem to substantiate this claim, and tantalum is definitely the better of the two metals.

All four tests conducted with lead in yttrium ended in complete failure of the capsules. Rapid solution attack and intermetallic formation are the mechanisms by which corrosion takes place. Lead did not climb the walls but alloyed directly with the yttrium to form a new compound. Gschneidner (34) does not report any information on the lead-yttrium system since it has not as yet been studied extensively. Considerable expansion of the capsules occurred, leaving a hollow interior. Upon sectioning these capsules and rinsing with water, it was noticed that an exothermic reaction occurs giving off enough heat to make the capsule too

hot to touch by hand. The lowest comparative rating of "1" was given to these tests since the corrosion reaction is so rapid, taking place in less than 12 hours.

The comparison test employing lead in Inconel showed signs of decarburization and grain boundary attack. These types of attack are clearly evident in the photomicrographs shown in Figure 15e and Figure 15f. This system was given a comparative rating of "8".

Corrosion by Tin and Its Thorium and Uranium Alloys

The majority of the tests conducted in this investigation were with tin, uranium-tin, and thorium-tin in the selected container materials. Five tests with an alloy of uranium, bismuth, and tin prepared in graphite crucibles were run in tantalum. Bismuth was chosen because of its early success in tantalum (28, 29) and the higher percentage of uranium which is soluble in it (18, 46, 56, 65). All thirty-eight of the tests are tabulated in Table 6. Figure 16 through Figure 25 contain photomicrographs of the specimens examined. It will be noticed that a number of the tests include results obtained from two metallographic specimens. This was done either because the tin attacked one region of the capsule more predominantly or because an alloy was used for the test in which a separation of the constituents was observed between the top and bottom parts of the liquid metal.

Eight static and one 135° dynamic, isothermal tests were conducted in niobium. These tests varied from 650 to 1100°C and from 194 to 2023 hours. Three of these tests failed including the 135° rocking furnace test using

Figure 16. Corrosion attack to niobium by tin (reduced 20 per cent)

a. Test Number 30 at 700°C for 622 hours (500X)

b. Test Number 31 at 900°C for 660 hours (top specimen, 500X)

c. Test Number 31 at 900°C for 660 hours (bottom specimen, 100X)

d. Test Number 32 at 600°C for 2500 hours (top specimen, 250X)

e. Test Number 32 at 600°C for 2500 hours (bottom specimen, 500X, polarized light)

f. Test Number 33 at 1100°C for 225 hours (250X)

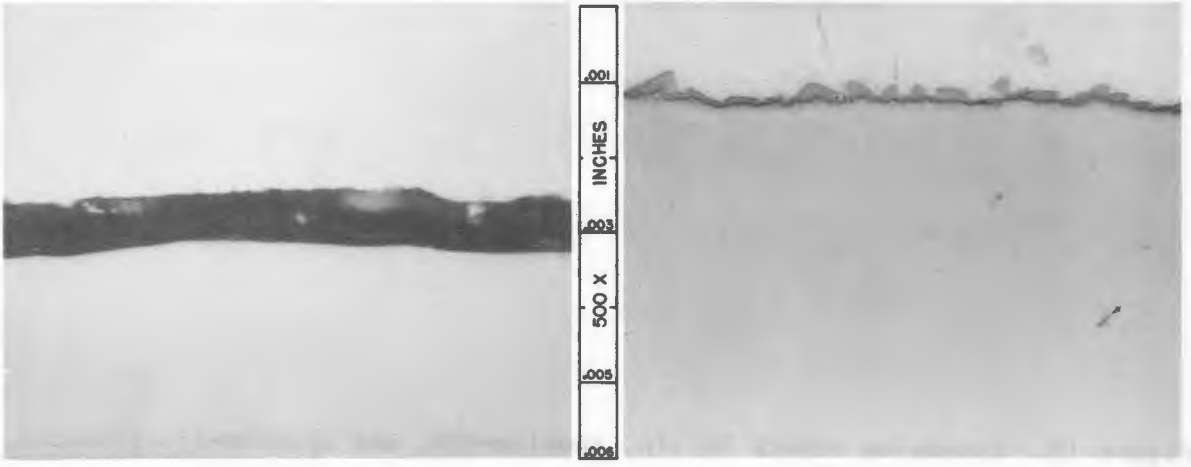
.001
INCHES
.003
500 X
.005
.006

a b

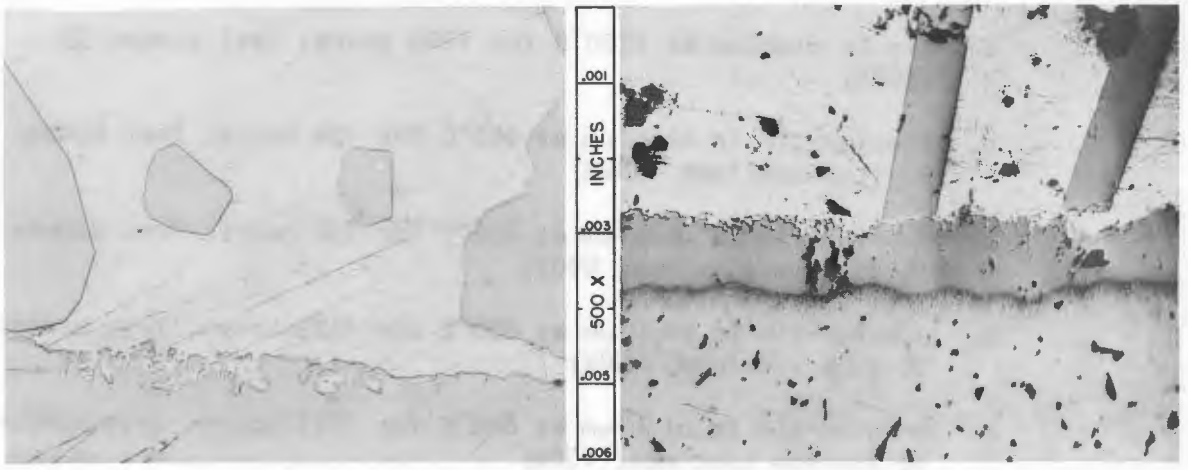
.001
INCHES
.003
500 X
.005
.006

c d

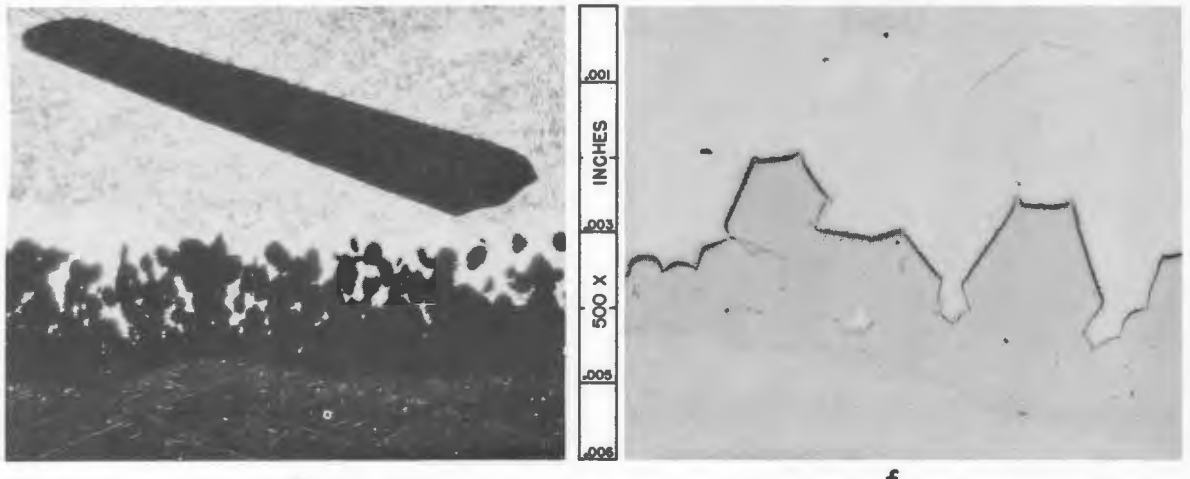
.001
INCHES
.003
500 X
.005
.006

e f

Figure 17. Corrosion attack by tin, thorium-tin, and uranium-tin (reduced 20 per cent)

a. Tin in niobium at 1100°C for 1000 hours; Test Number 35 (500X)

b. Thorium-tin in niobium at 650°C for 194 hours; Test Number 36 (top specimen, 500X)

c. Thorium-tin in niobium at 650°C for 194 hours; Test Number 36 (bottom specimen, 500X)

d. Uranium-tin in niobium at 800°C for 1225 hours; Test Number 38 (top specimen, 150X)

e. Uranium-tin in niobium at 800°C for 1225 hours; Test Number 38 (bottom specimen, 150X)

f. Tin in tantalum at 700°C for 576 hours; Test Number 39 (500X)

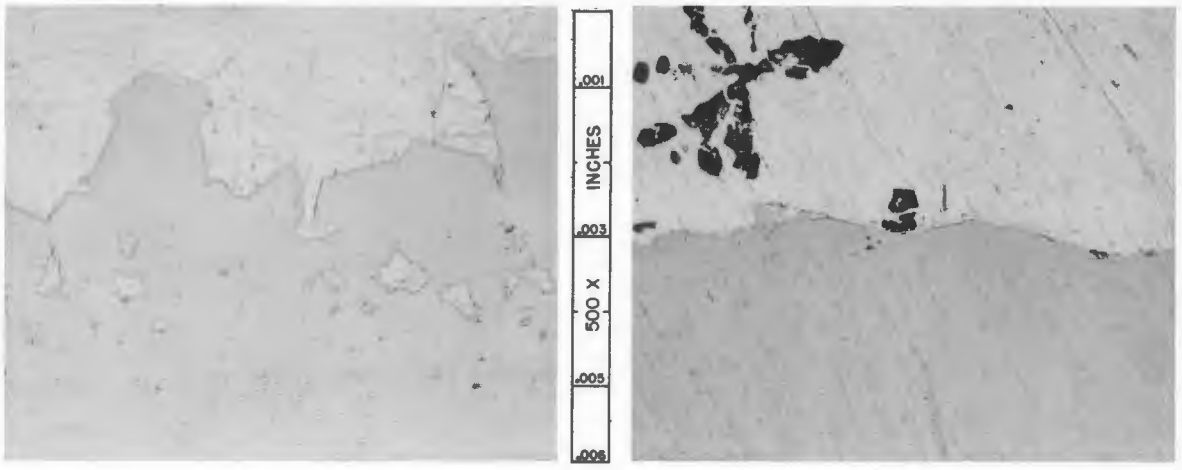
.001
INCHES
.003
500 X
.005
.006

a b

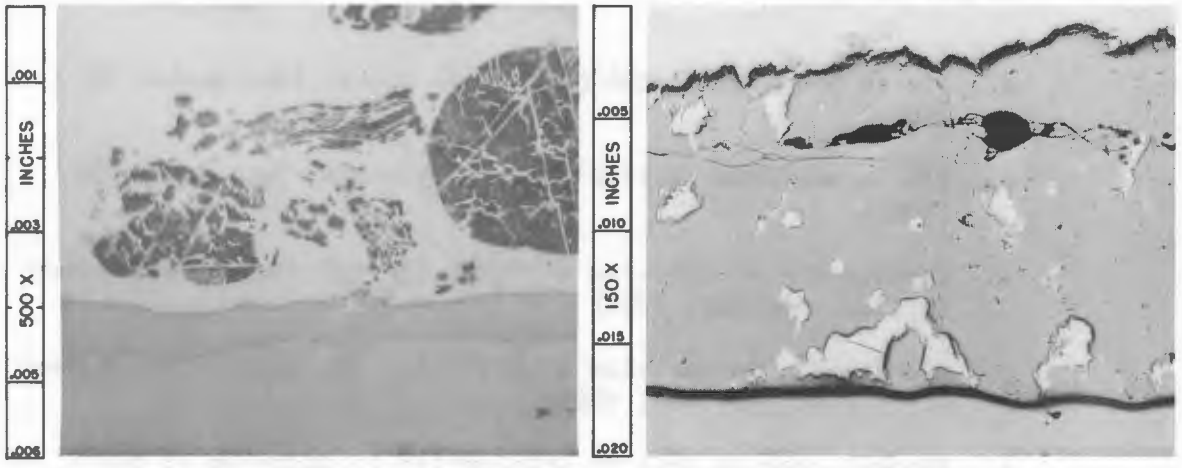
.001
INCHES
.003
500 X
.005
.006
.005
INCHES
.010
150 X
.015
.020

c d

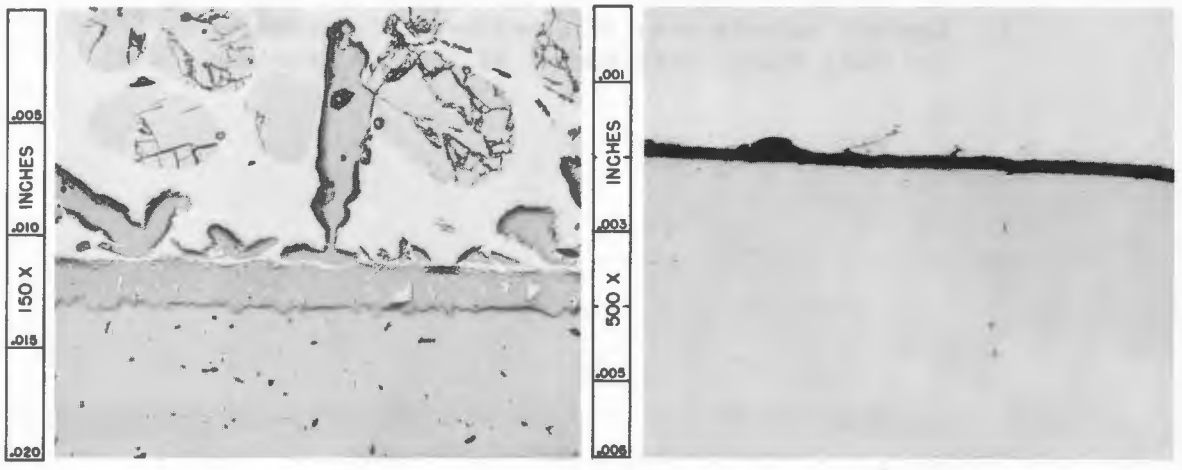
.005
INCHES
.010
150 X
.015
.020
.001
INCHES
.003
500 X
.005
.006

e f

Figure 18. Corrosion attack by tin and uranium-tin in tantalum (reduced 20 per cent)

a. Tin in tantalum at 900°C for 1500 hours; Test Number 40 (500X)

b. Tin in tantalum at 1100°C for 1255 hours; Test Number 41 (500X)

c. Uranium-tin in tantalum at 650°C for 192 hours; Test Number 42 (top specimen, 500X)

d. Uranium-tin in tantalum at 650°C for 192 hours; Test Number 42 (bottom specimen, 500X)

e. Dynamic capsule test of uranium-tin in tantalum at 800°C for 2023 hours; Test Number 43 (top specimen, 500X)

f. Dynamic capsule test of uranium-tin in tantalum at 800°C for 2023 hours; Test Number 43 (bottom specimen, 500X)

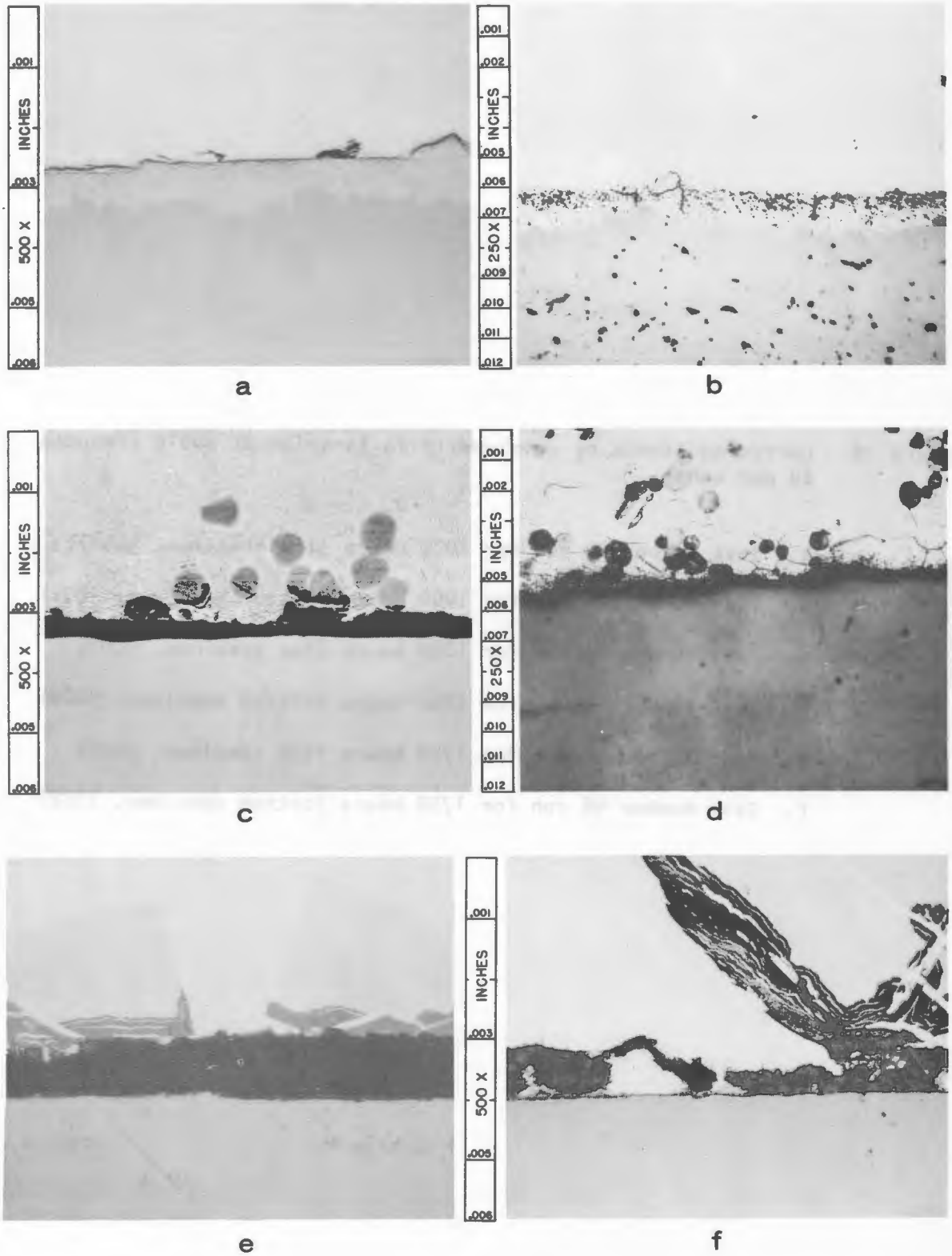
.001
INCHES
.003
500 X
.005
.006
.001
.002
INCHES
.005
.006
.007
250X
.009
.010
.011
.012
a
b
c
d
e
f

Figure 19. Corrosion attack by uranium-tin in tantalum at 800°C (reduced 20 per cent)

a. Test Number 44 run for 1000 hours (top specimen, 500X)

b. Test Number 44 run for 1000 hours (bottom specimen, 500X)

c. Test Number 45 run for 1000 hours (top specimen, 500X)

d. Test Number 45 run for 1000 hours (bottom specimen, 500X)

e. Test Number 46 run for 1750 hours (top specimen, 250X)

f. Test Number 46 run for 1750 hours (bottom specimen, 250X)

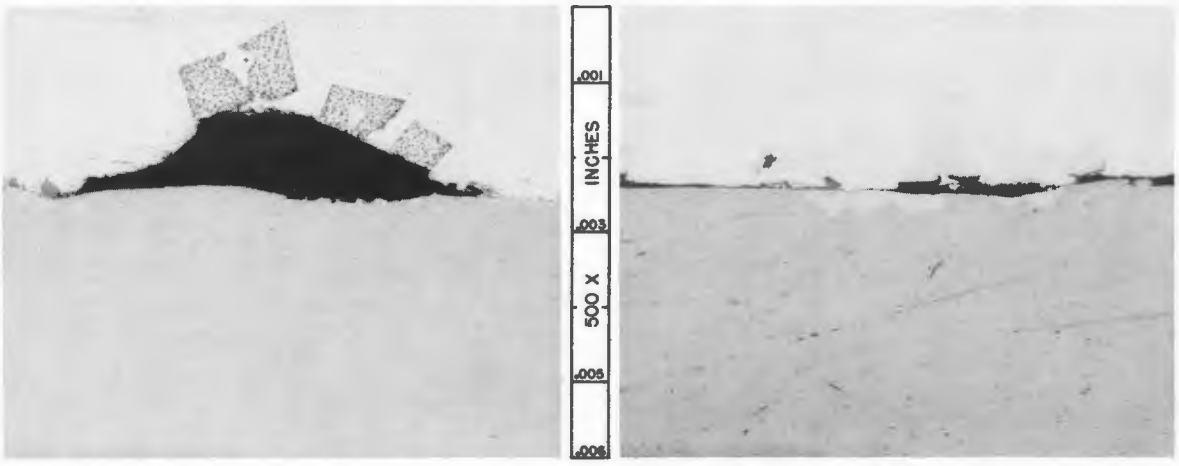
.001
INCHES
.003
500 X
.005
.006

a b

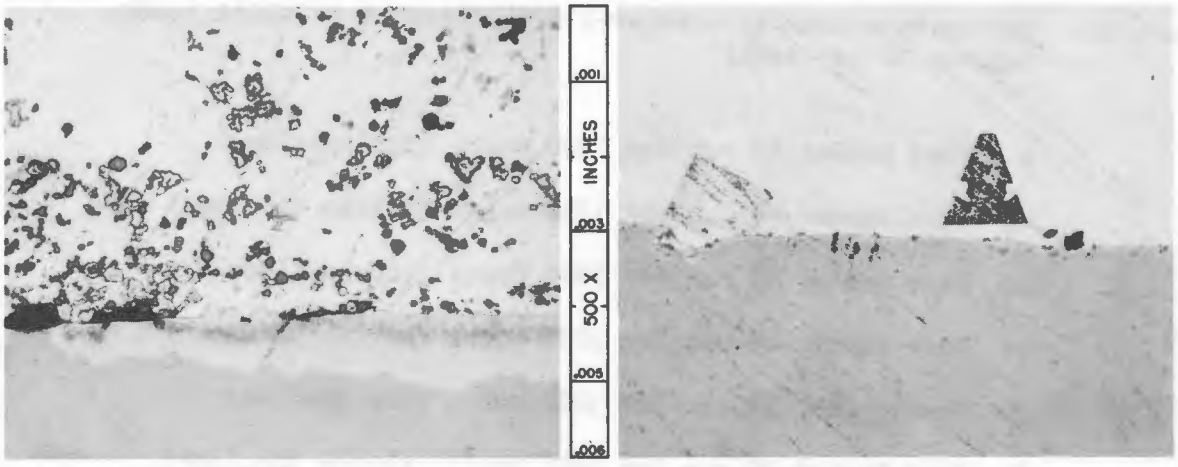
.001
INCHES
.003
500 X
.005
.006

c d

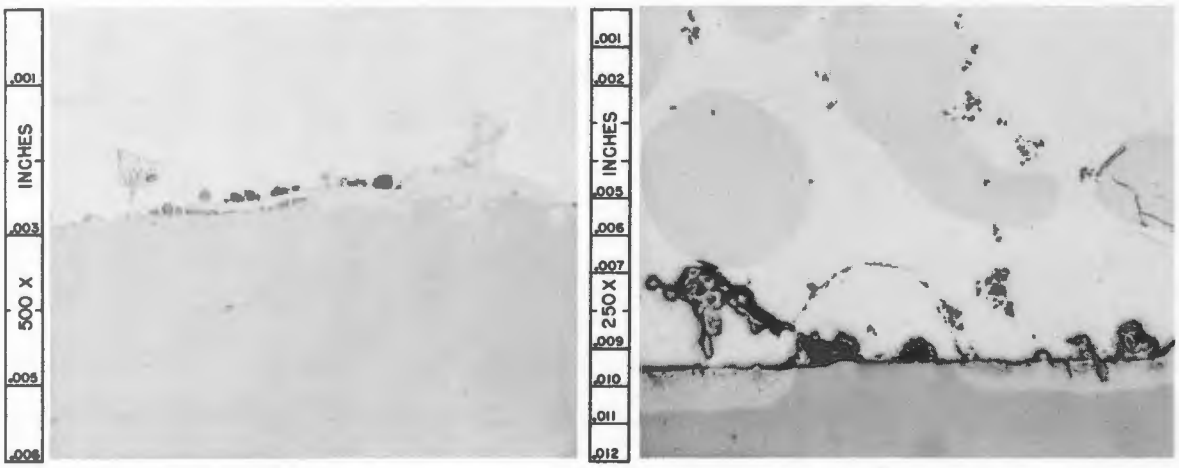
.001
INCHES
.003
500 X
.005
.006
.001
.002
INCHES
.005
.006
.007
250X
.009
.010
.011
.012

e f

Figure 20. Corrosion attack by uranium-tin in tantalum at 800°C (500X, reduced 20 per cent)

a. Test Number 47 run for 1750 hours (top specimen)

b. Test Number 47 run for 1750 hours (bottom specimen)

c. Test Number 48 run for 3000 hours (top specimen)

d. Test Number 48 run for 3000 hours (bottom specimen)

e. Test Number 49 run for 3000 hours (top specimen)

f. Test Number 49 run for 3000 hours (bottom specimen)

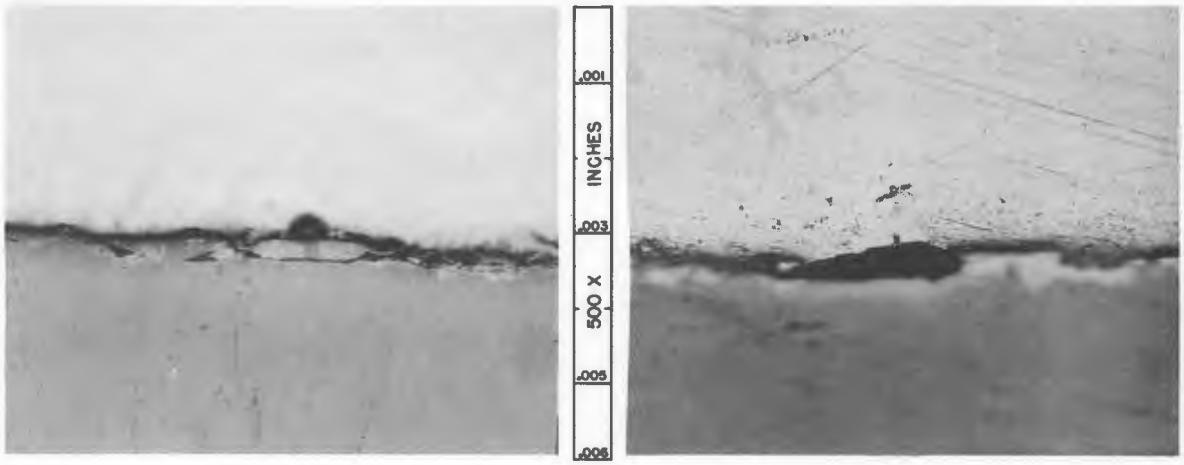
.001
INCHES
.003
500 X
.005
.006

a b

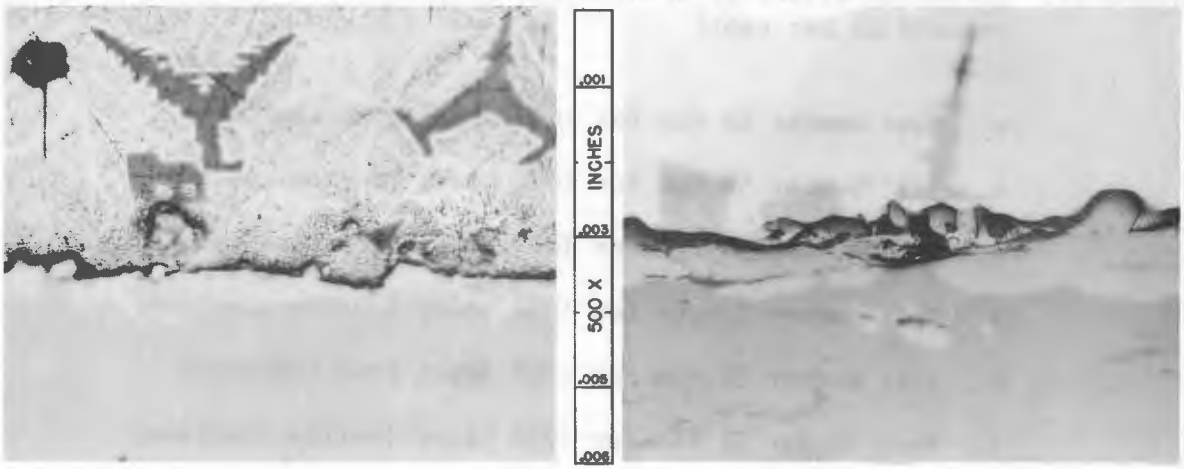
.001
INCHES
.003
500 X
.005
.006

c d

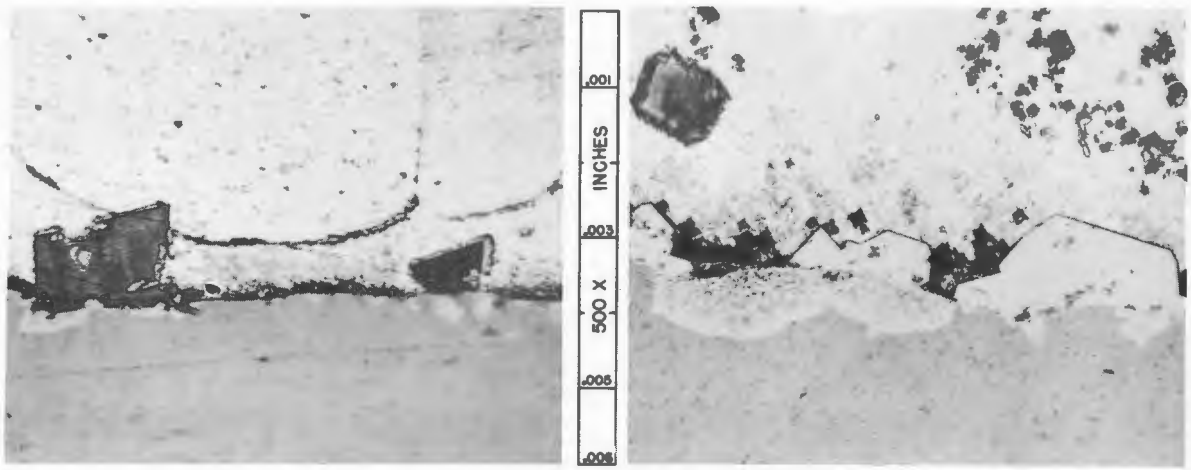
.001
INCHES
.003
500 X
.005
.006

e f

Figure 21. Corrosion attack by uranium-tin in tantalum at 950°C (500X, reduced 20 per cent)

a. Test Number 50 run for 1000 hours (top specimen)

b. Test Number 50 run for 1000 hours (bottom specimen)

c. Test Number 51 run for 1000 hours (top specimen)

d. Test Number 51 run for 1000 hours (bottom specimen)

e. Test Number 52 run for 1750 hours (top specimen)

f. Test Number 52 run for 1750 hours (bottom specimen)

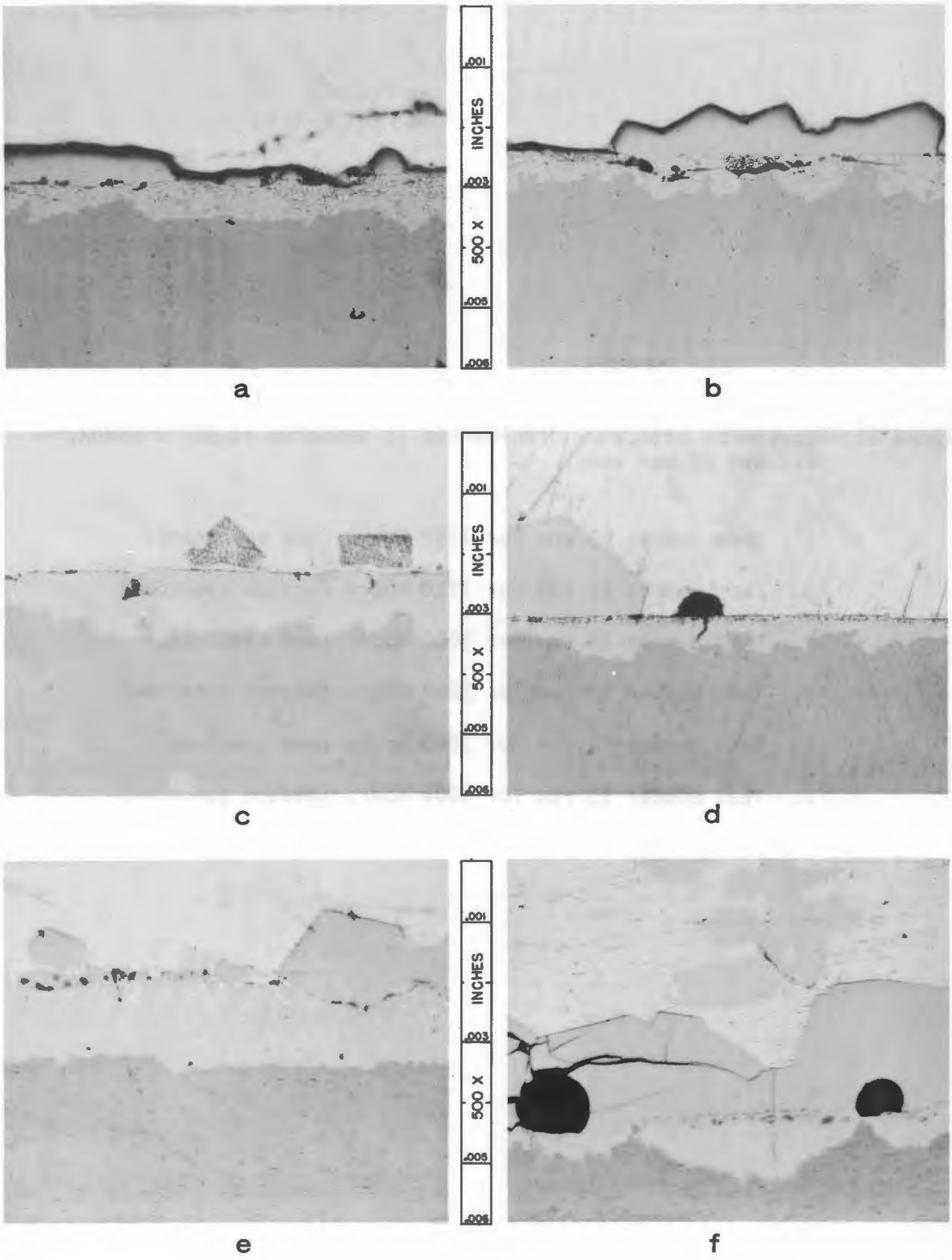
.001
INCHES
.003
500 X
.005
.006
a
b
c
d
e
f

Figure 22. Corrosion attack by uranium-tin in tantalum at 950°C (500X, reduced 20 per cent)

a. Test Number 53 run for 1750 hours (top specimen)

b. Test Number 53 run for 1750 hours (bottom specimen)

c. Test Number 54 run for 3000 hours (top specimen)

d. Test Number 54 run for 3000 hours (bottom specimen)

e. Test Number 55 run for 3000 hours (top specimen)

f. Test Number 55 run for 3000 hours (bottom specimen)

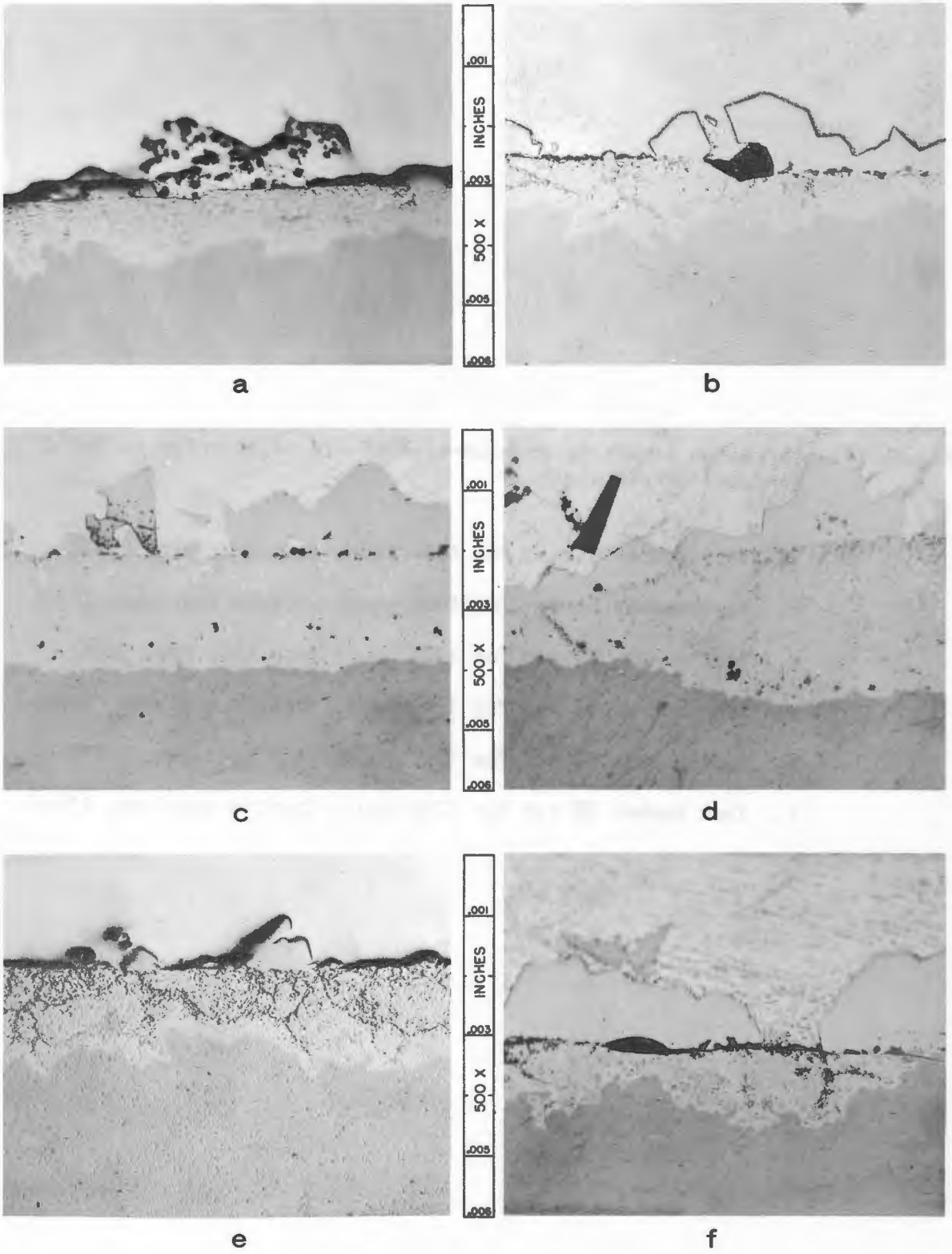
.001
INCHES
.003
500 X
.005
.006
a
b
c
d
e
f

Figure 23. Corrosion attack by uranium-bismuth-tin in tantalum at 950°C (reduced 20 per cent)

a. Test Number 56 run for 1000 hours (top specimen, 250X)

b. Test Number 56 run for 1000 hours (bottom specimen, 250X)

c. Test Number 57 run for 1000 hours (top specimen, 500X)

d. Test Number 57 run for 1000 hours (bottom specimen, 500X)

e. Test Number 58 run for 1750 hours (top specimen, 250X)

f. Test Number 58 run for 1750 hours (bottom specimen, 250X)

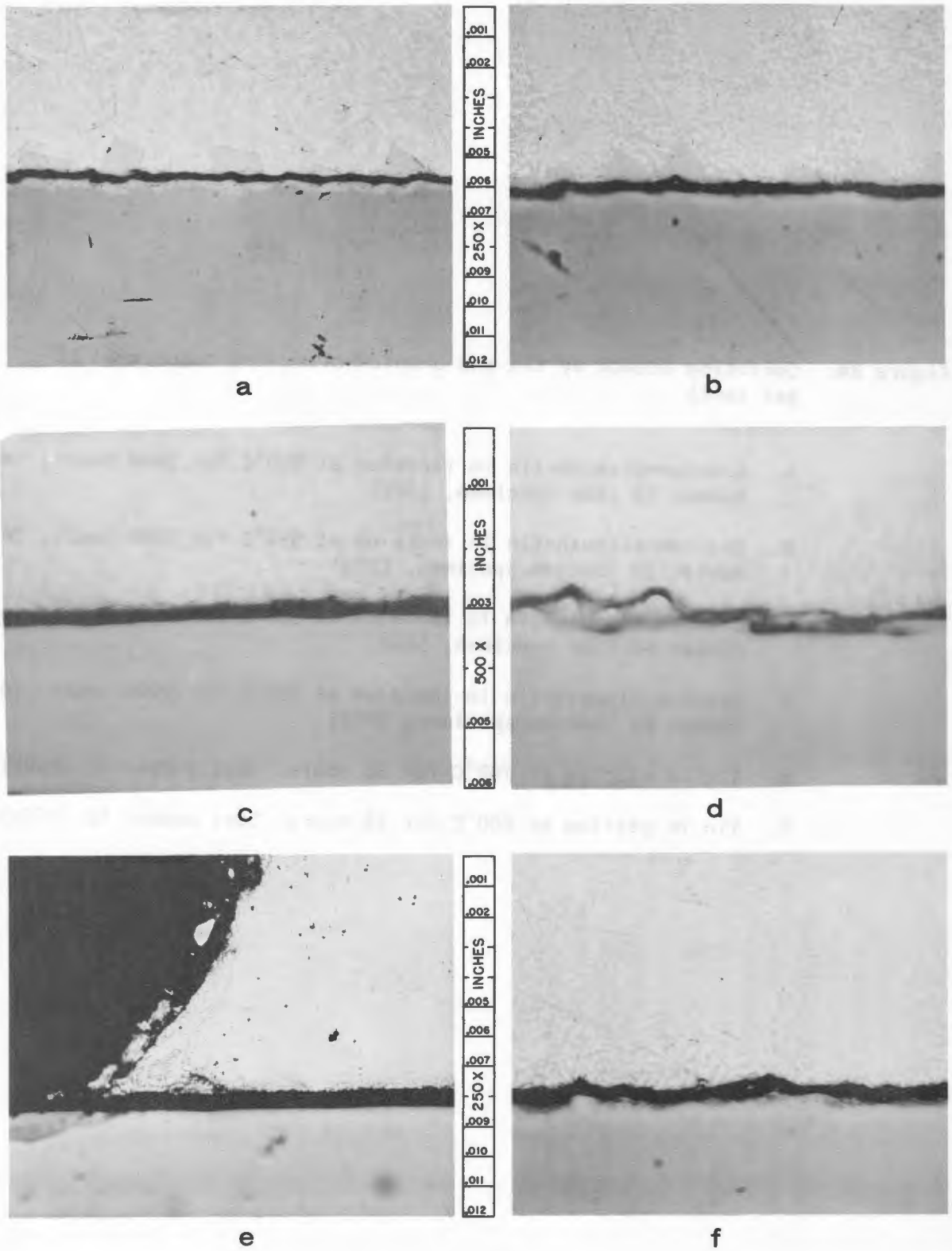
.001
.002
INCHES
.005
.006
.007
250 X
.009
.010
.011
.012
a
b
.001
INCHES
.003
500 X
.005
.006
c
d
.001
.002
INCHES
.005
.006
.007
250 X
.009
.010
.011
.012
e
f

Figure 24. Corrosion attack by tin and uranium-bismuth-tin (reduced 20 per cent)

a. Uranium-bismuth-tin in tantalum at 950°C for 3000 hours; Test Number 59 (top specimen, 250X)

b. Uranium-bismuth-tin in tantalum at 950°C for 3000 hours; Test Number 59 (bottom specimen, 250X)

c. Uranium-bismuth-tin in tantalum at 950°C for 3000 hours; Test Number 60 (top specimen, 500X)

d. Uranium-bismuth-tin in tantalum at 950°C for 3000 hours; Test Number 60 (bottom specimen, 500X)

e. Tin in yttrium at 700°C for 52 hours; Test Number 61 (250X)

f. Tin in yttrium at 800°C for 36 hours; Test Number 62 (150X)

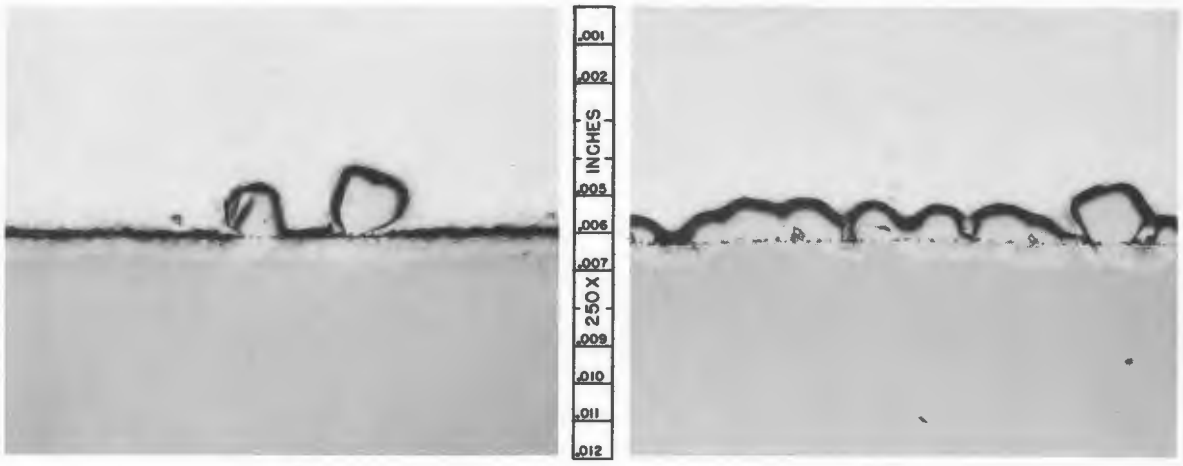
.001
.002
INCHES
.005
.006
.007
250 X
.009
.010
.011
.012

a b

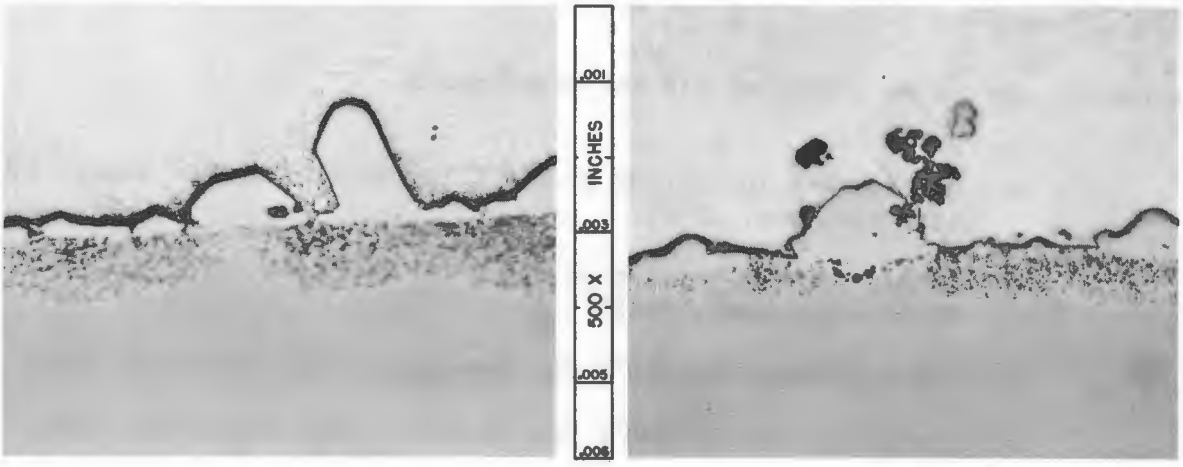
.001
INCHES
.003
500 X
.005
.008

c d

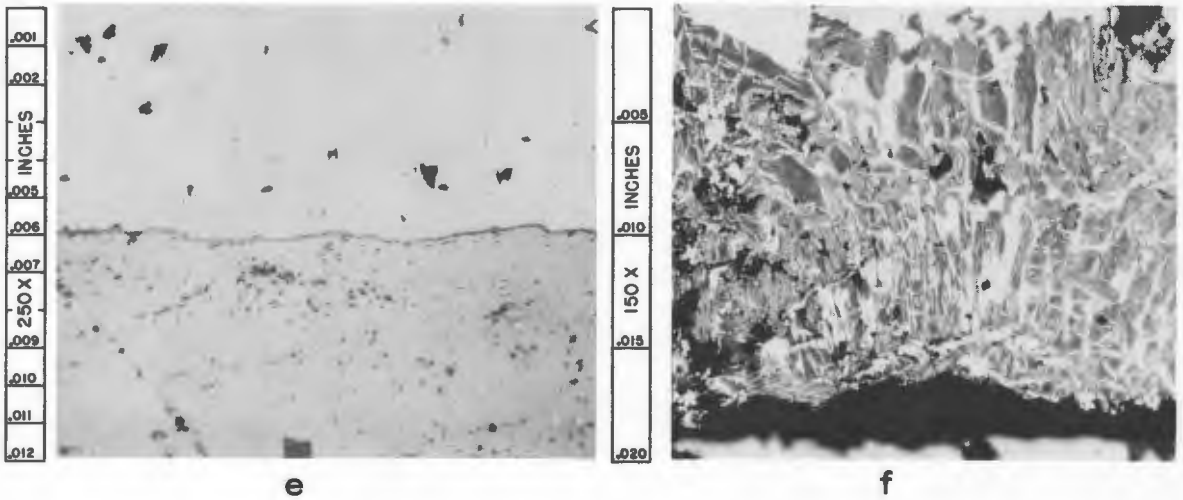
.001
.002
INCHES
.005
.006
.007
250 X
.009
.010
.011
.012
.005
INCHES
.010
150 X
.015
.020

e f

Figure 25. Corrosion attack by tin and uranium-tin

a. Uranium-tin in yttrium at 850°C for 64 hours; Test Number 64 (top specimen, 100X)

b. Uranium-tin in yttrium at 850°C for 64 hours; Test Number 64 (bottom specimen, 100X)

c. Tin in Inconel at 700°C for 244 hours; Test Number 65 (50X)

d. Tin in Inconel at 800°C for 72 hours; Test Number 66 (500X)

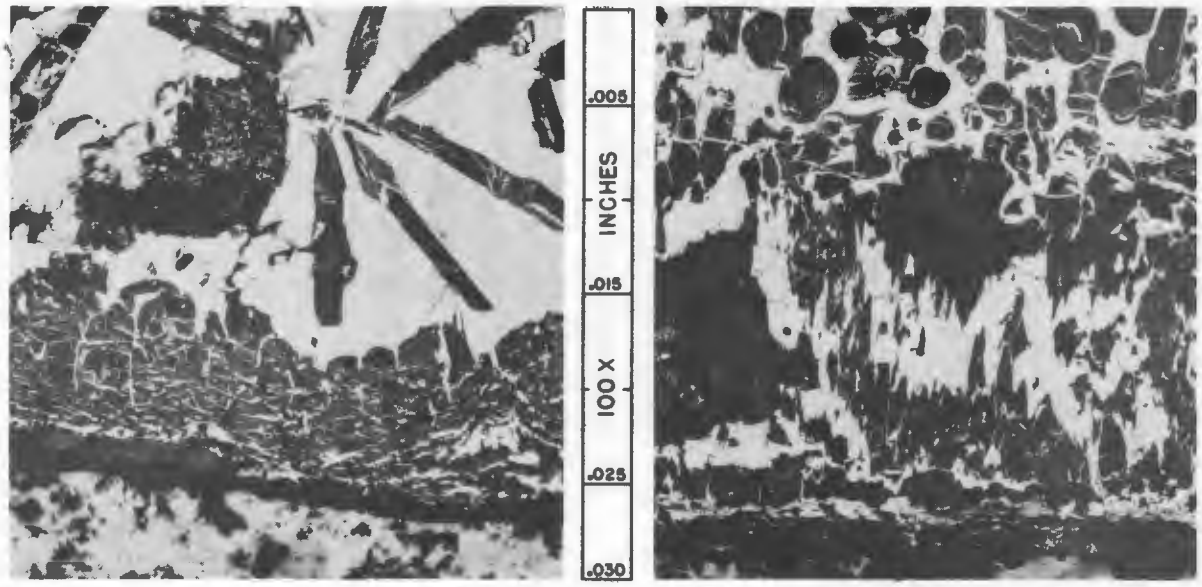
.005
INCHES
.015
100 X
.025
.030

a b

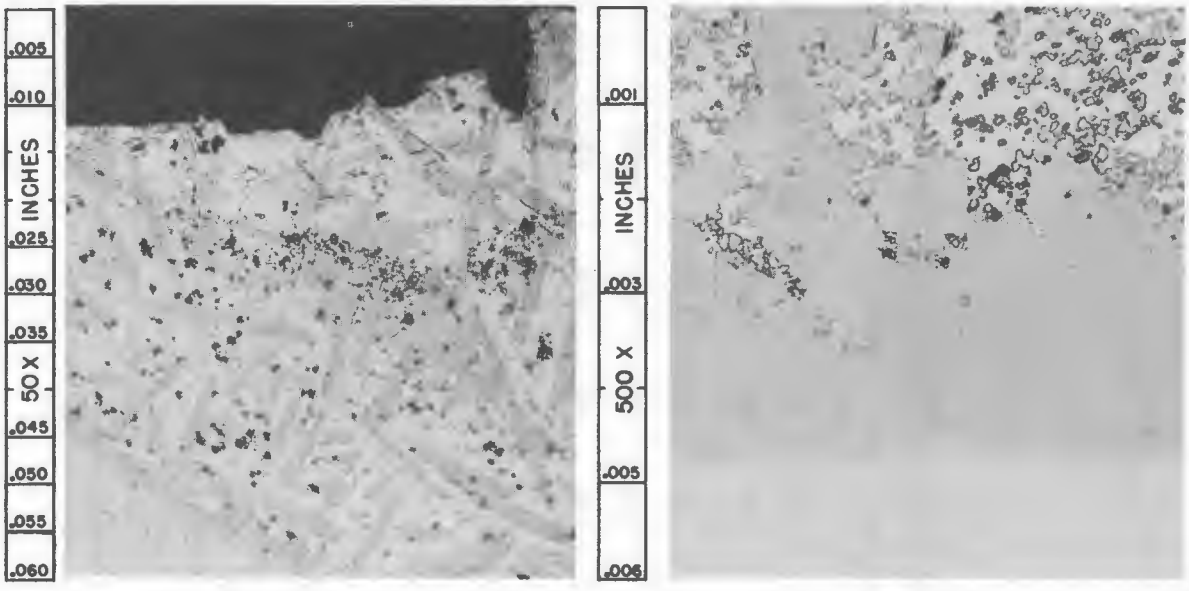
.005
.010
INCHES
.025
.030
.035
50 X
.045
.050
.055
.060
.001
INCHES
.003
500 X
.005
.006

c d

Table 6. Corrosion data for tin and its thorium and uranium alloys

Test Number	Corrosion system	Test temperature °C	Duration of test hours	Container wall thickness[a] inches	Penetration depth of corrosion inches	Type of corrosion attack[b]	Intermetallic compound formation inches	Arbitrary comparative ratings	Remarks
30	Sn in Nb	700	622	0.030	None	None	None	10	Sn sample easily removed from capsule. Meniscus was turned down--no wetting (Figure 16a).
31	Sn in Nb	900	660	0.030	Top[c] Complete Bottom 0.003	1a, 3 1a, 3	<0.001 <0.0015	4	Most severe attack at meniscus (Figure 16b). Globules in Figure 16c are precipitated Sn from cooling.
32	Sn in Nb	600	2500	0.030	Top[c] 0.006 Bottom 0.006	1a, 1c, 3 1a, 1c, 3	<0.010 <0.010	7	Wetting of walls. Intermetallic compound crystal facets shown in Figure 16d. Figure 16e shows extent of Type 3 attack of bottom specimen with polarized light.
33	Sn in Nb	1100	225	0.030	0.010	1a, 3	0.010	5	Wetting but no climbing of walls. Nb detected in Sn as a trace (Figure 16f).
34	Sn in Nb	1100	929	0.030	Complete	1a, 3	>0.010	5	Capsule top failed, possibly a faulty weld. No photomicrograph. Data from capsule bottom.
35	Sn in Nb	1100	1000	0.030	0.021	1a, 3	>0.012	5	Greatest attack at meniscus. Wetting but no climbing of walls (Figure 17a).
36	Th-Sn in Nb[d,e]	650	194	0.030	Top[c] 0.003 Bottom <0.001	1a, 3 1a, 3	<0.001 <0.001	5	Liquid wet and climbed walls (Figure 17b). Th settled to bottom on cooling (Figure 17c).
37	Th-Sn in Nb[d,e]	800	2023	0.030	Complete	1a, 3	>0.015	5	135° rocking furnace test. Capsule failed just before test ended. No photomicrograph.
38	U-Sn in Nb[e,f]	800	1225	0.030	Top[c] 0.013 Bottom 0.005	1a, 3 1a, 3	0.019 0.013	4	Liquid wet walls. Greatest attack at meniscus (Figure 17d). Th and Nb precipitated out (Figure 17e).
39	Sn in Ta	700	576	0.031	None	None	None	10	Sn did not wet walls and was easily removed from the capsule. No attack (Figure 17f).
40	Sn in Ta	900	1500	0.030	<0.0005	1a, 2	<0.001[g]	9	Very slight attack. Sn wet walls (Figure 18a).

[a] Tolerance of ±0.001 inch.

[b] Refer to section titled Corrosion by Liquid Metals.

[c] Two metallographic specimens were examined.

[d] 5.0 wt. % Th-Sn alloy; Th precipitates from solution upon cooling (39).

[e] Constituents of liquid alloy were not premelted.

[f] 5.0 wt. % U-Sn alloy; melting point approximately 450 to 500°C.

[g] Depth of inward diffusion into tantalum surface, instead of intermetallic formation.

Table 6 (Continued)

Test Number		Test temperature °C	Duration of test hours	Container wall thickness[a] inches	Penetration depth of corrosion inches	Type of corrosion attack[b]	Intermetallic compound formation[g] inches	Arbitrary comparative ratings	Remarks
41	Sn in Ta	1100	1255	0.030	0.001	1a, 2	<0.002[g]	9	Slight diffusion of Sn into Ta (Figure 18b).
42	U-Sn in Ta[e,f]	650	192	0.030	Top[c] None Bottom None	None None	None None	10	U-Sn easily removed from capsule. Meniscus turned was turned down. Top specimen (Figure 18c). U concentrated near bottom (Figure 18d).
43	U-Sn in Ta[e,f]	800	2023	0.031	Top[c] <0.0005 Bottom <0.0005	2 2	<0.0005 <0.0005	10	135° rocking furnace test. Meniscus turned down (Figure 18e). U concentrated near bottom (Figure 18f).
44	U-Sn in Ta[h,i]	800	1000	0.030	Top[c] <0.0003 Bottom <0.0005	2 2	<0.0003 <0.0005	9.5	Slight diffusion into Ta (Figure 19a). U-Sn wet capsule walls. U concentrated near bottom (Figure 19b).
45	U-Sn in Ta[h,i]	800	1000	0.030	Top[c] <0.0005 Bottom 0.001	2 2	<0.0005 0.001	9.5	See note above for Test No. 44. Top specimen: Figure 19c. Bottom specimen: Figure 19d.
46	U-Sn in Ta[h,i]	800	1750	0.030	Top[c] <0.0008 Bottom <0.002	1a, 2 1a, 2	<0.0008 <0.002	9.5	See note above for Test No. 44. Slight solution attack and precipitation of Ta detected. Top specimen: Figure 19e. Bottom specimen: Figure 19f.
47	U-Sn in Ta[h,i]	800	1750	0.030	Top[c] <0.0005 Bottom <0.0008	1a, 2 1a, 2	<0.0005 <0.0008	9.5	See note above for Test No. 46. Top specimen: Figure 20a. Bottom specimen: Figure 20b.
48	U-Sn in Ta[h,i]	800	3000	0.030	Top[c] <0.001 Bottom <0.0015	1a, 2 1a, 2	<0.001 <0.0015	9.5	See note above for Test No. 46. Top specimen: Figure 20c. Bottom specimen: Figure 20d.
49	U-Sn in Ta[h,i]	800	3000	0.030	Top[c] <0.0005 Bottom <0.001	1a, 2 1a, 2	<0.0005 <0.001	9.5	See note above for Test No. 46. Top specimen: Figure 20e. Bottom specimen: Figure 20f.
50	U-Sn in Ta[h,i]	950	1000	0.031	Top[c] <0.0015 Bottom <0.0015	1a, 2 1a, 2	0.002 0.002	9	See note above for Test No. 46. Top specimen: Figure 21a. Bottom specimen: Figure 21b.
51	U-Sn in Ta[h,i]	950	1000	0.030	Top[c] <0.0015 Bottom <0.0015	1a, 2 1a, 2	<0.0015 <0.0015	9	See note above for Test No. 46. Top specimen: Figure 21c. Bottom specimen: Figure 21d.
52	U-Sn in Ta[h,i]	950	1750	0.031	Top[c] <0.0015 Bottom <0.002	1a, 2 1a, 2	<0.0015 <0.002	9	See note above for Test No. 46. Top specimen: Figure 21e. Bottom specimen: Figure 21f.
53	U-Sn in Ta[h,i]	950	1750	0.030	Top[c] <0.0015 Bottom <0.0015	1a, 2 1a, 2	<0.0015 <0.0015	9	See note above for Test No. 46. Top specimen: Figure 22a. Bottom specimen: Figure 22b.

[h] 1.0 wt. % U-Sn alloy; melting point approximately 400 to 450°C.

[i] Alloy premelted in graphite crucibles at 1250°C.

Table 6 (Continued)

Test Number	Corrosion system	Test temperature °C	Duration of test hours	Container wall thickness[a] inches	Penetration depth of corrosion inches	Type of corrosion attack[b]	Intermetallic compound formation inches	Arbitrary comparative ratings	Remarks
54	U-Sn in Ta[h,i]	950	3000	0.030	Top[c] <0.0015 Bottom <0.002	Ia, 2 Ia, 2	0.002[g] 0.003[g]	9	See note for Test No. 46. Top specimen: Figure 22c. Bottom specimen: Figure 22d.
55	U-Sn in Ta[h,i]	950	3000	0.030	Top[c] <0.0015 Bottom <0.002	Ia, 2 Ia, 2	<0.002[g] 0.002[g]	9	See note for Test No. 46. Top specimen: Figure 22e. Bottom specimen: Figure 22f.
56	U-Bi-Sn in Ta[i,j]	950	1000	0.031	Top[c] <0.0003 Bottom <0.0003	Ia, 2 Ia, 2	<0.0003[g] <0.0003[g]	9.5	Slight attack. Alloy wet but did not climb walls. Little U concentrated at bottom. Top specimen: Figure 23a. Bottom specimen: Figure 23b.
57	U-Bi-Sn in Ta[i,j]	950	1000	0.030	Top[c] <0.0005 Bottom <0.0005	Ia, 2 Ia, 2	<0.0005[g] <0.0005[g]	9.5	See note above for Test No. 56. Top specimen: Figure 23c. Bottom specimen: Figure 23d.
58	U-Bi-Sn in Ta[i,j]	950	1750	0.030	Top[c] <0.0008 Bottom <0.0008	Ia, 2 Ia, 2	<0.0008[g] <0.0008[g]	9.5	See note above for Test No. 56. Top specimen: Figure 23e. Bottom specimen: Figure 23f.
59	U-Bi-Sn in Ta[i,j]	950	3000	0.031	Top[c] <0.001 Bottom <0.001	Ia, 2 Ia, 2	<0.001[g] <0.001[g]	9.5	See note above for Test No. 56. Top specimen: Figure 24a. Bottom specimen: Figure 24b.
60	U-Bi-Sn in Ta[i,j]	950	3000	0.030	Top[c] <0.001 Bottom <0.001	Ia, 2 Ia, 2	<0.0015[g] <0.0015[g]	9.5	See note above for Test No. 56. Top specimen: Figure 24c. Bottom specimen: Figure 24d.
61	Sn in Y	700	52	0.055	Complete	Ia, 3	>0.030	2	Sn wet but did not climb capsule walls (Figure 24e). Greatest attack at bottom.
62	Sn in Y	800	36	0.055	Complete	Ia, 3	>0.020	2	See note above for Test No. 61 and Figure 24f.
63	Sn in Y	600	84	0.055	Complete	Ia, 3	>0.060	2	Sn wet and climbed capsule wall. Failure through capsule top. No photomicrograph.
64	U-Sn in Y[e,f]	850	64	0.055	Complete	Ia, 3	>0.010	3	U-Sn wet but did not climb walls. Separation of alloy noticed (Figure 25a). Bottom: Figure 25b.
65	Sn in Inconel	700	244	0.113	0.057	Ia, 3	>0.010	2	Greatest attack at meniscus. Sn did not climb walls (Figure 25c).
66	Sn in Inconel	800	72	0.113	0.075	Ia, 3	>0.003	2	See note above for Test No. 65 and Figure 25d.
67	Bi in Y[k]	950	200	0.055	Complete	--[l]	--[l]	3	No photomicrograph. Failure at meniscus.

[j] 1.0 wt. % U-Bi-Sn alloy (bismuth-tin eutectic at 57 wt. % Bi-43 wt. % Sn); melting point approximately 242°C.

[k] Used as a test comparison against tests 61, 62, and 63.

[l] Not determined.

thorium-tin. Uniform solution attack followed by intermetallic compound formation are the modes of corrosion. The most severe attack almost always occurred at the meniscus level, possibly because of the increased activity at the surface of the liquid. Tin wet the niobium capsule walls in all but Test Number 30 which was run at 700°C for 622 hours. In this case the tin was easily removed from the capsule after sectioning. Another test (Number 32) run at 600°C for 2500 hours did wet the walls and could not be pried out, while a third test (Number 36) containing a 5.0 wt. % thorium-tin alloy at 650°C for 194 hours also wet and climbed the capsule walls. It is not readily clear why this one test did not wet the walls unless the condition of the capsule's surface was different or the test temperature and time duration were significant. A second test at 700°C was not run for a comparison, so a definite explanation was not made.

Thorium-tin from Test Number 36 was analyzed spectrographically and found to contain niobium present as a trace with interference. Test Number 35 also indicated the presence of niobium as a trace, while Test Numbers 30 and 32 showed niobium present as a faint trace with interference. The results of these tests are best explained by examining Table 6 and the photomicrographs for each test.

Pure tin in tantalum tests were run at 700, 900, and 1100°C. At 700°C the tin was observed not to wet the walls and was easily removed from the capsule after sectioning. At the higher temperatures, however, tin always wet the capsule walls but did not climb above the meniscus level. Very slight solution attack and up to 0.001 inch inward diffusion of the liquid-metal atoms into the tantalum were noticed in Test Numbers 40 and 41, the

latter being more pronounced. Following these tests, two capsules containing a 5.0 wt. % uranium-tin alloy were run at 650 and 800°C, respectively. The liquid metals in both of these tests were easily pried from the capsules since there had been no wetting and the meniscus was turned down. The latter test (Number 43) was run for 2023 hours in the 135° rocking furnace. Both capsules exhibited a separation of the uranium which probably occurred during cooling. Spectrographic results of the two layers indicated that separation of the uranium had indeed happened. Tantalum was detected as present as a faint trace with interference, but a blank tin sample also submitted indicated tantalum present as a faint trace with interference so that definite conclusions could not be made on the basis of these results. Test Number 41 run at 1100°C showed some solution attack since tantalum was detected as a trace.

To further check for inward diffusion of liquid-metal atoms into the tantalum container walls, twelve capsule tests were run for varying lengths of time up to 3000 hours. Six of the tests were conducted at 800°C and six at 950°C. These tests employed a 1.0 wt. % uranium-tin alloy previously melted in graphite crucibles at 1250°C. By premelting, it was hoped that separation of the uranium would be prevented; however, some uranium was observed to concentrate near the bottom. Both series of tests showed signs of slight uniform solution attack (Type 1a) and inward diffusion of the liquid-metal atoms into the tantalum lattice (Type 2 attack). Less than 0.002 inch of solution attack occurred and less than 0.003 inch of inward diffusion occurred. All of the samples wet the container walls but exhibited no tendency to climb them. Intermetallic compound formation

was not believed to have occurred since Miller (52) reports Ta_3Sn, the only intermediate compound, seems to be formed by a peritectic reaction between 1200 and 1550°C. Attack was more severe in the series run at 950°C than with those at 800°C, since the observed inward diffusion was greater. Etching did not reveal any grain boundary attack.

Since a separation of uranium had occurred in the twelve capsule tests described above, it was decided to combine 2.0 wt. % uranium with the bismuth-tin eutectic (57 wt. % bismuth-tin) in hopes that the higher solubility limit of bismuth for uranium would solve the problem. Five capsule tests (Numbers 56 through 60) were run at 950°C for periods up to 3000 hours. In this series corrosion attack of Types 1a and 2 still occurred but to a lesser degree than before. The greatest attack amounted to less than 0.001 inch of Type 1a and less than 0.0015 inch of Type 2. Two metallographic specimens were again examined and it was noted that little uranium separation had taken place. Wetting of the container walls did occur but no climbing tendency was noticed. The tantalum capsule tests of uranium-bismuth-tin were rated at "9.5", while those with uranium-tin at 800°C were rated "9.5" and those at 950°C at "9". Photomicrographs for all of these two test series are shown in Figure 16 through Figure 25.

Three tests of pure tin in yttrium and one test of uranium-tin in yttrium were all deemed failures as a result of complete penetration of the 0.055 inch wall. Types 1a and 3 corrosion attack occurred, with the most severe penetration at the bottom except for Test Number 63 where climbing of the walls and top end failurewere noted. Separation of the uranium in Test Number 64 was again noticed. These tests were rated at

"2" except for the uranium-tin test which was given a "3" rating because a lesser degree of intermetallic compound formation had occurred.

As comparison tests two capsules of tin in Inconel were run. Each resulted in severe solution attack and intermetallic compound formation. The greatest attack occurred at the meniscus penetrating over 50% of the way through the capsule walls. No climbing of the walls by the liquid metal was observed. Both tests received an arbitrary comparative rating of "2".

One final test of bismuth in yttrium was put into Table 6 to compare with tests 61, 62, and 63. Run at 950°C for 200 hours, the test resulted in complete penetration of the yttrium capsule at the meniscus. No analyses were conducted since the material inside the Inconel and tantalum sheaths had turned into a black powder.

Corrosion by Zinc

The last major phase of corrosion testing concludes with the results of nine isothermal tests with zinc in the selected container materials.

Four tests were run in niobium, three in tantalum, one in yttrium, and one in Inconel. Corrosion results are found in Table 7 and Figure 26. Each of the tests in niobium was run at 800°C, and each penetrated the 0.030 inch capsule wall. Solution attack (Type 1a) and intermetallic compound formation (Type 3) caused the capsule failures, but each time the zinc corroded through at the level of the inner surface of the end caps. Corrosion attack also occurred along the sides of the capsules but not severely as at the ends. It is theorized that a form of restrained

Table 7. Corrosion data for isothermal tests with zinc

Test Number	Corrosion system	Test temperature °C	Duration of test hours	Container wall thickness[a] inches	Penetration depth of corrosion inches	Type of corrosion attack[b]	Intermetallic compound formation inches	Arbitrary comparative ratings	Remarks
68	Zn in Nb	800	168	0.030	Complete	1a, 3[c]	--	2	Zn corroded through bottom cap and top cap leaving 0.010 inch walls.
69	Zn in Nb	800	100	0.030	Complete	1a, 3[c]	--	2	See note above. Greater attack occurred at the bottom cap.
70	Zn in Nb	800	102	0.030	Complete	1a, 3[c]	--	2	See note above for Test No. 69.
71	Zn in Nb	800	50	0.030	Complete	1a, 3	0.0003	2	Zn corroded through bottom cap. Figure 26a and data for top end.
72	Zn in Ta	800	400	0.030	Top[d] <0.0015 Bottom <0.002	1a 1a	None None	8	Slight solution attack. Etching did not reveal any intergranular attack (Figure 26b). Zn condenced on walls. Ta precipitate in bottom specimen (Figure 26c).
73	Zn in Ta	800	600	0.031	<0.0025	1a, 1c, 2	0.001[e]	7	Figure 26d shows evidence of Type 1c and 2 attack, and Figure 26e Type 1a. Zn wet but did not climb the walls.
74	Zn in Ta	900	1030	0.031	<0.0015	1a, 3	<0.0005	8	360° rotating capsule test. Slight intermetallic compound formation at interface (Figure 26f).
75	Zn in Y	700	90	0.055	Complete	1a, 3	>0.110	2	Severe attack.. Zn climbed walls and alloyed with Y, causing expansion of the capsule.
76	Zn in Inconel	800	306	0.113	0.061	3, 6	>0.040	3	Zn climbed walls and diffused into Inconel forming intermetallic compound. Greatest attack at meniscus.

[a] Tolerance of ±0.001 inch.

[b] Refer to section titled Corrosion by Liquid Metals.

[c] Based on the results of Test No. 71.

[d] Two metallographic specimens were examined.

[e] Intermetallic compound formation occurred within the tantalum (Figure 26d).

Figure 26. Corrosion attack by zinc (reduced 20 per cent)

a. Zinc in niobium at 800°C for 50 hours; Test Number 71 (500X)

b. Zinc in tantalum at 800°C for 400 hours; Test Number 72 (top specimen, 500X)

c. Zinc in tantalum at 800°C for 400 hours; Test Number 72 (bottom specimen, 250X)

d. Zinc in tantalum at 800°C for 600 hours; Test Number 73 (250X)

e. Zinc in tantalum at 800°C for 600 hours; Test Number 73 (second photomicrograph, 250X)

f. Dynamic capsule test of zinc in tantalum at 900°C for 1030 hours; Test Number 74 (250X)

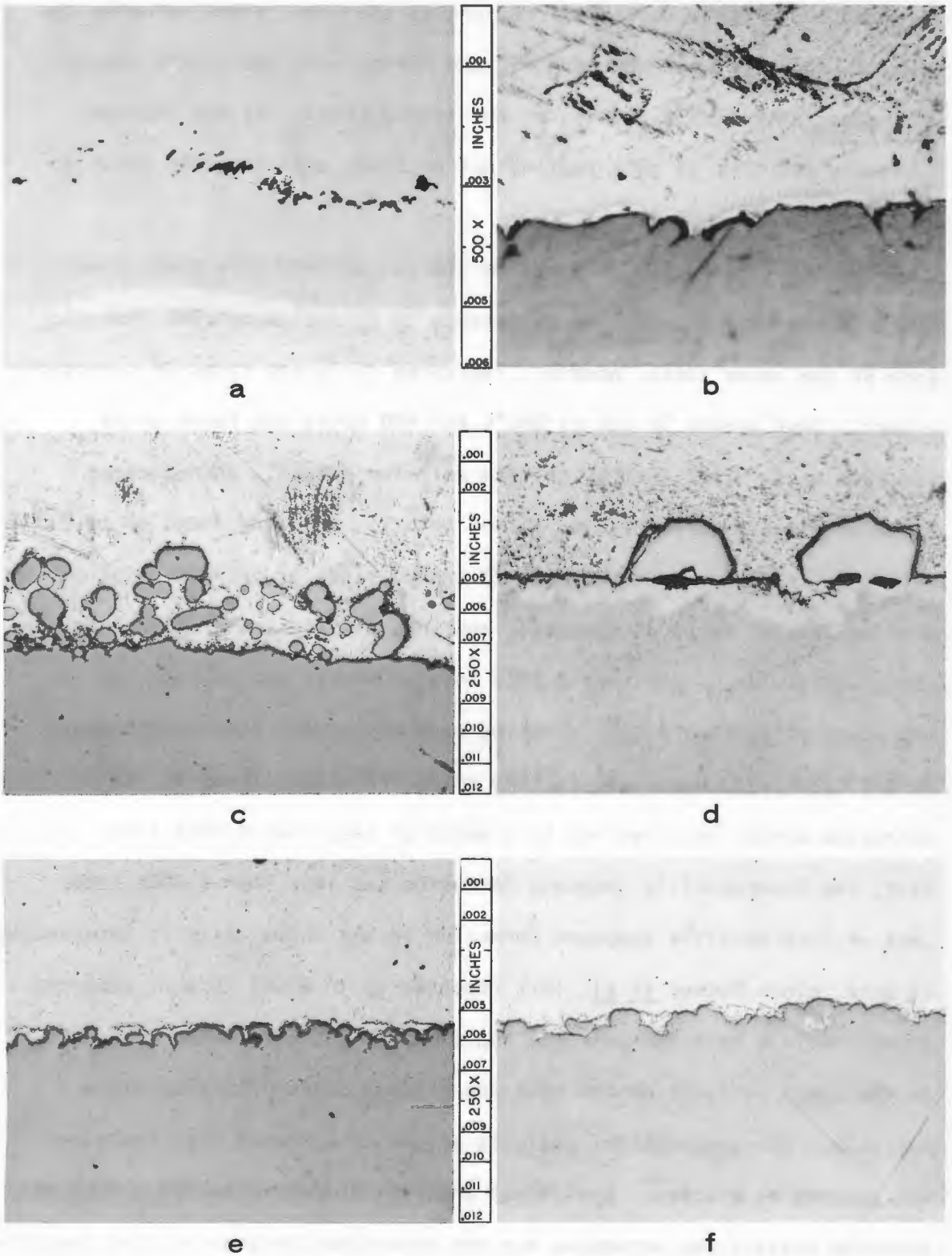
.001
INCHES
.003
500 X
.005
.006
a
b
.001
.002
INCHES
.005
.006
.007
250X
.009
.010
.011
.012
c
d
.001
.002
INCHES
.005
.006
.007
250X
.009
.010
.011
.012
e
f

or crevice corrosion caused the failure at the ends, since normally the crevice formed between the spun cap and tubing wall has little chance to contact appreciable amounts of the liquid metal. At any rate an increased activity in this region, not normally expected, did occur to cause the failure.

The tests conducted in tantalum did not exhibit this phenomenon. Tantalum showed a much better resistance to corrosion by zinc than niobium. Each of the three tests, however, indicated different types of corrosion attack. Test Number 72 run at 800°C for 400 hours was found to be attacked up to 0.002 inch by uniform solution attack. Upon cooling tantalum globules precipitated out of solution and were found up to 0.010 inch from the walls. Test Number 73 showed signs of uniform solution attack, crystal facet development, and inward diffusion of zinc into the tantalum lattice. Less than 0.0025 inch of attack occurred during the 600 hours at 800°C. A 360° rotating test was conducted for 1030 hours at 900°C, only 7° below the boiling point for zinc. Types 1a and 3 corrosion attack occurred but to a depth of less than 0.0015 inch. In fact, the intermetallic compound formation was less than 0.0005 inch. Lack of intermetallic compound formation in the three tests is interesting to note, since DeKany et al. (22) reported up to 0.003 inch of compound formation in a test run only 100 hours at 750°C. Zinc vapor condensed on the upper surfaces as the test was allowed to cool in a stationary position. Spectrographical analysis of the zinc showed that tantalum was present as a trace. Analytical analysis to determine the amount of tantalum present was attempted but not determined because of zinc precipi-

tate interference. Test Number 72 also showed tantalum present as a trace, while only a faint trace was detected in a sample of zinc from Test Number 73. The best indication of the corrosion attack, however, still lies with the metallographical analyses.

The one test of zinc in yttrium ended in total penetration of the capsule walls by solution attack and intermetallic compound formation. Considerable swelling of the capsule occurred as the intermetallic compound formed. Zinc climbed the walls to alloy with all of the available yttrium surface present. Gschneidner (34) reports that yttrium is soluble in liquid zinc at 600°C to an extent of 0.18 wt. %, but additional information on the system is not available.

The comparison test (Number 76) of zinc in Inconel was run at 800°C for 306 hours. Zinc climbed the capsule walls, diffused 0.061 inch into the Inconel walls, and formed an intermetallic compound. As a consequence Inconel-tin received an arbitrary comparative rating of "8". Zinc-niobium and zinc-yttrium each received a "2" while zinc-tantalum showed enough promise for a "7" and "8" rating.

CONCLUSIONS

The various types of corrosive attack of solid metals by liquid metals have been described, and an example of each has been presented. The driving forces for these types of attack have been discussed, and methods of corrosion inhibition presented. The various criteria for selecting fuel and fertile alloys and suitable container materials were considered.

Niobium, tantalum, yttrium, and Inconel have been exposed to molten aluminum, lead, tin, zinc, and their respective thorium and uranium alloys for various testing times and at temperatures ranging from 600 to 1100°C. From the results presented in Table 4 through Table 7 and Figure 12 through Figure 26, the following conclusions have been drawn:

1. Yttrium was found to be inadequate as a container material for aluminum, bismuth, lead, tin, and zinc at temperatures above 600°C except for short term capabilities. Lead, tin, and zinc severely attack yttrium above 600°C to cause failure in less than 50 hours. Yttrium was arbitrarily rated slightly better for containing uranium-aluminum and bismuth. Spectrographical analysis of several samples of the yttrium tubing used for the capsule tests showed varying degrees of copper impurity present from 30 to 1000 ppm, indicating that all of the copper had not been removed by pickling after the extrusion process. Failure of a number of yttrium capsules with the liquid metals tested, however, can be blamed almost entirely on the poor corrosion resistance of the metal and not on the impurities present.

2. Niobium was severely attacked by aluminum and zinc and to a lesser degree by tin. A slight amount of attack occurred with lead, although several tests indicated that no attack had taken place. Below 900°C niobium shows considerable promise for containment of lead and thorium-lead. Uranium-lead in niobium will need additional information since a number of high percentage uranium alloys, such as uranium-chromium and uranium-manganese, show rapid failure in niobium (9).

3. Tantalum proved to be superior to the other materials tested except for the tantalum-tungsten alloy tested with uranium-aluminum. This refractory metal shows excellent promise for containment of lead and uranium-lead but would be of limited value for use with tin and uranium-tin. Little or no detectable corrosion was noted with lead, but slight amounts of solution attack and inward diffusion into the container walls was seen with liquid tin. Tantalum is recommended as a satisfactory containment metal for these two liquid metals and their uranium alloys at temperatures up to 1100°C for periods in excess of 3000 hours.

Alloying uranium-tin with bismuth proved encouraging since the amount of corrosion attack was reduced as well as increasing the solubility of uranium in the alloy. Bismuth appears to be less corrosive to tantalum than tin.

Liquid zinc in tantalum was found to cause slight amounts of solution attack and intermetallic compound formation. Zinc in tantalum was rated at a slightly lesser value than tin in tantalum. Failure of the former system did not occur, and it is felt that tantalum would be capable of containing zinc at temperatures up to 900°C for periods in excess of 2000 hours without capsule failure.

Molten aluminum and uranium-aluminum were very corrosive to tantalum at 800°C in only 200 hours, although failure had not occurred. Alloying with uranium seemed to increase the corrosive nature of aluminum towards tantalum.

4. Tantalum-tungsten showed slightly better corrosion resistance to uranium-aluminum than tantalum, but cannot be compared with other liquid metals since only two test capsules were run. The alloy shows promise but presents difficulties in convenience of fabrication and welding.

5. Inconel was tested with pure liquid aluminum, lead, tin, and zinc for comparison with the other containment metals tested with these liquid metals. Varying amounts of corrosion attack were noted with all four systems. Lead was the least corrosive, but the other liquid metals all severely attacked the alloy. Inconel proved slightly better than niobium for containment of aluminum and zinc, better than yttrium for lead and zinc, and similar to yttrium for aluminum and tin.

6. Of the four container materials used with all the liquid-metal elements in the investigation, tantalum showed the best overall corrosion resistance. Niobium was second best, followed by Inconel and yttrium.

7. The most promising systems, excluding consideration of slurries, would be uranium-lead and thorium-lead in tantalum and uranium-bismuth-tin in tantalum. Additional work is recommended for these systems and for uranium- and thorium-tin in tantalum, employing the use of corrosion inhibitors.

RECOMMENDATIONS FOR FURTHER STUDY

There are many involved problems in the field of liquid-metal corrosion that should be carefully studied. The following items are listed.

1. Further static and particularly dynamic capsule testing is needed on the systems thorium-lead and uranium-lead in niobium. Dynamic capsule tests are recommended in order to prevent separation of the fuel or fertile constituent. If the systems look promising, then fabrication of a small-scale, forced-circulation loop would be justified.

2. Corrosion by tin, thorium-tin, uranium-tin, and uranium-bismuth-tin in tantalum should be carefully studied in light of the mechanism of attack and possible factors affecting the amount of corrosion. Dynamic tests including a possible test loop system should be considered.

3. Zinc in tantalum looks promising although some attack does occur. This system should be studied in the same manner as suggested in Number 2 above.

4. A forced-circulation loop should be constructed of tantalum and used to circulate lead and uranium or thorium additions to the lead. Mass transfer in addition to regular corrosion mechanisms which might occur could then be studied. Raseman and Weisman (56), Clifford (15, 16), and Fisher et al. (28, 29, 30) are useful references to consider in the design, construction, and operation of a liquid-metal circulating loop system.

5. Corrosion studies with alloys of uranium and the lead-bismuth eutectic should be considered and possibly incorporated with Recommendation Number 4 above.

6. Uranium-mercury which was recommended from Table 1, but not considered in this investigation due to the difficulty of alloy preparation, is worthy of study. A tantalum capsule containing mercury was run by the author at 800°C for 127 hours. Although the vapor pressure had caused the tantalum end caps to bulge and crack, allowing the mercury to escape, no corrosion attack was noticed. Alloying with uranium would lower the vapor pressure and possibly provide a promising liquid-metal fuel.

7. Corrosion by an alloy of 76 wt. % aluminum-18 wt. % thorium-6 wt. % uranium melting at 630°C (4) has been previously tested in niobium, tantalum and yttrium (9, 28, 29), but it should be investigated further for possible use especially in tantalum and yttrium.

8. Inhibition experiments should be conducted with all systems tested as a means of trying to check corrosion attack. In particular, additions or deletions of oxygen, hydrogen, nitrogen, carbon, and other elements should be considered as mentioned in the Corrosion Attack Inhibitors section of this report. Numerous references are appearing in the literature which stress the importance of these factors.

9. Slurries mentioned in Table 3 and by McCoy (49) should be given consideration but only in forced-circulation loop tests in order to keep the dispersion adequately mixed.

10. Other container materials besides those already tested in this investigation should be tried since the means of finding suitable containers is largely a matter of trial and error. Tantalum-tungsten is especially recommended in spite of the fact that tubing is not available and square capsules must be fabricated.

11. The possibility of using refractories and ceramic coatings was mentioned previously. The high melting points and oxide, carbide, and nitride compositions predict promising corrosion resistance. Several reports (6, 13, 19) indicate some of the work which has already been done in this area. Since the field is relatively new from the standpoint of liquid-metal corrosion, continual research should be conducted.

12. The fact that a number of the systems investigated failed or suffered appreciable corrosion attack does not mean that such a system would be nonpractical. Indeed, the rates of corrosion for all the systems is of importance and should be determined so that knowledge of a particular system's short term applicableness is known.[a]

13. The phenomenon of wetting by the liquid metal was observed in the majority of capsule tests. However, several capsule walls were not wet, and in these cases little or no corrosion attack was noted. Therefore, the factors which influence wetting should be studied and correlated to corrosion attack.

14. The strength characteristics of the containment materials to be used in a liquid-metal system should be studied, since corrosion has been known to increase as the result of stress. Crevice corrosion is one common example which can occur.

15. Future work should be directed toward increasing the understanding of rate controlling steps of dissimilar-metal (concentration-gradient) mass transfer and temperature-gradient mass transfer. Understanding these

---

[a]Bluhm, D. D., Ames, Iowa. Static corrosion of niobium by molten uranium-chromium eutectic. Private communication. 1963.

phenomena will then allow corrective measures to be taken which will keep these types of corrosion to a minimum.

ACKNOWLEDGMENT

Thanks are expressed to the Oak Ridge National Laboratory for providing a number of photomicrographs depicting the various types of corrosion attack.

BIBLIOGRAPHY

1. Alder, K. F. Liquid metal fuel reactors. In Australian Atomic Energy Symposium. pp. 346-354. Sydney, Australia, Melbourne University Press. ca. 1958.

2. Amateau, M. F. The effect of molten alkali metals on containment metals and alloys at high temperatures. U. S. Atomic Energy Commission Report DMIC-169 [Battelle Memorial Institute. Defense Metals Information Center, Columbus, Ohio]. 1962.

3. Bett, F. L. Compatibility between solid and liquid metals. In Australian Atomic Energy Symposium. pp. 201-205. Sydney, Australia, Melbourne University Press. ca. 1958.

4. Bobeck, C. F. Alloys of aluminum, thorium, and uranium. Unpublished M.S. thesis. Ames, Iowa, Library, Iowa State University of Science and Technology. 1956.

5. Bonilla, C. F. Mass transfer in molten metal and molten salt systems. [First] International Conference on the Peaceful Uses of Atomic Energy Proceedings 9: 331-340. 1956.

6. Brasunas, A. deS. Interim report on static liquid-metal corrosion. U. S. Atomic Energy Commission Report ORNL-1647 [Oak Ridge National Laboratory, Tennessee]. 1954.

7. Brasunas, A. deS. A simplified apparatus for making thermal gradient dynamic corrosion tests: seesaw tests. U. S. Atomic Energy Commission Report ORNL CF-52-3-123 [Oak Ridge National Laboratory, Tennessee]. 1952.

8. Brasunas, A. deS. Subsurface void formation in metals during high temperature corrosion tests. U. S. Atomic Energy Commission Report ORNL CF-52-9-59 [Oak Ridge National Laboratory, Tennessee]. 1952.

9. Cash, R. J., Core, M. R., and Fisher, R. W. Ames Laboratory molten-metal corrosion studies: compilation report to June 30, 1963. U. S. Atomic Energy Commission Report IS-768 [Iowa State University of Science and Technology, Ames. Institute for Atomic Research] [To be published 1964].

10. Cathcart, J. V. and Manly, W. D. The mass-transfer properties of various metals and alloys in liquid lead. U. S. Atomic Energy Commission Report ORNL-2008 [Oak Ridge National Laboratory, Tennessee]. 1956.

11. Cathcart, J. V. and Manly, W. D. A technique for corrosion testing in liquid lead. U. S. Atomic Energy Commission Report ORNL-1737 [Oak Ridge National Laboratory, Tennessee]. 1954.

12. Chelius, J. and Christophenson, R. G. Refractory metals. Machine Design 35, No. 22: 61-65. 1963.

13. Chemical engineering division summary report: October, November, and December, 1954. U. S. Atomic Energy Commission Report ANL-5388 [Argonne National Laboratory, Illinois]. 1955.

14. Chiotti, P. and Gill, K. J. Phase diagram and thermodynamic properties of the thorium-zinc system. Metallurgical Society of the American Institute of Mining, Metallurgical, and Petroleum Engineers Transactions 221: 573-579. 1961.

15. Clifford, J. C. A loop for circulating liquid lead-bismuth mixtures: corrosion and equipment studies. Unpublished M.S. thesis. Ames, Iowa, Library, Iowa State University of Science and Technology. 1958.

16. Clifford J. C. A loop for circulating liquid lead-bismuth mixtures: corrosion studies and operation. Unpublished Ph.D. thesis. Ames, Iowa, Library, Iowa State University of Science and Technology. 1960.

17. Collins, J. F. and Stephan, H. R. The solubility of metals and alloys in lead-bismuth eutectic at temperatures up to 2200°F. U. S. Atomic Energy Commission Report NEPA-1803 [Fairchild Engine and Airplane Corporation, NEPA Division, Oak Ridge, Tennessee]. 1951.

18. Cordovi, M. A. Static corrosion behavior of construction materials in an environment of liquid bismuth base metals at 550°C. U. S. Atomic Energy Commission Report BNL-179 [Brookhaven National Laboratory, Upton, New York]. 1952.

19. Coultas, T. A. Corrosion of refractories by tin and bismuth. U. S. Atomic Energy Commission Report NAA-SR-192 [North American Aviation, Inc., Downey, California]. 1952.

20. Cygan, R. Circulation of lead-bismuth eutectic at intermediate temperatures. U. S. Atomic Energy Commission Report NAA-SR-253 [North American Aviation, Downey, California]. 1953.

21. Danielson, G. C., Murphy, G., Peterson, D., and Rogers, B. A. Interim report of an investigation of the properties of thorium and some of its alloys. U. S. Atomic Energy Commission Report ISC-200 [Iowa State College, Ames]. 1952.

22. DeKany, J. P., Lavendel, H. W., and Burris, L., Jr. Studies of corrosion by molten zinc and cadmium systems. U. S. Atomic Energy Commission Report ANL-6243 [Argonne National Laboratory, Illinois]. 1960.

23. Deville, R. E. and Foley, W. R. Liquid metal fuel reactor experiment: liquid bismuth dynamic corrosion tests. U. S. Atomic Energy Commission Report BAW-1253 [Babcock and Wilcox Company, Alliance, Ohio]. 1960.

24. Eldred, V. W. Interactions between solid and liquid metals and alloys. United States Atomic Energy Commission Report AERE-X/R-1806 [Great Britain Atomic Energy Research Establishment, Harwell, Berkshire, England]. 1955.

25. Epstein, L. F. Corrosion by liquid metals. [First] International Conference on the Peaceful Uses of Atomic Energy Proceedings 9: 311-317. 1956.

26. Epstein, L. F. Static and dynamic corrosion and mass transfer in liquid metal systems. I. Liquid Metals Technology. Chemical Engineering Progress Symposium 53, No. 20: 67-81. 1957.

27. Finniston, H. M. Some studies of corrosion in liquid metal. In Australian Atomic Energy Symposium. pp. 189-196. Sydney, Australia, Melbourne University Press. ca. 1958.

28. Fisher, R. W. and Fullhart, C. B. Feasibility studies on molten metal reactor components. Second United Nations International Conference on the Peaceful Uses of Atomic Energy Proceedings 7: 216-222. 1958.

29. Fisher, R. W. and Fullhart, C. B. Problems in fabricating and operating a circulating molten metal system. Unpublished paper presented at Nuclear Technical Symposium, American Chemical Society, Boston, Massachusetts, April 8, 1959. Multilith. Ames, Iowa, Iowa State University of Science and Technology, Institute for Atomic Research. ca. 1959.

30. Fisher, R. W. and Winders, G. R. High temperature loop for circulating liquid metals. I. Liquid Metals Technology. Chemical Engineering Progress Symposium 53, No. 20: 1-6. 1957.

31. Friedlander, G. and Kennedy, J. W. Nuclear and radiochemistry. New York, N. Y., John Wiley and Sons, Inc. c1955.

32. Frost, B. R. T., Addison, C. C., Chitty, A., Geach, G. A., Gross, P., James, J. A., Metcalfe, G. J., Raine, T., and Sloman, H. A. Liquid metal fuel technology. Second United Nations International Conference on the Peaceful Uses of Atomic Energy Proceedings 7: 139-165. 1958.

33. Fundamental and applied research and development in metallurgy. Progress report for March, 1958. U. S. Atomic Energy Commission Report NMI-2068 [Nuclear Metals, Inc., Cambridge, Massachusetts]. 1958.

34. Gschneidner, K. A., Jr. Rare earth alloys. New York, N. Y., D. Van Nostrand Co., Inc. c1961.

35. Guidoboni, E. S., Huntress, A. M., and Loewenstein, P. Yttrium fabrication. U. S. Atomic Energy Commission Report NMI-1228 [Nuclear Metals, Inc., Cambridge, Massachusetts]. 1959.

36. Gurinsky, D. H. and Weeks, J. R. The metallurgy of a liquid fuel reactor. New York Academy of Science Transactions Series 2, 21, No. 1: 28-34. 1958.

37. Haefling, J. F. and Daane, A. H. The immiscibility limits of uranium with rare-earth metals. Metallurgical Society of the American Institute of Mining, Metallurgical, and Petroleum Engineers Transactions 215: 336-338. 1959.

38. Hampel, C. A. Corrosion properties of tantalum, columbium, molybdenum, and tungsten. Corrosion 14, No. 12: 29-32. 1958.

39. Hansen, M. and Anderko, K. Constitution of binary alloys. New York, N. Y., McGraw-Hill Book Company, Inc. 1958.

40. Hodgman, C. D., ed. Handbook of chemistry and physics. 44th edition. Cleveland, Ohio, The Chemical Rubber Publishing Company. c1962.

41. Holman, W. Materials for liquid metal systems. U. S. Atomic Energy Commission Report ASAE-26 [American Standard. Atomic Energy Division, Redwood City, California]. 1957.

42. Hopkins, E. H. and Peterson, D. T. The application of wax laps to vibratory polishers. U. S. Atomic Energy Commission Report IS-439 [Iowa State University of Science and Technology, Ames. Institute for Atomic Research]. 1962.

43. Kammerer, O. F., Weeks, J. R., Sadofsky, J., Miller, W. E., and Gurinsky, D. H. Zirconium and titanium inhibit corrosion and mass transfer of steels by liquid heavy metals. Metallurgical Society of the American Institute of Mining, Metallurgical, and Petroleum Engineers Transactions 212: 20-25. 1958.

44. Kaufmann, A. R. Reactor fuels. Nucleonics 15, No. 9: 142-146. 1957.

45. Kelman, L. R., Wilkinson, W. D., and Yaggee, F. R. Resistance of materials to attack by liquid metals. U. S. Atomic Energy Commission Report ANL-4417 [Argonne National Laboratory, Illinois]. 1950.

46. Klamut, C. J., Schweitzer, D. G., Chow, J. G. Y., Meyer, R. A., Kammerer, O. F., Weeks, J. R., and Gurinsky, D. H. Material and fuel technology for an LMFR. Second United Nations International Conference on the Peaceful Uses of Atomic Energy Proceedings 7: 173-195. 1958.

47. Lane, J. A., MacPherson, H. G., and Maslan, F., eds. Fluid fuel reactors. Reading, Massachusetts, Addison-Wesley Publishing Co., Inc. c1958.

48. Lyon, R. N., ed. Liquid-metals handbook. U. S. Atomic Energy Commission Report NAVEXOS P-733(Rev.) [Office of Naval Research, Washington, D. C.]. 1952.

49. McCoy, M. A. A reactor using UO_2-NaK slurry. Unpublished M.S. thesis. Ames, Iowa, Library, Iowa State University of Science and Technology. 1957.

50. Manly, W. D. Fundamentals of liquid-metal corrosion. U. S. Atomic Energy Commission Report ORNL-2055 [Oak Ridge National Laboratory, Tennessee]. 1956.

51. Miles, F. T. and Williams, C. Liquid metal fuel reactor. [First] International Conference on the Peaceful Uses of Atomic Energy Proceedings 3: 125-133. 1956.

52. Miller, G. L. Tantalum and niobium. New York, N. Y., Academic Press, Inc. 1959.

53. Nathans, M. W. A survey of metal solubilities in liquid zinc. U. S. Atomic Energy Commission Report ANL-5753 [Argonne National Laboratory, Illinois]. 1957.

54. Powell, G. W. Niobium-uranium alloys as container material for molten uranium eutectic alloys. U. S. Atomic Energy Commission Report NMI-1183 [Nuclear Metals, Inc., Cambridge, Massachusetts]. 1957.

55. Pray, H. A., Peoples, R. S., and Boyd, W. K. Corrosion by molten bismuth. U. S. Atomic Energy Commission Report BMI-773 [Battelle Memorial Institute, Columbus, Ohio]. 1952.

56. Raseman, C. J. and Weisman, J. Liquid metal fuel reactor (LMFR) processing loops. I. Design, construction, and corrosion data. U. S. Atomic Energy Commission Report BNL-322(T-55) [Brookhaven National Laboratory, Upton, New York]. 1954.

57. Reference data manual. Nucleonics 18, No. 11: 147-210. 1960.

58. Saller, H. A. and Rough, F. A. Compilation of U. S. and U. K. uranium and thorium constitutional diagrams. U. S. Atomic Energy Commission Report BMI-1000 [Battelle Memorial Institute, Columbus, Ohio]. 1955.

59. Smithells, C. J., ed. Metals reference book. Vols. 1 and 2. New York, N. Y., Interscience Publishers, Inc. 1955.

60. Spedding, F. H. The molten metal fuel reactor. U. S. Atomic Energy Commission Report ISC-318(Del.) [Iowa State College, Ames]. 1953.

61. Taylor, J. W. Inhibition of liquid-metal corrosion. United States Atomic Energy Commission Report AERE-M/TN-35 [Great Britain Atomic Energy Research Establishment, Harwell, Berkshire, England]. 1956.

62. Thamer, B. J. The containment of liquid-metal fuels at 500-1000°C. Atomic Energy Review 1, No. 2: 3-36. 1963.

63. Thompson, D. H. and Fisher, R. W. Performance characteristics of an electromagnetic pump. U. S. Atomic Energy Commission Report IS-188 [Iowa State University of Science and Technology, Ames. Institute for Atomic Research]. 1960.

64. Thompson, D. H. and Murphy G. Engineering design considerations for a liquid-metal in-pile loop. Unpublished Ph.D. thesis. Ames, Iowa, Library, Iowa State University of Science and Technology. 1963.

65. Tipton, C. R., Jr., ed. Reactor handbook. Vol. 1: Materials. 2nd edition. New York, N. Y., Interscience Publishers, Inc. 1960.

66. Udy, M. C. and Boulger, F. W. The properties of thorium alloys. U. S. Atomic Energy Commission Report BMI-89 [Battelle Memorial Institute, Columbus, Ohio]. 1951.

67. Waldron, M. B. Phase diagrams of plutonium alloys studied at Harwell. In Coffinberry, A. S. and Miner, W. N., eds. The metal plutonium. pp. 231-234. Chicago, Illinois, The University of Chicago Press. c1961.

68. Weeks, J. R. and Gurinsky, D. H. Solid metal-liquid metal reactions in bismuth and sodium. In Liquid metals and solidification. pp. 106-161. Cleveland, Ohio, American Society for Metals. c1958.

69. Weeks, J. R. and Klamut, C. J. Liquid metal corrosion mechanisms. U. S. Atomic Energy Commission Report BNL-6102 [Brookhaven National Laboratory, Upton, New York]. 1962.

70. Weeks, J. R. and Klamut, C. J. Reactions between steel surfaces and zirconium in liquid bismuth. Nuclear Science and Engineering 8: 133-147. 1960.

71. Weeks, J. R., Klamut, C. J., Silberberg, M., Miller, W. E., and Gurinsky, D. H. Corrosion problems with bismuth uranium fuels. [First] International Conference on the Peaceful Uses of Atomic Energy Proceedings 9: 341-355. 1956.

72. Weinberg, A. M., Howe, J. P., Jette, E. R., Wilhelm, H. A., Rogers, B. A., and Foote, F. G. Nuclear metallurgy. American Institute of Mining and Metallurgical Engineers. Institute of Metals Division Special Report Series No. 1. 1955.

APPENDIX A

Chemical Analyses of Metals and Alloys Used in the Investigation

The materials involved in this investigation were obtained from commercial sources and were used in essentially the as-received condition. Tables 8 and 9 represent data obtained from the suppliers while Table 10 summarizes the results of spectrographical analyses run on the metals.

It should be recognized that additional impurities might have been added during handling and preparation of the materials for testing although usual precautions were taken. This contamination has not been determined because of the difficulties of such a determination and the questionable significance of the data if obtained.

Table 8. Composition of metals used in the liquid-metal alloys

Metal	Source	Purity wt. %	Impurities wt. %[a]	Remarks
Aluminum	National Bureau of Standards	99.99	Cu, Fe, Si, Mn, Mg, Ca, Cr, Ni,	No analysis was supplied. Impurities detected by spectrographic analysis.
Bismuth	Baker Chemical Company	99.985+	Ag, 0.005 Pb, 0.0005 As, 0.00005 Sb, 0.001 Cu, 0.0005 Fe, 0.002 Zn, 0.005	Commercial grade. Reported as a typical analysis.
Lead	Fisher Scientific Company	99.99+	As, 0.00003 Ag, 0.0001 Fe, 0.0003	Commercial grade. Reported as a typical analysis.

[a]Reported as wt. % unless otherwise noted.

Table 8 (Continued)

Metal	Source	Purity wt. %	Impurities wt. %[a]	Remarks
Lead (Continued)			Sb, 0.001 Bi, 0.0004 Sn, 0.003 Cu, 0.0003	
Tin	Baker Chemical Company	99.9+	As, 0.00001 Cu, 0.0003 Fe, 0.002 Pb, 0.005 Zn, 0.0005 other, 0.007	Commercial grade. Reported as a typical analysis.
Zinc	Baker Chemical Company	99.99	As, 0.000001 Fe, 0.005 Pb, 0.002	Commercial grade. Reported as a typical analysis.
Thorium	Ames Laboratory	99.7+	N, 84 ppm C, 250 ppm Al, < 25 ppm Ca, < 50 ppm Be, 110 ppm Si, < 50 ppm Mg, < 20 ppm Zn, < 20 ppm Fe, 80 ppm Mn, < 20 ppm B, < 0.5 ppm Cd, < 0.2 ppm	Billet No. A1702. Wet-chemistry analysis.
Uranium	National Lead Company of Ohio	99.8--99.9	N, 55 ppm C, 30 ppm Fe, 100 ppm Si, 31 ppm Cr, 24 ppm Cu, 8 ppm Mg, 61 ppm Mn, 11 ppm Ni, 56 ppm	Average of 21 derbies.

Table 9. Composition of container materials

Material	Source	Purity wt. %	Impurities ppm[a]	Remarks
Niobium (Annealed)	Wah Chang Corporation	99.9+	Al, < 20 C, < 30 Cr, < 20 Cu, < 40 Fe, < 100 H, < 2.3 Mg, < 20 Mn, < 20 Mo, < 20 N, 72-99 Ni, < 20 O, 110-180 Pb, < 20 Si, < 100 Sn, < 20 Ta, 470-490 Ti, < 150 V, < 20 W, < 300 Zn, < 20 Zr, < 500	Analysis reported by supplier.
Tantalum (Annealed)	Fansteel Metallurgical Company	99.9	Nb, < 500 W, < 200 Fe, < 100 Mo, < 50 O, < 70 Zr, < 50 Ni, < 50 C, < 50 N, < 50	Reported as a typical analysis by the supplier.
Yttrium[b] (Annealed)	Ames Laboratory Extruded by Nuclear Metals, Inc.	99.6	O, 1190 F, 580 C, 217 N, 142 Fe, 200[c] Ni, 200[c] Ca, < 10	Billet No. 346.

[a] Reported as ppm unless otherwise noted.

[b] Impurities before extrusion.

[c] Estimated at the values of previous billets.

Table 9 (Continued

Material	Source	Purity wt. %	Impurities ppm[a]	Remarks
Yttrium (continued)			Mg, < 15 Ti, 0.5 wt.%[c] Zr, < 50[c] Cu, < 100[b,c]; 1000[d] Si, < 100[c] B, < 10[c]	
Tantalum-tungsten	National Research Corporation	90Ta-10W	C, 20 Cr, < 10 Fe, 20 Ni, < 10 O, 13 N, 20 W, 12.0 wt.%	Analysis reported by supplier.
Inconel	International Nickel Company, Incorporated	Ni-Cr-Fe	Ni, >72.0 wt.% Cr, 14-17 wt.% Fe, 6-10 wt.% Mn, < 1.0 wt.% C, < 0.15 wt.% Cu, < 0.5 wt.% Si, < 0.5 wt.% S, < 0.015 wt.%	Limits of composition

[d]Copper impurity after extrusion.

Table 10. Spectrographical analysis of the metals used in the investigation

Metal	Reported strengths				
	Weak	Very weak	Trace	Faint trace	Very faint trace
Aluminum	Si	Cu	Fe	Ca,Cr,Mg,Ni,Mn	
Bismuth			Cu	Si,Mg,Ni	Ca
Lead				Mg,Cu,Ca,Al,Cr	
Niobium			Mg,Si	B,Fe,Ni,Zr	
Tantalum			Mg,Nb	Ca,Fe,Si,Ti,V,Zr	
Thorium		Be		Al,Cr,Fe,Si,Ni	
Tin		Ni	Pb,Sb	Fe,Cu	Si,Mg,Ca
Yttrium		Cu,Cr,Fe	Ni,Si	Al,Mg,Mn	Ca
Zinc			Sn,Pb	Si,Cu,Mg,Cr	Ca

APPENDIX B

Table II. Physical properties of the materials used in the investigation[a]

Property	Aluminum[A]	Bismuth[A]	Lead	Tin	Zinc	Niobium[B]	Tantalum[B]	Yttrium[C]	Thorium	Uranium
Atomic number	13	83	82	50	30	41	73	39	90	92
Atomic weight	26.98	208.99	207.21	118.70	91.22	92.91	180.95	88.91	232.05	238.07
Natural isotopes[D] (% abundance)	27(100%)[D]	209(100%)[D]	204(1.48%) 206(23.6 %) 207(22.6 %) 208(52.3 %)	112(0.95%); 114(0.65%) 115(0.34%); 116(14.24%) 117(7.57%); 118(24.01%) 119(8.58%); 120(32.97%) 122(4.71%); 124(5.98%)	64(48.99%) 66(27.81%) 67(4.11%) 68(18.56%) 70(0.62%)	93(100%)[D]	180(0.01+%)[D] 181(99.99 %)[D]	89(100%)[D]	232(100%)	234(0.0058%) 235(0.715 %) 238(99.28 %)
Lattice structures (transition temperatures)	FCC[E]	Rhombo[E]	FCC[E]	α, Cubic (18°C)[E] β, Tet (170°C) γ, Rhombo	HCP[E]	BCC[E]	BCC[E]	α, HCP(1490°C) β, BCC	α, FCC(1375°C)[A] β, BCC	α, Ortho(666°C)[A] β, Tet (771°C) γ, BCC
Thermal-neutron absorption cross section (barns)	0.215	0.032	0.170[F]	0.625[F]	1.1[F]	1.1	21.3	1.31[F]	7.56[F]	7.68[F]
Density at 20°C (gm/cm^3)[F]	2.70[F]	9.7[F]	11.3	7.29	7.14	8.6[F]	16.6[F]	5.51[F]	11.5	19.04(25°C)[A]
Melting point (°C)	660.2	271	327[A]	231.9[E]	419.5[E]	2468 ± 10	2997-3000	1502 ± 7	1750[A]	1132[G]
Boiling point (°C)	2327	1477	1740[A]	2200[E]	907[E]	5027 ± 100	5427 ± 100	2630	3000-4200	4200[E]
Thermal conductivity at 20°C (cal/sec/cm/°C)	0.503	0.019[E]	0.083[A]	0.156[E]	0.270[E]	0.125	0.130	0.035(25°C)	0.090(100°C)[A]	0.065
Specific heat at 20°C (cal/gm/°C)	0.214[G]	0.0294[G]	0.0306[G]	0.054[G]	0.0925[G]	0.065(100°C)	0.036(100°C)	0.079[G]	0.0276[G]	0.028[G]
Coefficient of linear thermal expansion at 25°C (°C^{-1})	25.5(10^{-6})[G]	-13.4(10^{-6})[E]	29.4(10^{-6})[G]	26.9(10^{-6})[G]	26.3(10^{-6})[G]	7.1(10^{-6})	6.6(10^{-6})	10.8(10^{-6})	12.3(10^{-6})[G]	a, 23.12(10^{-6})[A] b, -0.46(10^{-6}) c, 19.71(10^{-6})
Electrical resistivity 20°C (microhm-cm) 500°C 1000°C	2.66	116[E] 139.7	20.6[E] 104.6[E] 125.7[E]	12.8[E] 54.0[E] 68.6[E]	5.92[E] 36.1[E]	15.2(0°C) 35	12.5[E] 35 54	57(27°C)	13[A]	29.2[A] 52.0[A] 49.5[A]
Tensile strength at 20°C (psi)	--	--	--	--	--	50,000-110,000	50,000-180,000	45,000	25,000-80,000[A]	55,000-190,000[A]

[a] Reference citations for tabular data are designated as follows:
A means data from Reference 65 unless otherwise noted.
B means data from Reference 52 unless otherwise noted.
C means data from Reference 34 unless otherwise noted.
D means data from Reference 31.
E means data from Reference 59.
F means data from Reference 57.
G means data from Reference 40.